UNIVERSITY *of the*
WESTERN CAPE

THE USE OF REMOTE SENSING DATA TO MONITOR POOLS ALONG NON-PERENNIAL RIVERS IN THE WESTERN CAPE, SOUTH AFRICA.

by

DSL Seaton

Supervisor: **Prof D Mazvimavi**

Co-supervisor: **Dr T Dube**

UNIVERSITY *of the*
WESTERN CAPE

A thesis submitted in fulfilment of the requirements for the degree of Magister Scientiae

Faculty of Science

Department of Earth Science

Environmental and Water Science

University of the Western Cape

March 2019

http://etd.uwc.ac.za/

ABSTRACT

The lack of monitoring of non-perennial rivers is a major problem for water resources management, despite their significance in satisfying agricultural, economic and recreational needs. Pools in non-perennial rivers are not monitored, due to their remoteness. Remote sensing offers a promising alternative for the monitoring of changes in water storage in these pools.

This study aims to assess the extent to which remotely-sensed datasets can be used to monitor the spatio-temporal changes of water storage of pools along non-perennial rivers in the Western Cape. The objectives of this study are: (1) to determine a suitable image pre-processing and classification technique for detecting and monitoring surface water along non-perennial rivers, and (2) to describe the spatial and temporal changes of water availability of pools along non-perennial rivers, using remotely sensed datasets.

The Normalised Difference Water Index (NDWI), Modified NDWI (MNDWI), Normalised Difference Vegetation Index (NDVI), Automated Water Extraction Index for shadowed ($AWEI_{sh}$) and non-shadowed regions ($AWEI_{nsh}$) and the Multi-Band Water Index (MBWI) classification techniques were investigated in this study, using the Sentinel-2 and Landsat 8 datasets. In-situ measurements were used to validate the satellite-derived datasets, while the use of high resolution aerial photography and Digital-Globe WorldView imagery were further compared to the results. The results suggested that the NDWI is the most suitable classification technique for identifying water in pools along non-perennial rivers throughout the Western Cape. The NDWI applied to the Sentinel-2 Top-of-Atmosphere (TOA) reflectance dataset had the highest overall accuracy of 85%, when compared to the Sentinel-2 Dark Object Subtraction 1 (DOS1) atmospheric correction, Sentinel-2 Sen2Cor atmospheric correction, Landsat 8 TOA reflectance and Landsat 8 DOS1 atmospheric correction datasets. The incorporation of atmospheric correction was shown to eliminate surface water pixels in many of the smaller pools.

The NDWI was used to examine the pool dynamics along non-perennial rivers (the Nuwejaars, Breede, Touws and Tankwa Rivers), over a period of two years (2016 – 2017). The results were further compared to the daily mean rainfall and temperatures to better understand the causes of the spatio-temporal variability of pools in non-perennial rivers. As

UNIVERSITY of the
WESTERN CAPE

http://etd.uwc.ac.za/

expected, the results showed a good relationship between the rainfall, temperature and changing surface areas of water stored in the pools. Overall, the results underscored the relevance of using Sentinel-2 imagery for monitoring pool dynamics in non-perennial rivers, which was previously challenging when using coarse resolution multi-spectral sensors, such as the Moderate Resolution Imaging Spectroradiometer (MODIS).

Keywords:

Atmospheric correction

Hydroperiod classification

Landsat 8-OLI

Multiband methods

Non-perennial rivers

Pools

Remote sensing

Sentinel-2 MSI

Surface water area estimation

Time series

UNIVERSITY of the
WESTERN CAPE

http://etd.uwc.ac.za/

ACKNOWLEDGEMENTS

My thanks, first and foremost, go to my mother, father and brother, for pushing me to do the best I can. You have stood by me through the highs and lows, and for that I will be forever grateful. I would also like to extend my gratitude to my aunt and uncle for their help and support.

Secondly, I would like to extend my gratitude to Clinton Andries and Bernhard Schacht for their help and support over the course of this thesis. Thank you for the journey we have shared since our first year. I would also like to extend my gratitude to the students and staff who have supported me over the years and taught me so much.

Thirdly, I would like to thank the Institute for Water Studies and the Non-Perennial Rivers Project for funding me over the course of my studies, and for affording me the opportunity to undertake this project. The skills and knowledge I that have gained from this project will remain with me always. I would like to extend my gratitude to Alliance for Collaboration on Climate and Earth Systems Science (ACCESS) for providing the funding for me to take part in the 19th WaterNet Symposium.

Fourthly, I would like to thank the South African Weather Services (SAWS) and the Agricultural Research Council (ARC) for providing the necessary rainfall data that I required.

Finally, I would like to express my deep gratitude to my supervisors, Prof. Dominic Mazvimavi and Dr. Timothy Dube. Thank you for the valuable guidance, assistance and support during the course of this study. This thesis would not have been possible without your help.

UNIVERSITY of the
WESTERN CAPE

http://etd.uwc.ac.za/

DECLARATION

I declare that the thesis entitled "*An Assessment of Remotely-sensed Multiband Methods for Surface Water Monitoring along Non-perennial Rivers in the Western Cape, South Africa*" is my own work, that it has not been submitted before, for any degree or examination, at any other university, and that all the sources I have used or quoted have been indicated and acknowledged by means of complete references.

Full name: Dylan St Leger Seaton

Signed…… Date……...

http://etd.uwc.ac.za/

TABLE OF CONTENTS

UNIVERSITY of the
WESTERN CAPE

http://etd.uwc.ac.za/

UNIVERSITY of the
WESTERN CAPE

http://etd.uwc.ac.za/

UNIVERSITY of the
WESTERN CAPE

http://etd.uwc.ac.za/

LIST OF FIGURES

UNIVERSITY of the WESTERN CAPE

http://etd.uwc.ac.za/

UNIVERSITY of the
WESTERN CAPE

http://etd.uwc.ac.za/

UNIVERSITY of the WESTERN CAPE
http://etd.uwc.ac.za/

UNIVERSITY of the
WESTERN CAPE

http://etd.uwc.ac.za/

LIST OF TABLES

UNIVERSITY of the
WESTERN CAPE

http://etd.uwc.ac.za/

ABBREVIATIONS

AD	Allocation Disagreement
ARC	Agricultural Research Council
ASTER	Advanced Spaceborne Thermal Emission and Reflection Radiometer
AVHRR	Advanced Very High Resolution Radiometer
$AWEI_{nsh}$	Automated Water Extraction Index for non-shadowed regions
$AWEI_{sh}$	Automated Water Extraction Index for shadowed regions
BOA	Bottom of Atmosphere
DEM	Digital Elevation Model
DGPS	Differential Global Positioning System
DOS	Dark Object Subtraction
DWS	Department of Water and Sanitation
ESA	European Space Agency
ET	Evapotranspiration
MBWI	Multi-band Water Index
MNDWI	Modified Normalised Difference Water Index
MODIS	Moderate Resolution Imaging Spectrometer
MSI	Multi-spectral Imager
NDVI	Normalised Difference Vegetation Index
NDWI	Normalised Difference Water Index
NGI	National Geo-spatial Information
NIR	Near Infrared
OA	Overall Accuracy
OLI	Operational Land Imager

UNIVERSITY of the
WESTERN CAPE

http://etd.uwc.ac.za/

PA	Producers' Accuracy
QD	Quantity Disagreement
RMSE	Root Mean Square Error
RQIS	Resource Quality Information Services
SAR	Synthetic Aperture Radar
SAWS	South African Weather Services
SNAP	Sentinel Application Platform
SPOT	Satellite Pour l'Observation de la Terre
SWIR	Shortwave Infrared
TOA	Top of Atmosphere
UA	Users' Accuracy
USGS	United States Geological Survey
EO	Earth Observation
ML	Maximum Likelihood
ETM	Enhanced Thematic Mapper
TSWB	Temporary Surface Water Bodies

UNIVERSITY of the
WESTERN CAPE

http://etd.uwc.ac.za/

1. INTRODUCTION

1.1 Background

Freshwater is an irreplaceable natural resource that is essential for socio-economic development, agriculture and ecosystem functioning (Jiang et al., 2014; Rokni et al., 2015). Coastal and inland surface waters, such as wetlands, dams, lakes and rivers play a key role in climate variations and global carbon cycles, and they provide a fundamental resource to all life on earth (Mishra & Prasad, 2015). Despite this, the world is experiencing a surge of water-related crises (Eliasson, 2015). The result of global climate change and the effects of increasing water abstraction, arising from urbanisation and development, have caused water resources to become increasingly scarce (Mishra & Prasad, 2015; Zhou et al., 2017). Water use has been increasing at more than double the rate of the population growth (Changwony et al., 2017), while approximately four billion people live in conditions of severe water scarcity at least once a month each year (Mesfin & Arjen, 2016).

Non-perennial rivers offer an immense range of services to humans (Mathews & Richter, 2007). The natural flow regime of non-perennial rivers affects fish populations, the movement of nutrients, organic carbons and sediment and it contributes to channel formations (Seaman et al., 2016). High flows transport sediments, nutrients and organisms to downstream rivers. Extreme floods recharge aquifers, thereby ensuring water availability during the dry seasons for the growth of riparian vegetation (Jacobson et al., 1995; Rossouw et al., 2005). Low flows allow for the deposition of sediments and nutrients in river channels and river banks, for their stabilization (Poff et al., 1997; Wood & Armitage, 1997; King et al., 2003; Stromberg et al., 2007).

Pools occurring along non-perennial rivers play a significant role in flood control, groundwater recharge, pollution filters, as well as the recycling of nutrients, sediments and carbon deposition zones (Rhazi et al., 2011). Pools possess great value in terms of usage by society and by grazing and wildlife animals, as well as in agriculture and in the harvesting of medicinal plants (Smith et al., 2002; Zacharias & Zamparas, 2010; Rhazi et al., 2011). However, the extensive use of river water often results in ecological degradation and the loss

http://etd.uwc.ac.za/

of biological diversity (Poff et al., 1997; King et al., 2004) and information about its effects is limited or of poor quality (Kapangaziwiri et al., 2012).

The in-situ measurement of river flow is a primary method for monitoring surface water availability. These measurements provide an overview of the surface water availability, but they are labour-intensive and costly (Omute et al., 2012). Inadequate funding for the development of hydrological networks restricts the assessment of water resources in most countries (Smakhtin et al., 2004; Kapangaziwiri et al., 2012; Hughes et al., 2014; Solander et al., 2016). Therefore, alternative methods for surface water monitoring need to be explored in data-scarce areas, especially in developing countries.

Remote sensing is widely used for hydrological monitoring (Joseph, 2003; Rokni et al., 2014; Feyisa et al., 2014) and the monitoring of water resources, using remote sensing, is well-documented (Avisse et al., 2017; Sarp & Ozcelik, 2017). Remote sensors, such as MODIS, provide global coverage of surface water resources, with daily revisit times, but they have a coarse spatial resolution of 250 m to 1 km (Yamazaki et al., 2015). Very high resolution remote sensing datasets, such as WorldView-2 and SPOT have daily revisit times, but are extremely expensive. Other datasets, such as the Landsat series and Sentinel satellites have also been extensively used for surface water monitoring (Zhou et al., 2017). The Sentinel-2 MSI satellite that was launched in 2015 offers high spatial resolution data of 10 m, 20 m and 60 m, and a short revisit time of five days (ESA, 2015).

UNIVERSITY of the
WESTERN CAPE

As new satellites are being launched, remote sensing classification methods are continuously being developed. However, the accuracy of these classification methods varies greatly, and depends significantly on the sensor, the location, the features and overall outcome of the study. Several semi-automatic classification methods have been developed over the years to extract surface water information from optical satellite datasets. Multiband methods, or water-index methods, have been shown to be some of the most promising. This is due to their relatively high accuracy in water detection, their low-cost of implementation and their ease of use. As more satellites are being launched, new methods are being developed (Marcus & Fonstad, 2007). Improving surface water monitoring through remote sensing of non-perennial rivers directly improves the water resources management of these rivers. This study intends to enhance the knowledge on remotely-sensed classification methods for surface water mapping in non-perennial rivers, as well as to determine whether the Sentinel-2 MSI dataset is suitable for monitoring surface water in non-perennial rivers.

http://etd.uwc.ac.za/

1.2 Research Problem

Non-perennial rivers make up about two-thirds of all rivers in southern Africa (Rossouw et al., 2005; Rossouw, 2011), yet limited information about these river systems is available (Haas et al., 2009; Makungo et al., 2010). In-situ measurements provide sparse data without comprehensive coverage of the spatial variation of river water dynamics (Fausch & Bramblett, 1991; Puckridge, 1998).

The problem of selecting a suitable remote sensing dataset, in terms of its spatial resolution, return period and classification method, can be challenging (Soti et al., 2009). There is an inevitable trade-off between spatial resolution, return period and acquisition cost. Coarse resolution sensors, such as MODIS offers a daily revisit period across any region of the world, but is not feasible for mapping small pools along non-perennial rivers. Very high resolution sensors, such as SPOT, offer more detailed, and, thus, more accurate mapping; however, the high costs and limited number of spectral bands are not feasible for determining a large range of classification methods. Medium-resolution sensors, such as Landsat and Sentinel, offer freely available multispectral data, with short revisit times every five to fifteen days. However, the accuracy of surface water mapping also depends on the methods applied. No single multiband method has been shown to be the best (Fisher et al., 2016). This has led to uncertainty as to which method is most suitable for mapping surface water in non-perennial rivers. Therefore, there is a need to investigate the use of remotely-sensed datasets for monitoring the availability of surface water in non-perennial rivers.

UNIVERSITY of the
WESTERN CAPE

1.3 Research Questions

The following research questions were addressed:

a) How accurate are remote sensing datasets for mapping pools in non-perennial rivers? and
b) To what degree can the spatial and temporal changes of pools along non-perennial rivers be described?

http://etd.uwc.ac.za/

1.4 Aim and Objectives

1.4.1 Aim

The aim of this study is to assess the extent to which medium resolution multispectral imager datasets can be used to map and monitor surface water availability along non-perennial rivers, in the semi-arid environments of South Africa.

1.4.2 Objectives

The objectives of this study are:

a) to determine a suitable image pre-processing and classification technique for detecting and monitoring surface water along non-perennial rivers; and
b) to describe the spatial and temporal changes of pools along non-perennial rivers, using remotely-sensed datasets.

1.5 Significance of the Study

Non-perennial rivers and pools play a critical role in their surrounding habitats. However, the information on these systems and features is limited. Ecologists require information on pools in order to better understand their influence on their surrounding environment. There is a need to develop a fast, reliable and less costly method for identifying and mapping the occurrence and spatio-temporal dynamics of pools in non-perennial rivers. This study will explore the potential and limitations of using remotely-sensed datasets for the surface water mapping and monitoring of non-perennial rivers. This study will also provide a greater understanding of the dynamics of pools and non-perennial rivers in semi-arid environments, and it will contribute to future studies that aim to use remote sensing for surface water monitoring in non-perennial rivers.

http://etd.uwc.ac.za/

1.6 Thesis Outline

Chapter One introduces the background of the study, highlighting the significance of non-perennial rivers, which is followed by the research problem, research questions, aim and objectives.

Chapter Two presents the literature that has been reviewed. The different surface water classification methods are revised, and the necessary pre-processing steps required are shown. The chapter will conclude with a summary of the knowledge gaps that have been identified.

Chapter Three presents a description of the study areas. Firstly, a regional description of the Western Cape is presented, followed by a description of the research sites that were selected.

Chapter Four investigates the accuracy of remotely-sensed datasets for mapping pools in non-perennial rivers. This chapter presents the data collection and data analysis methods, followed by the results and a discussion of the major findings.

Chapter Five investigates the estimation of surface water availability for pools in non-perennial rivers. The chapter discusses the data collection and data analysis methods, followed by the results and a discussion of the major findings.

Chapter Six presents the general conclusions stemming from this study. It also answers the research questions and provides recommendations for future studies.

UNIVERSITY of the
WESTERN CAPE

http://etd.uwc.ac.za/

2. LITERATURE REVIEW

2.1 Introduction

The significance of non-perennial rivers and pools is well-documented, but few studies have examined the dynamics of these systems. This chapter will discuss the importance of pools and non-perennial rivers as a freshwater resource, in terms of the basic human needs and ecological needs. This will be followed by a review of past studies that used remote sensing to map and monitor surface water resources, and their advantages and limitations will be highlighted. This chapter will conclude with a summary and the knowledge gaps will be identified.

2.2 Non-perennial Rivers and pools

As discussed in Chapter 1, the flows of non-perennial rivers are highly variable and largely support their surrounding environments. However, according to scientist and ecologists, the terminology used for the different types of river flows and rivers is vaguely understood. Terms, such as 'ephemeral', 'temporary', 'intermittent', 'non-perennial', 'seasonal' and 'episodic', tend to confuse readers and researchers (Rossouw et al., 2005).

UNIVERSITY of the
WESTERN CAPE

2.2.1 Definition of Non-perennial Rivers

Several studies have aimed to standardise the definition of river flow regimes in South Africa. Uys & O'Keeffe (1997) described temporary flows as a blanket term for describing all flow regimes that are encountered in the hydrological state, where the flow is temporary. In a later study, Rossouw et al. (2005) described the perenniality of river systems as a quantitative percentage of the amount of water flow within a river channel in a year (Table 2.1). In this case, non-perennial rivers were used as a blanket term to encompass rivers with semi-permanent, ephemeral or episodic flows (Boulten & Suter, 1986; Jacobson et al., 1995). Ollis et al. (2013) described non-perennial rivers as rivers where flow is not continuous throughout the whole year, but pools may occur. To avoid confusion, this study will adopt the definition of Rossouw et al. (2005) and Ollis et al. (2013), who use the term non-perennial rivers to encompass all rivers that have a temporary flow throughout a year.

http://etd.uwc.ac.za/

Table 2.1 Categories of perenniality, as proposed by the study of Rossouw et al. (2005)

Perennial	**Non-perennial**					
	Semi-permanent	**Ephemeral**		**Episodic**		
May cease flow in extreme drought	No flow 1 – 25 %	No flow 26 – 75 %		No flow at least 76 %		
	Flows for at least 9 months			Flows briefly only after a flood event		
		Seasonal	Non-seasonal	Seasonal	Non-seasonal	

2.2.2 Definition of pools

Much like the definition of non-perennial rivers, the definition of pools also seems to be fragmented. Zacharias & Zamparas (2010) described pools as shallow water bodies that vary significantly in their size, shape, depth, as well as the duration of inundation and diversity of organisms. They are often inundated for at least a few months every year (winter/late spring), to allow for the development of aquatic/semi-aquatic vegetation and animal communities. While flow may cease for long periods in non-perennial rivers, some pools may hold water for more than a year, while others remain dry for more than one season, depending on their surrounding climate.

UNIVERSITY of the WESTERN CAPE

A well-documented description of pools was reviewed by Zacharias & Zamparas (2010). A summary of various studies in which the different names, sizes and descriptions of the pools are defined, is shown in Table 2.2. Mediterranean temporary ponds, for example, are varied ecosystems that exist throughout the world, which harbour a significant portion of aquatic biodiversity on a landscape scale. These ponds occur in Mediterranean climates (Rhazi et al., 2011) such as Europe, Australia, Western USA, South Africa and North Africa. For this study, the term ‘pools’ will be used when referring to surface water features.

http://etd.uwc.ac.za/

Table 2.2 Description of the variations of pool definitions throughout the world

Author	Area of study	Definition	Description/ characteristics	Size
Frazier & Page (2000)	Southern Murray-Darling Basin, Australia	Small pools	Small water bodies on floodplains/closed depressions in swales and backswamps	50 – 32 000 m^2
Buddemeier et al., (2002)	USA	Ponds	Small natural/artificial water bodies distinct from other water features such as lakes, reservoirs and large impoundments	600 – 900 m^2 and often as small as ≥25 m^2
Smith et al., (2002)	USA	Small water bodies	Loosely defined as having a surface water area approximately <10^4 m^2	<10 000 m^2
Lacaux et al., (2007)	Senegal, West Africa	Ponds	Small irregular shaped natural surface water bodies	1 000 – 20 000 m^2
Soti et al., (2009)	Senegal, West Africa	Small ponds	Isolated natural surface water bodies varying in size	<2 600 m^2
Zacharias & Zamparas (2010)	Europe, Australia, Western USA, South Africa, North Africa	Mediterranean temporary ponds	Shallow water bodies flooded in winter/end of spring for sufficiently long periods to allow for the development of vegetation and animal communities	<1 m^2 to several hectares
Rhazi et al., (2011)	Benslimane, Western Morocco	Pools/Mediterranean temporary ponds	Small shallow surface water bodies in Mediterranean climates	≥3 600 m^2
Ogilvie et al., (2018)	Tunisia	Small water bodies	Small reservoirs	10 000 m^2 – 100 000 m^2

UNIVERSITY of the WESTERN CAPE

http://etd.uwc.ac.za/

2.2.3 Monitoring surface water availability in rivers

Dam construction, river water abstractions, return flows and pollutants result in rivers being unable to support their surrounding ecosystems (Poff et al., 1997; Acreman & Dunbar, 2004; King et al., 2008). While these effects occur, they are often left unchecked, due to limited or poor monitoring strategies. Monitoring the surface water availability is essential for water resources management and achieving sustainable development. The traditional methods for monitoring surface water availability through river gauging stations are not always feasible, as they are costly and time consuming procedures. Remote sensing is a fast growing alterative for surface water monitoring. Remote sensing techniques provide a reduced time consuming and lower cost alternative to monitor surface water changes throughout entire river channels (Rahman & Di, 2017).

2.3 Development of Remote Sensing

Remote sensing is widely applied for monitoring changes in the land surface. Before the first Landsat satellite was launched in 1972, aerial photographs were captured on board low orbiting aircrafts, to map the spatial distribution of land cover types (Bakker et al., 2009). This provided accurate information to forest managers, ecologists, soil scientists, geologists and hydrologists. Aerial photography provides high spatial resolution data, but at the cost of low temporal frequency, with images being updated once every few years and only a limited spectral range being captured.

UNIVERSITY of the
WESTERN CAPE

Satellite imagery has advanced much further to provide continuous, accurate and reliable information on land surface and atmospheric changes, with high spatial, spectral and temporal frequencies. Explorer 6, which was launched by NASA in 1959, captured the first space photograph of the earth. Since then, many satellites have been launched for earth observations (Aggarwal, 2004). Sea surface temperature monitoring was achieved by using the Advanced Very High Resolution Radiometer (AVHRR). Ocean and land biomass can be successfully estimated by using the OrbView-2, and land cover monitoring is often mapped by using a range of freely available multispectral satellite images (Bakker, 2009). For example, Karimi & Bastiaansen (2015) did an extensive review highlighting the use of remotely-sensing for estimating evapotranspiration (ET), precipitation and land use. However, remote sensing has also extended into the field of estimating soil moisture content and surface water availability.

http://etd.uwc.ac.za/

2.4 Applications of Remote Sensing in Hydrology

2.4.1 Evapotranspiration and precipitation

Estimating actual ET through ground-based measurements is extremely difficult (Karimi & Bastiaansen, 2015). The quantification of ET rates is important for modelling climate change, hydrological processes and assessing environmental stresses on ecosystems (Kustas & Norman, 1996). Remote sensing techniques can provide spatially-distributed daily estimates of actual ET, making it possible to account for water loss through evaporation. Satellite sensors, such as the Advanced Very High Resolution Radiometer (AVHRR), Moderate Resolution Imaging Spectrometer (MODIS), Advanced Space borne Thermal Emission and Reflection Radiometer (ASTER) and Landsat, are able to estimate surface temperature over vast spatial scales with relatively high accuracies, to aid in ET estimations (Karimi & Bastiaansen, 2015).

Rain gauges still provide the main source of rainfall data, but in many countries rain gauge networks are inadequate and unable to provide data for producing reliable rainfall maps. Satellite-derived rainfall estimates assist in monitoring near real-time rainfall observations, to provide more spatially distributed estimates (Toté et al., 2015). Satellite sensors and datasets, such as Meteosat-8, Geostationary Operational Environmental Satellite (GOES), Special Sensor Microwave Imager (SSM/I), Tropical Rainfall Measuring Mission (TRMM), Advanced Microwave Sounding Unit (AMSU) and the Climate Hazards Group Infra-Red Precipitation with Stations (CHIRPS), are widely used to estimate precipitation (Toté et al., 2015).

UNIVERSITY of the
WESTERN CAPE

2.4.2 Soil moisture

Soil moisture plays a significant role in the hydrological cycle, as soil is an intermediate interface between the atmosphere, lithosphere, biosphere and hydrosphere (White, 2006; Moller, 2014). Soil moisture is responsible for controlling the rate and amount of precipitation infiltrating into the soil, as well as for the recharge into aquifers (Bronsert & Plate, 1997; Moller, 2014). Remote sensing techniques have been widely investigated to provide soil moisture data over a wider spatial scale than conventional ground-based methods (Moller, 2014). Microwave remote sensing techniques, for example, have been investigated since the 1970's and are particularly advantageous, because they can be used in all weather conditions, day or night, and can provide a direct measure of soil moisture content

http://etd.uwc.ac.za/

(Mekonnen, 2009; Moller, 2014). For example, Wang et al. (2007) developed a soil moisture estimation algorithm, using NDVI and Land Surface Temperature products from MODIS, and discovered a strong correlation between the two products, making it possible to generate soil moisture estimates at a moderate spatial resolution.

2.4.3 Water quality

The quality of water is a fundamental factor to take into account for water resources management. Contaminants degrade the waters' quality, causing environmental and human health problems (Liu et al., 2003). The Earth Observing One (EO-1), which was launched, in November 2000 by NASA, was designed as a technical demonstration for land applications, but showed promising use for monitoring water quality because of its on-board Hyperion Imaging Spectrometer sensor (Bakker et al., 2009). Brando & Dekker (2003) pioneered the use of Hyperion imagery to map coloured dissolved organic matter, chlorophyll, and total suspended matter simultaneously in estuarine and coastal water systems. Other satellite sensors, such as the AVHRR have shown promising results in monitoring inorganic sediment particles, phytoplankton pigments, dissolved organic material and turbidity (Liu et al., 2003).

2.4.4 Groundwater

Understanding the patterns and magnitude of groundwater-surface water interactions is also an important concept for water resources management (Fleckenstein et al., 2003a; Meijerink et al., 2007; Webb et al., 2008). Traditional methods, such as geochemical sampling and seepage measurements, are still the primary approaches for studying groundwater-surface water interactions (Liu et al., 2016), although temperature is also a robust tracer for groundwater-surface water interaction. This is due to the groundwater temperatures being relatively constant, while the surface water temperatures are more variable and depend on the local air temperature (Meijerink et al., 2007). One study by Liu et al. (2016) explored the Thermal Airborne Spectrographic Imager (TASI) to evaluate groundwater-surface water interaction. TASI datasets were compared with historic geochemical sampling data in the Heihe River, China and showed promising results as a fast alternative estimation tool for providing a better insight into groundwater-surface water interactions. Therefore, the use of remote sensing to assess temperature serves as a convenient and fast tool for obtaining general information regarding the groundwater-surface water interaction, but it cannot yet replace the traditional ground-based methods.

UNIVERSITY of the WESTERN CAPE
http://etd.uwc.ac.za/

2.4.5 Surface water

Remote sensing has been extensively used for mapping inland surface water bodies. Although the visual interpretation of satellite data still provides the best delineation of surface water, the approach is exceedingly time-consuming, especially with higher resolution images (Mishra & Prasad, 2015). Semi-automatic image processing methods have been developed to extract the surface water from satellite datasets. These methods are commonly grouped into three categories. The first category involves the single-band threshold methods, which makes use of the spectral values of single bands by applying a threshold value to discriminate water from non-water features (Sawunyama et al., 2006; Jiang et al., 2014; Feyisa et al., 2014; Rokni et al., 2014). This is possible because surface water has different spectral properties to other surfaces and can be identified, based on its reflected characteristics. For example, Near Infrared (NIR) is strongly absorbed by water, giving water an almost black colour in NIR images, and it provides a clear distinction between water and non-water features (Verdin, 1996; Soti et al., 2009). However, single band threshold methods often misclassify shadows, urban areas and other background features that have similar reflectance properties as water (Soti et al., 2009; Jiang et al., 2014; Du et al., 2016).

The second category involves the use of machine-learning classification techniques to identify water from multispectral imagery (Jiang et al., 2014). These techniques are found to be more accurate in surface water classification than single band approaches (Rokni et al., 2014; Jiang et al., 2014; Mishra & Prasad, 2015; Sisay, 2016). For example, supervised classification uses a set of training samples to gather reflectance values and to categorise pixels into groups (Rokni et al., 2014). However, these approaches have two major disadvantages. Firstly, the acquisition of training datasets often requires costly and time-consuming field reconnaissance visits. Secondly, if the training datasets incorporate two different features that have the same spectral values, the classified image will group those two features into the same category, causing misclassifications (Mishra & Prasad, 2015).

The third category consists of multiband methods, also called water index methods. These methods combine a number of spectral bands that use mathematical models to enhance water features, while simultaneously restricting or eliminating surrounding features (Jiang et al., 2014; Sisay, 2016). Multiband methods are widely used and constantly improving, with the new technologies and satellites that are being launched (Jiang et al., 2014; Rokni et al., 2014). Much like single band methods, multiband methods apply a threshold value to discriminate

UNIVERSITY of the WESTERN CAPE
http://etd.uwc.ac.za/

water from the background features. Multiband methods include more than one spectral band. This minimises the potential for two features, which share similar spectral responses, to be classified in the same category. The threshold value may vary, depending on the region of study, as well as the method applied (Fisher et al., 2016).

2.5 Multiband Methods

Among all multiband methods for surface water classification, the most well-known is the Normalised Difference Water Index (NDWI) by Mcfeeters (1996). The NDWI makes use of two spectral bands, the NIR and Green bands, which, when applied, suppress the presence of vegetation and land, while enhancing water features. However, the NDWI has been shown to misclassify built up areas as water. Xu (2006) developed the Modified NDWI (MNDWI), which takes advantage of the Mid-Infrared (MIR)/Shortwave Infrared (SWIR) bands, to suppress the reflectance of built-up features, while still enhancing surface water features.

Since then, the accuracy of surface water mapping has improved, with the advancements of multiband methods. Recently, Feyisa et al. (2014) attempted to develop a multiband method that not only eliminates the misclassification from built-up areas, but also from shadows. This because to shadow pixels also share similar spectral properties to water. The Automated Water Extraction Indices for shadow ($AWEI_{sh}$) and non-shadow ($AWEI_{nsh}$) regions were developed to improve the accuracy of surface water mapping by automatically suppressing background noise from shadow and non-water dark surfaces. Using a larger number of spectral bands than the NDWI and MNDWI, the $AWEI_{sh}$ and $AWEI_{nsh}$ were tested for their robustness, under different environmental conditions, to evaluate their accuracy. By using Landsat 5 datasets, Feyisa et al. (2014) compared the $AWEI_{sh}$, $AWEI_{nsh}$, MNDWI and the machine-learning Maximum Likelihood Classification (ML) methods in different areas of the world. The AWEI had the most promising results across all the regions of interests.

UNIVERSITY of the
WESTERN CAPE

2.5.1 Application of multiband methods on a global scale

Remotely-sensed datasets, such as MODIS provide oceanic and inland surface water monitoring on a global scale and at a daily rate. However, mapping surface water on a global scale is challenging because of the turbidity levels and surrounding features, and so multiband methods are often more suited for local and regional scale assessments. Nevertheless, Sharma et al. (2015) developed a robust Superfine Water Index (SWI) for mapping surface water on a global scale, using MODIS, and compared it to other widely-used

http://etd.uwc.ac.za/

multiband methods. The study showed that the performance of the water indices varied with different land cover types. Ultimately, the SWI explained 88 – 97% of the surface water variation in different land cover types, while the NDWI explained 58 – 81% of the surface water variation.

2.5.2 Application of multiband methods on a local scale

MODIS has very coarse spatial resolution and is not always suitable for monitoring surface water at local or regional scale. Multiband methods applied to Landsat datasets have been widely applied for surface water mapping and monitoring at local and regional scales. For example, Xu (2006) compared the accuracies of the NDWI and MNDWI for mapping the boundaries of the Bayi Reservoir and the Min River in China by using Landsat ETM+ data. The MNDWI achieved an accuracy of greater than 99% in both regions, while maintaining a default threshold value of zero.

Other studies have also attempted to compare the accuracy of multiband methods, by primarily using Landsat datasets. For example, Jiang et al. (2014) compared the accuracy of the NDWI, MNDWI, $AWEI_{sh}$ and $AWEI_{nsh}$ in mapping surface water throughout China, and it was found that the MNDWI and $AWEI_{sh}$ outperformed the NDWI. However, the accuracies tended to vary, depending on the multiband method applied and the area of study. Effects, such as mixed pixels and the confusion of water bodies with background noise, all depend on the dataset used and the method applied (Jiang et al., 2014). Fisher et al. (2016) also compared a range of multiband methods over different water and spectrally similar non-water land cover types, in eastern Australia. Their results suggested that the MNDWI is the most suitable for extracting the largest range of surface water bodies that have varying spectral properties, with a relatively high accuracy.

A more extensive study was undertaken by Zhou et al. (2017), who compared nine multiband methods across three sensors, namely the Landsat ETM+, Landsat OLI and the Sentinel-2 MSI, in the Poyang Lake Basin, China. All the multiband methods had reasonable overall accuracies ranging from 88 – 95%. However, the results suggested that the Landsat 8-OLI and Sentinel-2 MSI sensors were the most promising datasets and the NDWI and NDWIplusVI classification methods shared the same highest overall accuracy of 95%.

UNIVERSITY of the WESTERN CAPE
http://etd.uwc.ac.za/

2.5.3 Application of multiband methods for mapping small water bodies

Limited studies have explored the potential of monitoring non-perennial rivers and pools, using remote sensing. Haas et al. (2009) assessed the accuracy of mapping temporary small water bodies in the arid, semi-arid and sub-humid regions of sub-Saharan western Africa, using the SPOT VEGETATION (SPOT-VGT) instrument. SPOT-VGT has an automatic surface water body identification tool called Maximum Value Composites (MVC) (CNES, 1999), which identifies water and humid vegetation. Haas et al. (2009) showed the potential of mapping temporary small water bodies in arid and semi-arid regions. However, this simple image classification does not provide sufficient results, because the spectral signatures vary with the ecological conditions, and with a 10-day return period, high costs, and limited number of spectral bands, the SPOT-VGT sensor is not a feasible sensor.

Other studies have compared a range of multiband methods and various Earth Observation System (EOS) sensors for mapping ponds. For example, Soti et al. (2009) compared the accuracy of the MNDWI, NDWI1, NDWI2 and NDVI on the Quickbird, SPOT, MODIS and Landsat ETM+ datasets. The study involved collecting Global Positioning System (GPS) coordinates of 30 ponds for validation, and additional GPS coordinates of the non-water reference sites. Ponds as small as 1 100 m^2 were identified when using Landsat datasets. Landsat was preferable because of its higher resolution over MODIS, as well as its free availability. Jones et al. (2017) compared the accuracy of mapping reservoirs, using the NDWI, MNDWI1 and MNDWI2 on Landsat datasets to a global surface water datasets called the Global Surface Water Monthly Water History (GSW). Over 272 reservoirs were mapped, ranging from 900 m^2 – 720 000 m^2, and it was found that reservoirs mapped with the GSW were 19 % less accurate than those mapped with Landsat.

UNIVERSITY of the
WESTERN CAPE

2.5.4 Image classification accuracy

An accuracy assessment is a fundamental component in image classification, as this illustrates the validity and accuracy of a classified image, and it is often presented in the form of a confusion matrix, also called an error matrix or contingency table (Congalton et al., 1983). A confusion matrix provides unbiased information concerning the entire study area, in order to derive unbiased summary statistics on a classified image (Pontius & Millones, 2011). The overall accuracy, the error of omission, the error of commission, the producers' accuracy, the users' accuracy and the Kappa coefficient are all calculated from the matrix.

http://etd.uwc.ac.za/

The overall accuracy expresses the proportionality of correct classification in a map, based on reference sites (Brovelli et al., 2015). The error of omission refers to the reference sites omitted from the correct class in a classified map, to evaluate the accuracy for each class. The error of commission is in relation to the classified results, and it occurs when the classification method assigns pixels to a certain class that does not belong to it. The producers' accuracy is a mathematical result of the probability that a particular land cover type of an area on the ground is classified correctly. The users' accuracy illustrates the probability that the class on the map will be present on the ground i.e. reliability. The Kappa coefficient evaluates the degree to which a classification method has performed, compared to randomly assigning values i.e. was the classification technique more optimal than random pixel classification (Pontius & Millones, 2011).

However, the Kappa coefficient does not reveal information that is different from the overall accuracy, users' accuracy and producers' accuracy that aids in practical decision-making (Pontius & Millones, 2011). The Kappa coefficient often gives misleading and redundant information, while it is also complicated to compute, difficult to understand and its interpretations unhelpful. This led Pontius & Millones (2011) to develop an approach that focuses on the quantity and spatial allocation of disagreement between the classes in a map. The quantity disagreement calculates the difference between the reference map and classified map, due to a less than perfect match in the proportions of the classes. The allocation disagreement calculates the difference between the reference map and classified map, due to the less than optimal match in the spatial allocation of the classes. This allows the analyst to better understand the reasons for disagreement, based on the information in the matrix, and it presents the results in a more interpretable manner.

UNIVERSITY of the
WESTERN CAPE

2.5.5 Effects of shadows in surface water classification

In mountainous regions, or rough terrain, the topography has a strong influence on the recorded signals of space-borne optical sensors (Richter et al., 2009). Shadows pose a difficult problem in terms of image classification (Riaño et al., 2003; Zhou et al., 2014). They often become misclassified as false positive water pixels (Martha et al., 2010; Yamazaki et al., 2015), as they share similar spectral responses to water pixels.

A hillshade can be an optimal detector of the topography of shadow regions, without affecting the spatial and spectral properties of an image. A hillshade is a hypothetical image that is created from a DEM to identify shadow regions by using the sun's position (azimuth

http://etd.uwc.ac.za/

and zenith) at the time of the acquisition of the multispectral image (Martha et al., 2010). A hillshade is considered to be more reliable for shadow masking, since other potential sources of low brightness/similar reflectance, such as water, are avoided, ultimately improving the accuracy of the image (Martha et al., 2010; Yamazaki et al., 2015).

2.6 Image Pre-processing

2.6.1 Atmospheric correction

Gases and aerosols that are suspended in the atmosphere absorb, refract and scatter the electromagnetic radiation coming to earth's surface. These gases influence the radiation that is reflected from a target, by reducing the effect of the radiation. This process changes the properties that the sensor records (Gilabert et al., 1994; Chavez, 1996). Several mathematical procedures to correct for the atmospheric effects on satellite imagery have been developed. Above all, the simplest and most widely-used technique is the Dark Object Subtraction (DOS) procedure (Chavez, 1988; Song et al., 2001; Nguyen et al., 2015). DOS removes the haze or scattering effects caused by gases and aerosols, by assuming the existence of dark objects throughout an entire scene (image) with a value of zero and a horizontally homogenous atmosphere. The minimum Digital Number (DN) value in that scene is then attributed to the atmospheric effects and is subtracted from all of the pixels in that scene (Chavez, 1996).

UNIVERSITY of the
WESTERN CAPE

Over the years, more advanced atmospheric correction algorithms have been developed to further minimise the atmospheric effects on satellite images. Song et al. (2001) reviewed eight atmospheric correction techniques, using Landsat datasets, to assess their accuracies on image classification and change detection. The study found that recent and complicated atmospheric correction methods did not always lead to improved results. The simpler atmospheric correction methods, such as the Dark Object Subtraction 1 (DOS1) achieved accurate results when correcting for atmospheric effects. This was also shown in a study by Liang et al. (2001), in which the DOS atmospheric correction actually led to more accurate image classification and change detection products than other methods.

When mapping vegetation cover, several studies compared different atmospheric correction methods prior to image classification. Nguyen et al. (2015) compared the accuracy of DOS, the Fast Line-of-sight Atmospheric Analysis of Spectral Hypercubes (FLAASH), the Second Simulation of Satellite Signal in the Solar Spectrum (6S) and Top-Of-Atmosphere (TOA)

http://etd.uwc.ac.za/

reflectance imagery to estimate the Aboveground Biomass (AGB) in South Korean forests. The study found that the 6S atmospheric correction method and TOA reflectance products that were used prior to the image classification, outperformed all other atmospheric correction methods. Martins et al. (2017) compared the 6S, ACOLITE and the Sen2Cor processor on Sentinel-2 datasets, prior to classifying the Amazon floodplain Lakes in Brazil. After atmospheric correction, the results mimicked the in-situ measurements across the lakes and, Sen2Cor products showed the smallest Root Mean Square Error (RMSE), when compared to in-situ measurements. However, the results varied based on the classification method.

Despite several studies applying atmospheric correction for surface water classification and change detection (Feyisa et al., 2014; Rokni et al., 2015; Zhou et al., 2017; Masocha et al., 2018; Wang et al., 2018), they neglected to assess which atmospheric technique was best, and except in some cases, whether a TOA reflectance image was also evaluated for its accuracy in image classification. Li et al. (2013), Fisher et al. (2016) and Acharya et al. (2016) compared the accuracy of multiple classification methods by using TOA reflectance datasets from Landsat. All studies showed high accuracies in the surface water classification when using only Landsat TOA reflectance datasets, which indicates that no pre-processing may be required prior to image classification.

UNIVERSITY of the
WESTERN CAPE

2.7 Change Detection and Time Series Analysis

Timely surface water monitoring is needed to provide an insight into the surface water availability. Multi-period remote sensing datasets provide more information on surface water changes than single date satellite observations and historical maps. For example, Rokni et al. (2014) and Sarp & Ozcelik (2017) estimated the declining trends in the surface area, when using multi-date Landsat imagery in Iran and Turkey, respectively. Buddemeier et al. (2002) analysed the identification and distribution of artificial ponds in the USA to illustrate how pond development increased from 1930 to 2000.

Several studies have attempted to develop large datasets, in order to describe the changes of surface water availability around the world. Pekel et al. (2016) quantified global surface water changes from 1984 – 2015, using Landsat. The frequency of water presence was captured in a single product named Surface Water Occurrence (SWO), which estimated global surface water availability over a period of 31 years. Another study by Meuller et al. (2016) developed the Water Observations from Space (WOfS) public package to monitor the

http://etd.uwc.ac.za/

behaviour of surface water across the Australian continent, using Landsat from 1987 – 2014. The study found that a majority of the errors and misclassifications occurred along rivers, small surface water bodies and swamps, where water and vegetation was not distinctive and often caused mixed pixels.

2.7.1 Hydroperiod of pools in non-perennial rivers

Rivers are often classified, based on their hydrological flow regime. However, non-perennial rivers rarely flow, while pools are more common. Typically, for inland water systems that are not rivers, it is more suited to classify them according to their hydroperiod (Ollis et al., 2013). The hydrogeomorphic units of a river channel, such as the low flow channels, can also be categorised according to their hydroperiod (Montgomery et al., 2018). The hydroperiod of an open water body is the period of inundation or saturation for a given period of time (Ollis et al., 2013) i.e. the length of time that there is standing water at a location. By describing the hydroperiod of open water pools in non-perennial rivers, a deeper understanding of their physical characteristics, such as their occurrence and recurrence, can be established.

A hydroperiod of a water body is often classified into different classes. These classes have been modified over the years, but all follow a similar structure. Montgomery et al. (2018) modified a marsh hydroperiod classification system from Stewart & Kantrud (1971), which consisted of five classes, namely, an ephemeral pond (Class I), a temporary pond (Class II), a seasonal pond or lake (Class III), a semi-permanent pond or lake (Class IV) and a permanent pond or lake (Class V). Class I describes highly variable surface water that is only present for a brief period of time and has little associated ecological monetary value. Class II describes temporary ponds that are usually only present after rainfall or snowmelt. Class III describes seasonal surface water that is only present during the rainfall season. Class IV describes semi-permanent surface water that is present for most of the year, and Class V describes permanent water bodies. However, the modified hydroperiod classification system by Montgomery et al. (2018) excluded Class I, because ephemeral ponds have little ecological value, while Class IV and V were combined as a period of three years, which is too short to show the certainty of permanent surface water.

The modified hydroperiod classification system is shown in Table 2.3, where Class I has been removed, and Class IV and V were combined to describe semi-permanent and permanent open water bodies. The study detailed a framework for a new time-series classification approach, based on hydroperiod and hydro-climatic conditions. With overall accuracies

UNIVERSITY of the WESTERN CAPE
http://etd.uwc.ac.za/

ranging from 89 – 95%, the results suggest that remotely-sensed datasets can be used to determine the hydroperiod and permanence of surface water bodies.

Table 2.3 Modified wetland hydroperiod classification for pools in non-perennial rivers, based on Stewart & Kantrud (1971) and Montgomery et al. (2018)

Type	Duration	Description
Temporary (Class II)	1 – 2 months	Water present for short time after snowmelt or rainfall.
Seasonal (Class III)	3 – 4 months	Water present throughout growing season, dry by end of summer.
Semi-permanent/permanent (Class IV and V)	5 + months	Water present for most/all year round, except in drought conditions.

2.8 Summary

The significance of non-perennial rivers is well-documented. However, the monitoring of non-perennial rivers is limited. Therefore, water resources management strategies cannot be effectively implemented. Remote sensing, using optical satellite datasets, has emerged as an alternative approach to monitor surface water availability, as opposed to traditional timely and costly field methods. However, no study has managed to determine the most suitable image pre-processing and classification technique for monitoring surface water availability in non-perennial rivers, more specifically, pool dynamics. This has made water resources management in these environments very difficult, if not complex.

Though some studies have highlighted that atmospheric correction is not a necessary step, other studies have documented its importance. This creates confusion about when it is most appropriate to correct for atmospheric effects, prior to image classification. Literature has also shown that the use of multiband methods provides a fast, reliable semi-automatic approach to identify surface water, but it does not specify which method is more suitable over the other.

The use of Landsat for surface water classification and change detection is still widely applied. For example, Pekel et al. (2016) and Meuller et al. (2016) have developed large datasets of optical multispectral imagery for surface water monitoring. However, these

UNIVERSITY of the WESTERN CAPE
http://etd.uwc.ac.za/

studies have not shown the potential of monitoring non-perennial rivers. With the launch of the Sentinel-2 MSI satellite, there is new potential for monitoring smaller water bodies with more frequent intervals. Ultimately, methods investigating remote sensing for monitoring surface water availability in non-perennial rivers, located in semi-arid to arid regions, has not been widely addressed. Therefore, this study aims at addressing these gaps in knowledge that have been highlighted above.

http://etd.uwc.ac.za/

3. DESCRIPTION OF THE STUDY AREA

3.1 Introduction

This study assessed a suitable remote sensing image classification system to identify surface water along non-perennial rivers throughout the Western Cape Province. The Western Cape is situated on the south-western region of South Africa where the majority of rivers are non-perennial. For this purpose, four separate rivers in the Western Cape were assessed in four different drainage regions. A regional description of the Western Cape will be discussed, followed by a brief description of the selected study sites.

3.2 Regional Description of the Western Cape

3.2.1 Climate

Situated along the southern west coast of South Africa (Figure 3.1), the Western Cape covers an estimated area of 129 462 km^2, and it has a distinctive climate and geological structure. The province is described as being biophysically unique, when compared to the rest of southern Africa (Pasquini et al., 2013). This is attributed to the Western Cape having an almost Mediterranean-type climate, with warm-dry summers and cool-wet winters. The Western Cape has three dominant rainfall zones, namely winter, late summer and year-round rainfall regimes, as well as the highest rainfall variability in South Africa, with rainfall recorded as low as 60 mm/year and as high as 3 345 mm/year (Provincial Spatial Development Framework, 2005). The average temperatures within the Western Cape are 23 °C in summer and 13 °C in winter.

3.2.2 Land cover

The Western Cape is home to some of the largest biodiversity hotspots. Three main biomes are dominant in the Western Cape, namely the Fynbos biome, the Succulent Karoo Biome, and the Nama Karoo Biome (Magoba, 2014). A large portion of land cover within the Western Cape consists of cultivated lands, with small regions of densely cultivated orchards and vineyards. About 43% of land in the Western Cape is used for animal production, 36% for cropland and agriculture, 13% for settlements and infrastructure and 8% for commercial forests, protected areas and other land use types, such as mining (Provincial Spatial Development Framework, 2005).

http://etd.uwc.ac.za/

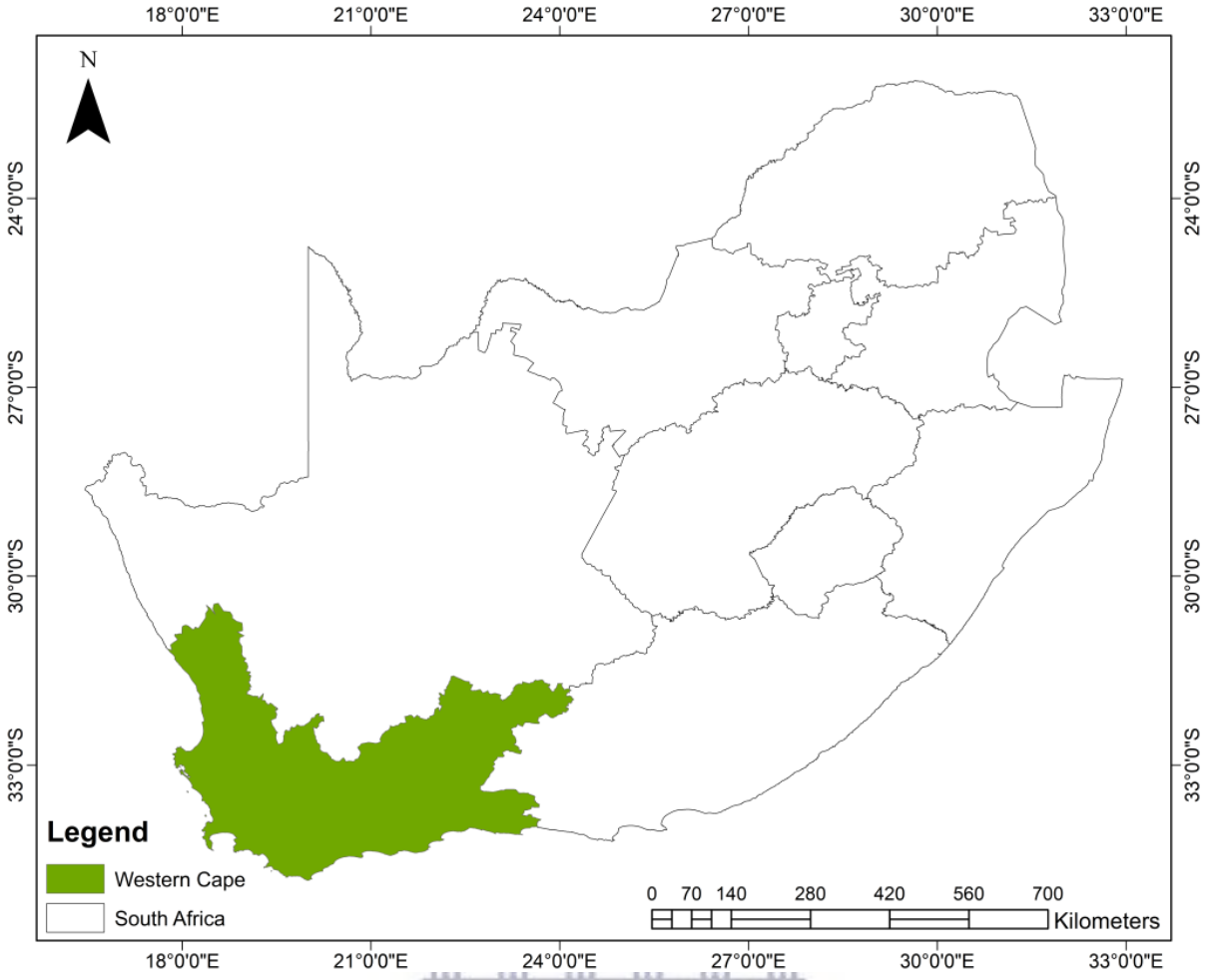

Figure 3.1 Location of the Western Cape regional study area within South Africa

UNIVERSITY of the
WESTERN CAPE

3.2.3 Geology

Many of the Western Cape rock types are comprised of sedimentary rocks that have been formed from materials laid down by wind and erosion. The Western Cape topography ranges from coastal planes, edged with steep cliffs and sandy beaches, over dramatic mountain ranges, enclosing secluded valleys, to the wide cosmic inland plains of the Karoo. The Cape Folded Belt is a prominent feature that is described as an L-shaped band that is comprised of erosion-resistant quartzitic sandstone mountains, alternating with plains and valleys underlain by softer shales, that were formed from lava activity and sedimentation (Provincial Spatial Development Framework, 2005). A detailed illustration of the geology is shown in Figure 3.2.

http://etd.uwc.ac.za/

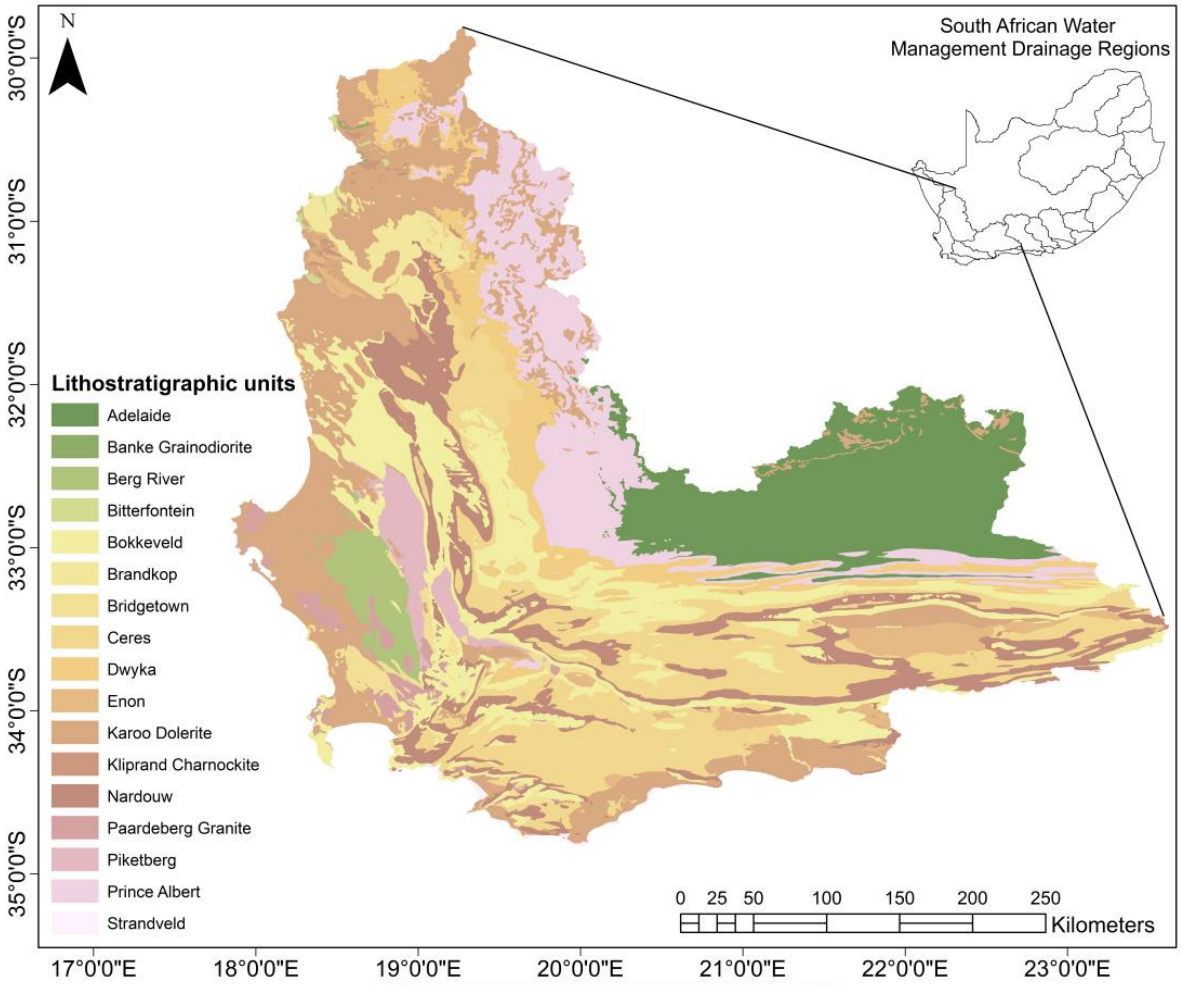

Figure 3.2 Geological lithostratigraphic units of the Western Cape

UNIVERSITY of the
WESTERN CAPE

3.2.4 River systems

River network datasets were obtained from the Department of Water and Sanitations (DWS) Resource Quality Information Services (RQIS), that were developed in April 2016 (http://www.dwaf.gov.za/iwqs/gis_data/river/rivs500k.aspx). The DWS classified river networks are based on their flow regimes, i.e. they are either perennial, non-perennial, dry or unknown (Berhanu et al., 2015; DWS, 2016). Four main drainage regions fall within the Western Cape. Figure 3.3 illustrates the Berg, Breede, Olifants and Gouritz drainage regions. All rivers within the boundaries of these drainage regions are shown in Figure 3.3, which highlights their river class. Non-perennial rivers are primarily found further inland, while the perennial rivers are located nearer the coast. Many non-perennial rivers also seem to be tributaries of the perennial rivers throughout the province (Figure 3.3).

http://etd.uwc.ac.za/

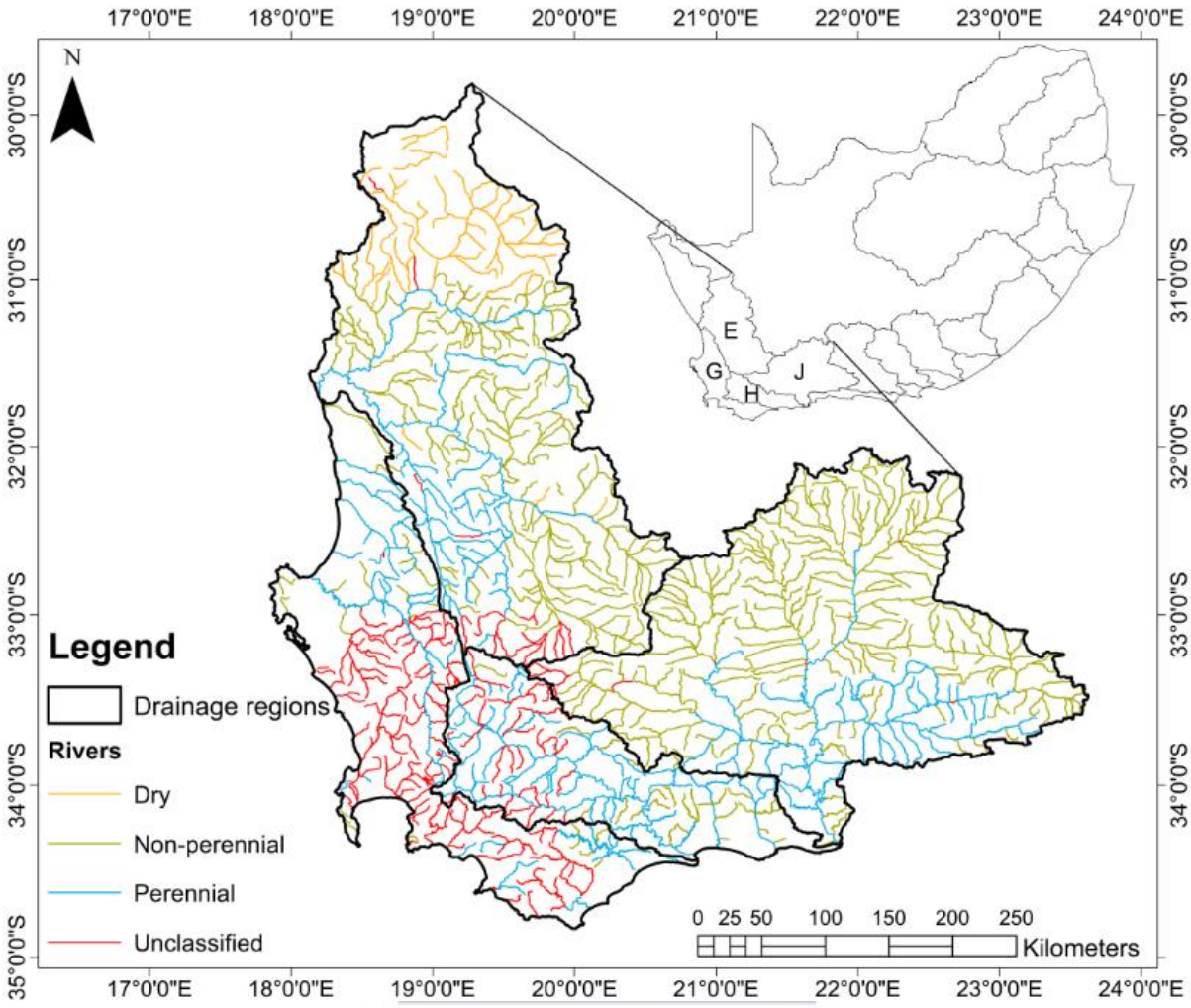

Figure 3.3 River network systems within the Berg (G), Breede (H), Olifants (E) and Gouritz drainage (J) regions. Source: DWS (2016).

UNIVERSITY of the
WESTERN CAPE

3.3 Research Sites

The focus of this study is to explore the use of remote sensing to map and monitor surface water availability along non-perennial rivers within the Western Cape. Therefore, using the river network datasets from RQIS, a few major non-perennial rivers were selected in various regions of the province. This was undertaken to assess the performance of the classification techniques in different land cover zones and to evaluate the use of remote sensing in rivers of different aridity. The rivers selected were the Nuwejaars (Figure 3.4), Breede (Figure 3.6), Touws (Figure 3.8) and the Tankwa Rivers (Figure 3.10).

The Nuwejaars, Touws and Tankwa Rivers are considered to be some of the major non-perennial rivers in the Western Cape Province, while the Breede River is considered to be a major perennial river system. These rivers vary in location, size and aridity. The Nuwejaars

http://etd.uwc.ac.za/

River has a narrow channel width, it is surrounded by riparian vegetation, and it has a seasonal flow regime. The Breede River, although classified as a perennial river, has a more non-perennial flow regime, specifically in the upper parts of the river. The Touws River has a wider channel width than the Nuwejaars River and is situated in a more arid environment. Flow in the Touws River is limited to only a few days a year. The Tankwa River is situated in an extremely arid environment where surface water is present for only a brief period of time.

These rivers were also selected, based on the availability of higher resolution aerial photography and satellite imagery. The higher resolution datasets were used to compare the classified maps of coarser remotely-sensed datasets. Lastly, these rivers are surrounded by extensive agricultural and other socio-economic activities, which highlights the need for the implementation of accurate monitoring. As this study is part of a larger ongoing catchment monitoring project, the results presented here will provide more information on these systems.

3.3.1 The Heuningnes Catchment

The Heuningnes Catchment is situated at the southern-most tip of Africa, along the Agulhas Plain (Figure 3.4). The catchment has an estimated area of 1 938 km^2 (HilLand Associates, 2008). The Agulhas Plain has a unique low gradient topography, resulting in significant wetland development. The topography of the Heuningnes Catchment is described as having a gently rolling, coastal low-land landscape. The catchment experiences a Mediterranean climate with hot dry summers and cold wet winters. It has a mean annual rainfall of 500 mm/year, and temperatures range between 10 ºC in winter and 28 ºC in summer (HilLand Associates, 2008). The dominant geological formations of the catchment include the Table Mountain Group and Bokkeveld Group (Kraaij et al. 2009), with the major rock types being sandstone, quartzite and shale (Bickerton, 1984).

The catchment has various lakes, pans, vleis and wetlands. The two major vleis are the Voelvlëi (estimated 8 km^2) and Soetendalsvlei (estimated 20 km^2). The major river is the Heuningnes River, which feeds into an estuary and drains into the Indian Ocean. The two major tributaries of the Heuningnes River are the Kars River (which is estimated to be 82 km long), and the Nuwejaars River (which is estimated to be 35 km long) which feeds through Voelvlëi, finally draining into Soetendalsvlei.

UNIVERSITY of the WESTERN CAPE
http://etd.uwc.ac.za/

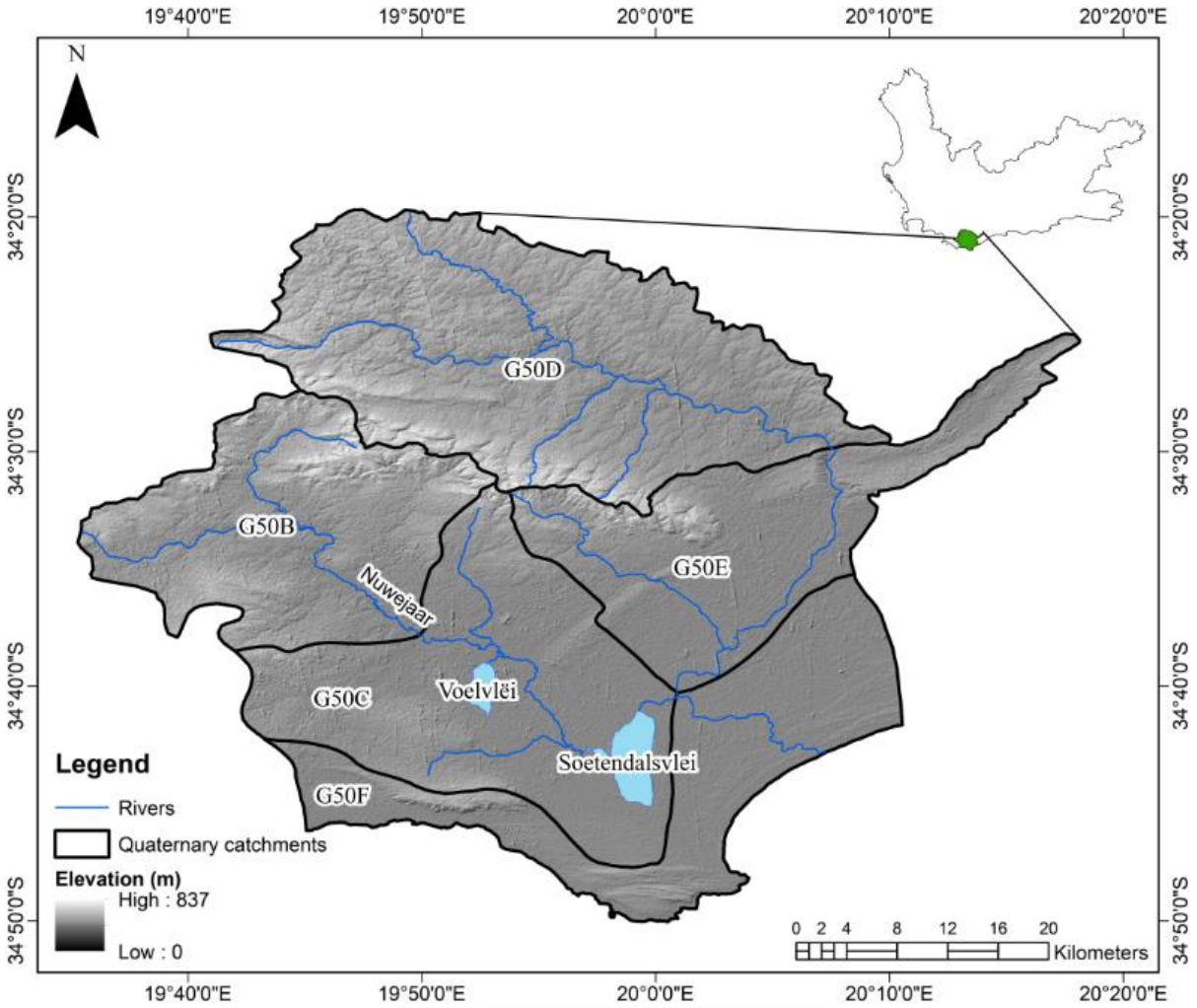

Figure 3.4 Location of the Heuningnes Catchment within the Western Cape, including the rivers and the two major lakes

UNIVERSITY of the WESTERN CAPE

The Heuningnes Catchment has a mean annual precipitation (MAP) of 466 mm/yr and Mean Annual Runoff (MAR) of 26 mm/yr. In this catchment, the rainfall gradually increases from April, reaching a peak between June and September (Figure 3.5). Thereafter, the rainfall decreases from December to March, with the lowest recordings during January and February. The river flows have a similar seasonal pattern to that of the rainfall (Figure 3.5). However, the highest flows tend to occur during the August period. This is because rainfall occurs during the June to July period, generating runoff in the catchment and along the Nuwejaars River. This then fills up the pools along the Nuwejaars River, which would otherwise dry up.

http://etd.uwc.ac.za/

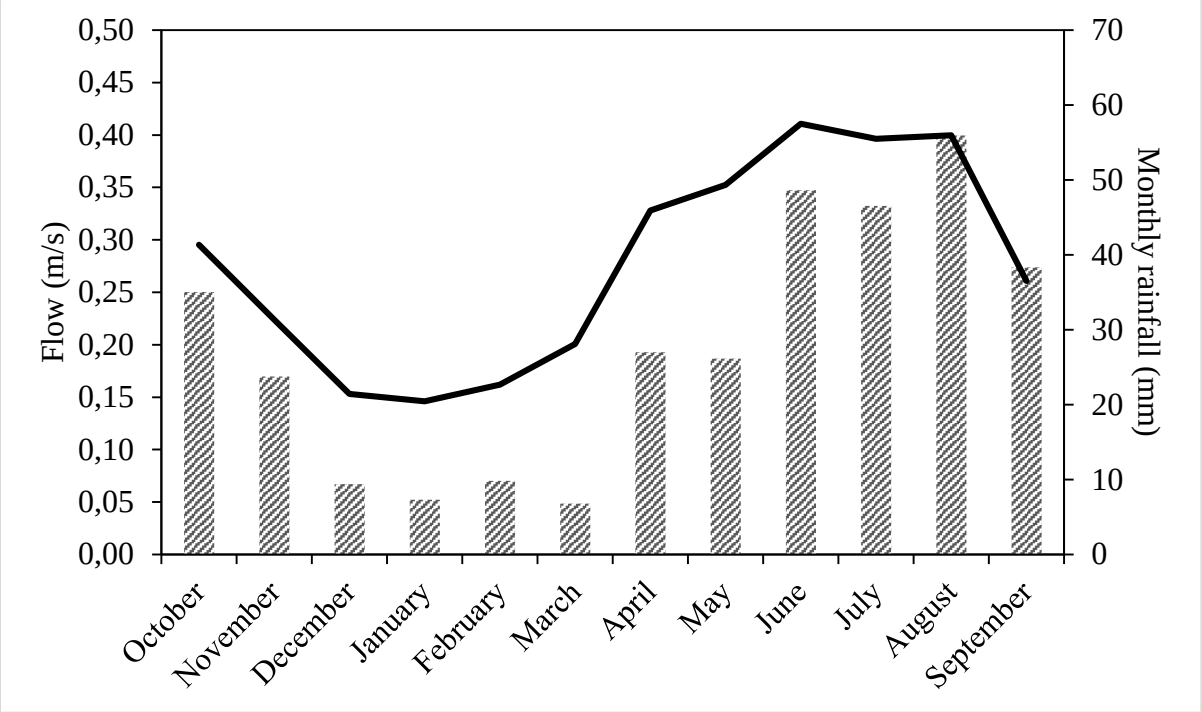

Figure 3.5 Naturalised mean monthly flow (bars) and mean monthly rainfall (line) for the Nuwejaars Catchment having a MAP of 466 mm/yr, and MAR of 26 mm/yr. Source: WR2012

3.3.2 The Breede Catchment

The Breede Catchment is situated between the Berg and Gouritz drainage region and has an estimated area of 12 600 km^2. The Breede River system is one of the large systems in the Cape Floristic Region, and it is associated with the semi-arid Karoo region. The dominant geological formation is the Bokkeveld Group, with the major rock types consisting of sandstone and shale. The region receives about 80% of its precipitation between April and September, and it is brought by mid-latitude cyclones. Being a variable mountainous area, the spatial variation of rainfall ranges from 400 – 2 300 mm/year (Daniels et al., 2006; Steynor et al., 2009). The major river system is the Breede River, which drains the inter-mountain fault basin of the Hex and Langeberg Mountains (Figure 3.6). The river has an estimated length of 313 km and flows through key agricultural regions (Steynor et al., 2009).

http://etd.uwc.ac.za/

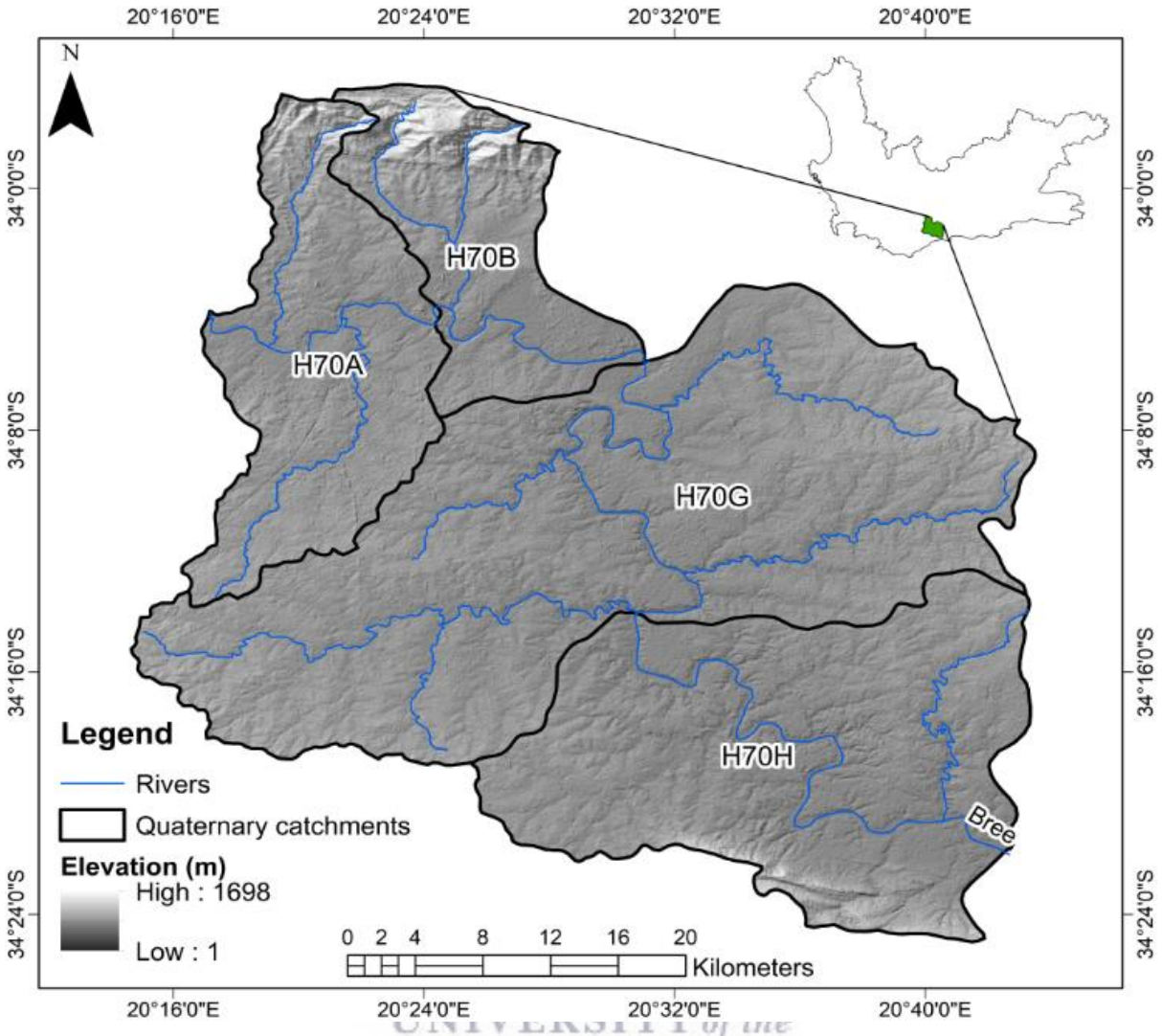

Figure 3.6 Location of the Breede Catchment within the Western Cape and rivers

The Breede Catchment has an MAP of 488 mm/yr and an MAR of 56 mm/yr. In this catchment, rainfall does not follow the same seasonal pattern as the Nuwejaars Catchment. Rainfall gradually increases from February, peaking in April, decreasing in June and then increasing again in August (Figure 3.7). Thereafter, rainfall decreases from November to January, with the lowest recordings during December. The river flows show a seasonal pattern similar to that of the rainfall (Figure 3.7). However, the highest flows tend to occur during the August to November period, peaking in August and September. Despite the rainfall peaking in April, the highest flows are not seen during that period (Figure 3.7). Although the flows decrease during the summer months, they are still relatively high throughout the year, indicating that the pools in the Breede River are filled throughout most of the year.

http://etd.uwc.ac.za/

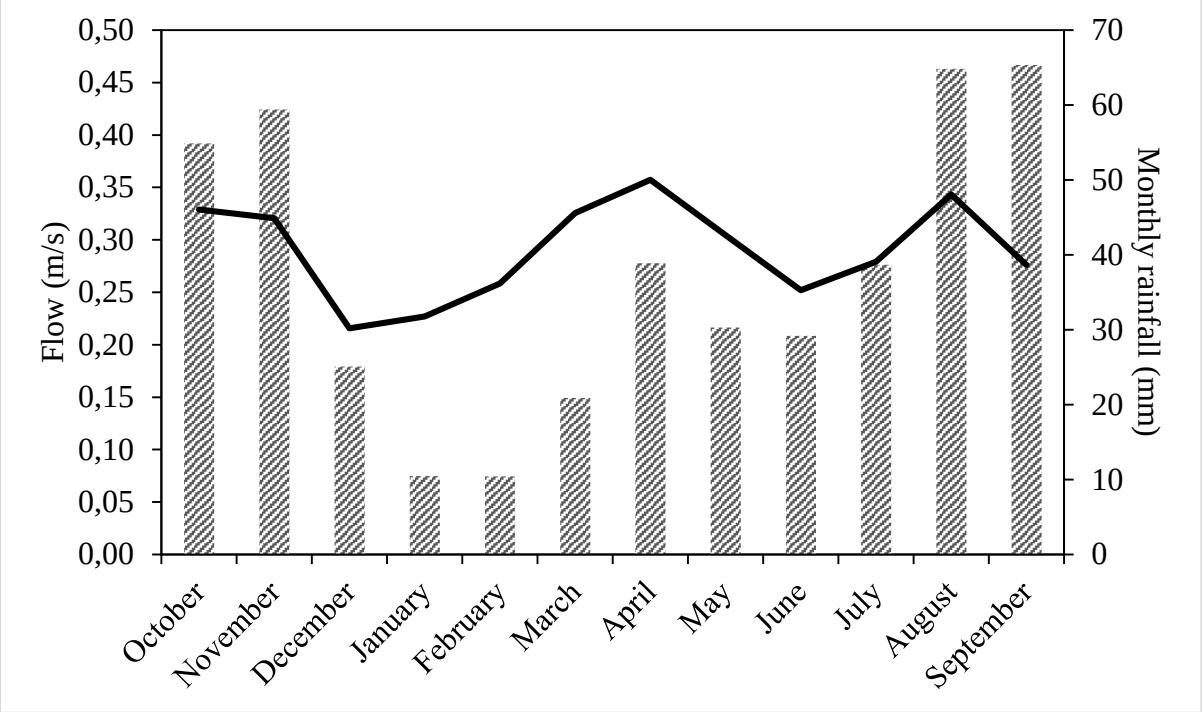

Figure 3.7 Naturalised mean monthly flow (bars) and mean monthly rainfall (line) for the Breede Catchment having a MAP of 488 mm/yr, and MAR of 56 mm/yr. Source: WR2012

3.3.3 The Touws Catchment

The Touws River Catchment is situated in the Gourtiz drainage region, above the Cape Folds Belt. The Touws sub-catchment has an estimated surface area of 2 627 km^2 and lies within the boundaries of the Klein Karoo (Maitre et al., 2009) (Figure 3.8). In the mountainous regions, the rainfall ranges from 900 – 1 400 mm/year. Summer temperatures range from 22 – 25 °C and winters from 18 – 21 °C (Petersen et al., 2017). The area receives a high potential solar radiation throughout the year, resulting in a high evaporation rate (Maitre et al., 2009). The catchment is dominated by the Bokkeveld geological formation, with mainly sandstone and shale rock types. The Touws River is a non-perennial river system with an estimated length of 140 km.

http://etd.uwc.ac.za/

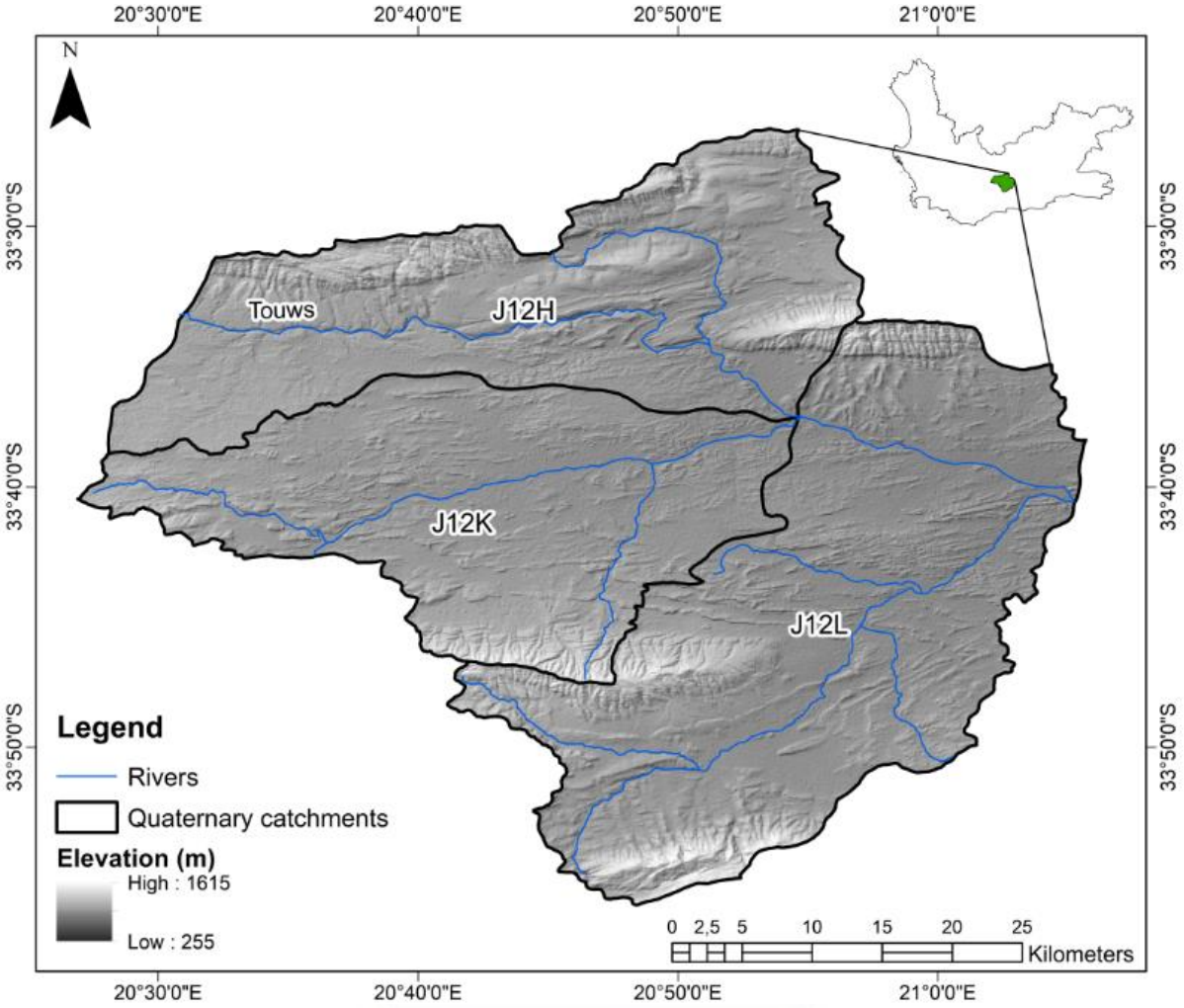

Figure 3.8 Location of the Touws River Catchment within the Western Cape and rivers

UNIVERSITY of the
WESTERN CAPE

The Touws Catchment has a MAP of 256 mm/yr and MAR of 7 mm/yr. In this catchment, rainfall also does not follow the same seasonal pattern as the Nuwejaars Catchment. Rainfall increases minimally from January, peaking in April, and only decreasing in August (Figure 3.9). Thereafter, rainfall decreases between November and January, with the minimal recordings during December. River flows do not show a seasonal pattern for rainfall (Figure 3.9). Flows are relatively constant throughout the year, peaking in April, decreasing in June and July, and then increasing again in August. There are moderate flows during October to February, despite a decrease in the mean monthly rainfall, indicating sporadic rainfall during the summer months (Figure 3.9). The moderately lower flows in the Touws River suggest that pools have little time to fill up and may only fill during, and immediately after, rainfall events.

http://etd.uwc.ac.za/

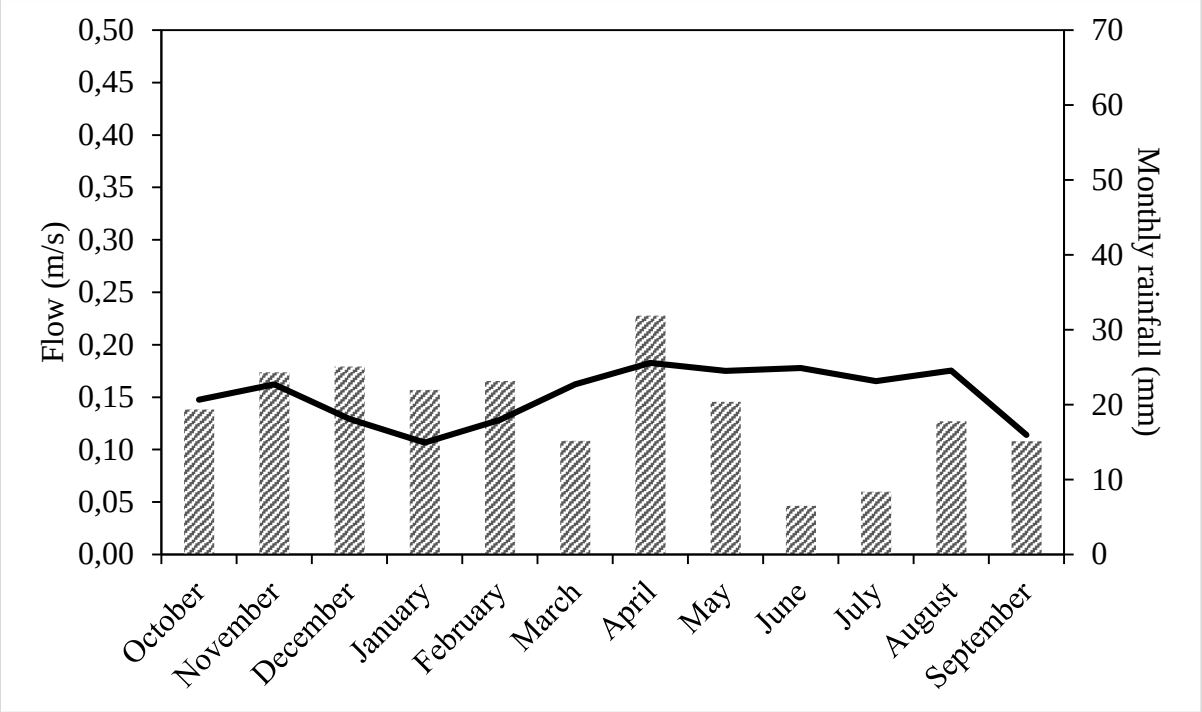

Figure 3.9 Naturalised mean monthly flow (bars) and mean monthly rainfall (line) for the Touws Catchment having a MAP of 256 mm/yr, and MAR of 7 mm/yr. Source: WR2012

3.3.4 The Tankwa Karoo Catchment

The Tankwa Karoo Catchment is situated in the Olifants/Doorn drainage region, and it is partially within the boundaries of the Tankwa Karoo National Park. The sub-catchment falls within the boundaries of the Western Cape and the Northern Cape provinces (Figure 3.10). The sub-catchment has an estimated area of 4 471 km^2. The region experiences a mean rainfall of 500 mm/year, with 25% of the mean annual precipitation falling in summer. The mean minimum winter temperature is 6 °C, while the mean maximum summer temperature is 39 °C (Strauss et al., 2014). The geology of the region consists mainly of Bokkeveld Group shales, Witteberg Group sandstones and quartzite, and sediments of the Karoo Supergroup (Strauss et al., 2014). The main river is the Tankwa River, which has an estimated length of 146 km. The Tankwa River drains into the Oudebaaskraal Dam (Figure 3.10), which attracts more than 100 bird species.

http://etd.uwc.ac.za/

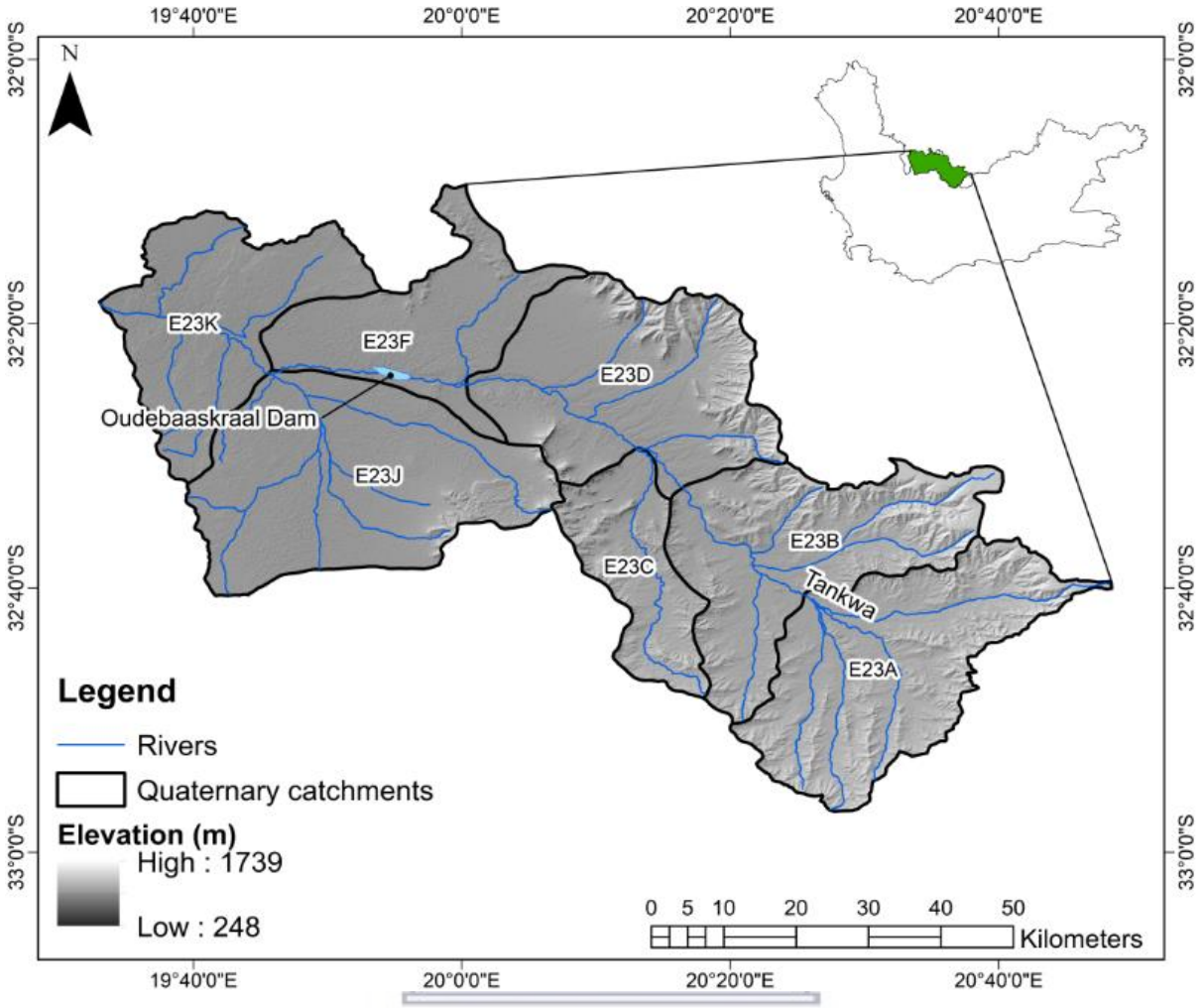

Figure 3.10 Location of Tankwa River Catchment within the Western Cape and rivers

UNIVERSITY of the
WESTERN CAPE

The Tankwa Catchment has a MAP of 189 mm/yr and MAR of 5 mm/yr, which is the lowest of all of the rivers assessed. In this catchment, rainfall follows a broad seasonal pattern. Rainfall increases gradually from February to June, peaking in June, and it decreases significantly from July to January (Figure 3.11). River flows also show a general seasonal pattern to the rainfall (Figure 3.11). Almost no flow is recorded from September to March, and it only starts increasing in April, eventually peaking in June. Flows then decrease in July and follow the same pattern as that of the rainfall for the catchment. The low flows in the Tankwa River Catchment suggest that pools have little time to fill up and may only fill during, and immediately after, rainfall events.

http://etd.uwc.ac.za/

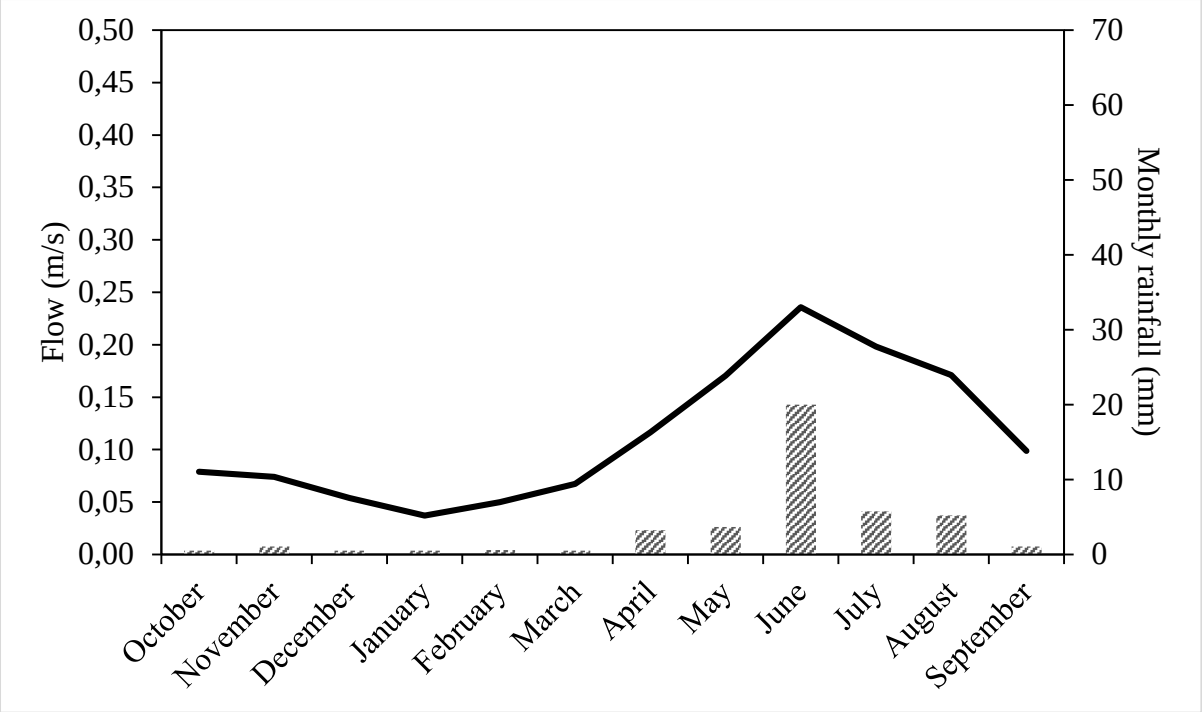

Figure 3.11 Naturalised mean monthly flow (bars) and mean monthly rainfall (line) for the Tankwa Catchment having a MAP of 189 mm/yr, and MAR of 5 mm/yr. Source: WR2012

UNIVERSITY of the
WESTERN CAPE

http://etd.uwc.ac.za/

4. DETERMINATION OF APPROPRIATE METHODS FOR MAPPING POOLS IN NON-PERENNIAL RIVERS

4.1 Introduction

Chapter 2 of this study discussed the various classification methods that are used in remote sensing to identify and map surface water. Multiband methods are semi-automatic classification methods for surface water mapping and are widely considered to be highly accurate (Ji et al., 2015; Wang et al., 2015; Acharya et al., 2016; Sisay, 2016; Rahman & Di, 2017; Masocha et al., 2018). This chapter addresses the first objective, which is to determine the most optimal multiband method for surface water detection in non-perennial rivers, with varying climatic and land cover types throughout the Western Cape. The first section describes the materials and methods that are necessary to assess the accuracy of remotely-sensed datasets for surface water classification. The second section describes the results of each method in which various pre-processed techniques are used. The third section provides a discussion of the results, a summary of the overall findings, as well as the limitations that were found in this study. Figure 4.1 illustrates the methodological steps that are taken in a flow diagram, and Objectives 1 and 2 are indicated by the checked boxes.

UNIVERSITY of the
WESTERN CAPE

4.2 Materials and Methods

Based on the problem outlined in Chapter 1, as well as the literature reviewed in Chapter 2, medium-resolution multispectral imagers may be suitable for mapping surface water along non-perennial rivers. Despite MODIS having a daily return period, the resolution of the dataset is too coarse, and despite the high resolution of SPOT, the return period and expensive costs makes these two datasets unfeasible. The Sentinel-2 MSI and Landsat 8-OLI sensors were shown by previous studies to be suitable for mapping small water bodies.

Therefore, this study assessed the performance of Sentinel-2 MSI and Landsat 8-OLI datasets for surface water monitoring in non-perennial rivers. The study used a comparative analysis approach, in order to determine the most suitable remote sensing product, the pre-processing method and the classification method for surface water mapping in non-perennial rivers. Preliminary sites were selected, based on the availability of validation data. This included a combination of in-situ field measurements and high resolution imagery, as well as variability

http://etd.uwc.ac.za/

in climatic and land cover differences, and was based on the premise of being part of an ongoing catchment monitoring project. Higher resolution datasets were also included in this study, to further compare the performance of the classification techniques applied to Sentinel-2 and Landsat 8. The high resolution datasets are WorldView-2 imagery and aerial photography.

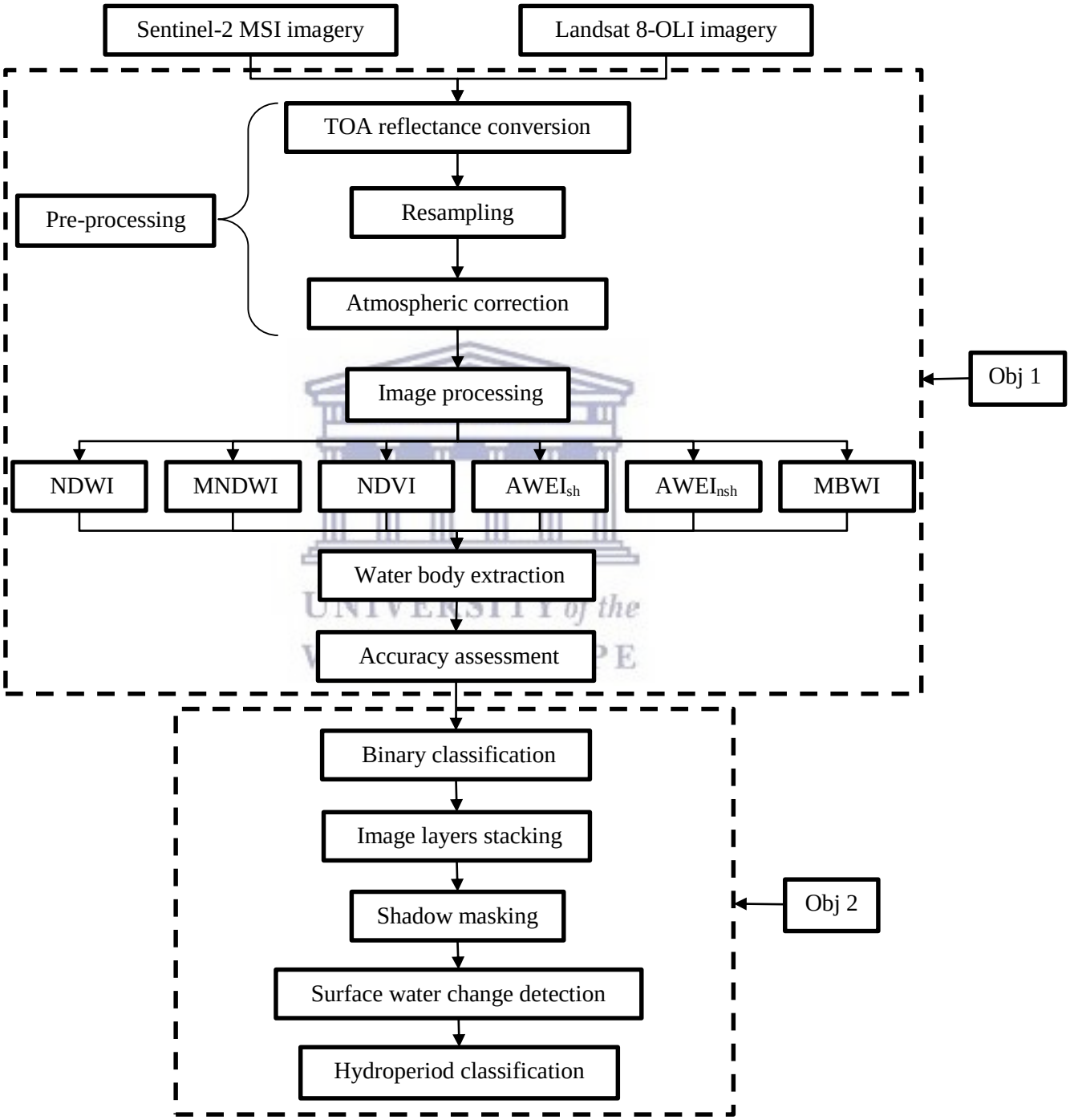

Figure 4.1 Methodological flowchart. Obj 1 refers to the steps undertaken to complete Objective 1, and Obj 2 refers to the step undertaken to complete Objective 2

http://etd.uwc.ac.za/

4.2.1 Data collection

Remote sensing data

The Sentinel-2 MSI is a sun synchronous, multi-spectral imaging sensor with a 290 km swath width. Sentinel-2 is a constellation of two satellites, namely Sentinel-2A and 2B, which was launched in June 2015 and March 2017, respectively (ESA, 2015). Sentinel-2 has thirteen spectral bands, ranging from the visible and near infrared, to the shortwave infrared (Chemura et al., 2017). Four bands have a spatial resolution of 10 m, six bands have a spatial resolution of 20 m and three bands have a spatial resolution of 60 m (Table 4.1). Sentinel-2 data was downloaded via the European Spaces Agency's Copernicus Open Access Hub (https://scihub.copernicus.eu/), as Level-1C TOA reflectance products (ESA, 2015).

Table 4.1 Summary table illustrating the different remotely-sensed products used in this study and their specifications

Sensor	Resolution	Source	Number of spectral bands
Sentinel-2 MSI	10 – 60 m	ESA	13
Landsat 8-OLI	15 – 100 m	USGS	11
WorldView-2	0.5 m	DigitalGlobe	3
Aerial photography	0.5 m	NGI	3

UNIVERSITY of the WESTERN CAPE

Landsat 8-OLI is a medium spatial resolution multi-spectral imager with a 190 km swath width. The satellite was launched in February 2013, with global imagery being captured over eleven spectral bands. One panchromatic band is available at a 15 m spatial resolution, eight bands have a spatial resolution of 30 m and two bands have a spatial resolution of 100 m (Table 4.1). Landsat-8 OLI data was downloaded via the United States Geological Survey's Earth Explorer website (http://earthexplorer.usgs.gov), as a Level-1 terrain corrected product, in raw Digital Number (DN) format. No atmospheric correction was applied to the datasets.

The National Geo-Spatial Information (NGI) agency of South Africa has high resolution aerial photography for South Africa, which is updated every 3 to 5 years (DRDLR, 2013). Aerial photographs consist of a red, blue and green colour composite, with a spatial resolution of 0.5 m. Aerial photography is often used for the validation of lower resolution images. For this study, aerial photography was compared to the classified maps of the

http://etd.uwc.ac.za/

Sentinel-2 and Landsat 8 datasets. Aerial photographs were obtained for the Western Cape from September to October 2016 (Table 4.2).

DigitalGlobe offers a pan-sharpened 0.5 m spatial resolution multispectral WorldView-2 dataset **t**hat is radiometrically and sensor corrected (Table 4.1) (DigitalGlobe, 2018). The WorldView-2 data were purchased in October 2017, during a period of on-site field visits. The dataset covered a reach of the Touws River in the area of Plathuis (Figure 4.2). The region in Figure 4.2 was selected, based on previous reconnaissance visits, its accessibility, and the abundance of pools that were identified. Multiple Sentinel-2 and Landsat 8 datasets were downloaded from 2016 to 2017, for comparison against the higher resolution datasets.

Attention was paid to the dates on which the remotely-sensed datasets were captured. Table 4.2 shows the rivers that were selected, based on the availability of the remote sensing datasets throughout the Western Cape. The presence of surface water in these rivers varied in shape, size, depth and land cover.

Table 4.2 Dates of relevant remote sensing datasets for the rivers of study

Rivers	Aerial photograph	Sentinel-2 MSI	Landsat 8-OLI	WorldView-2
Breede River	2016/09/04	2016/09/10	N/A	N/A
Nuwejaars River	2016/09/18	2016/10/03		
Tankwa River	2016/10/13	2016/10/13	2016/09/30	
Touws River	N/A	2017/10/20	201710/28	2017/10/17

UNIVERSITY of the WESTERN CAPE

In-situ measurements

The in-situ measurements of the Touws River were collected as part of an ongoing catchment monitoring project. The Touws River is classified as a non-perennial river within the Gouritz River system catchment (RQIS, 2012). The region of Plathuis was scoped for pools through field reconnaissance visits and with the aid of Google Earth Pro. The boundaries of the two pools were digitised, using a Differential Global Positioning System (DGPS), as indicated by the green points in Figure 4.2. GPS points were recorded from 20 – 25 November 2017, using a sub-meter DGPS with a range of error of < 1 m. The pools were digitised by using the Hartebeesthoek94_Lo19 coordinate reference system. The surveyed data were uploaded into ArcGIS software and the areas of the pools were calculated, and used as a reference dataset for the accuracy assessments of the classification method assessed in this study.

http://etd.uwc.ac.za/

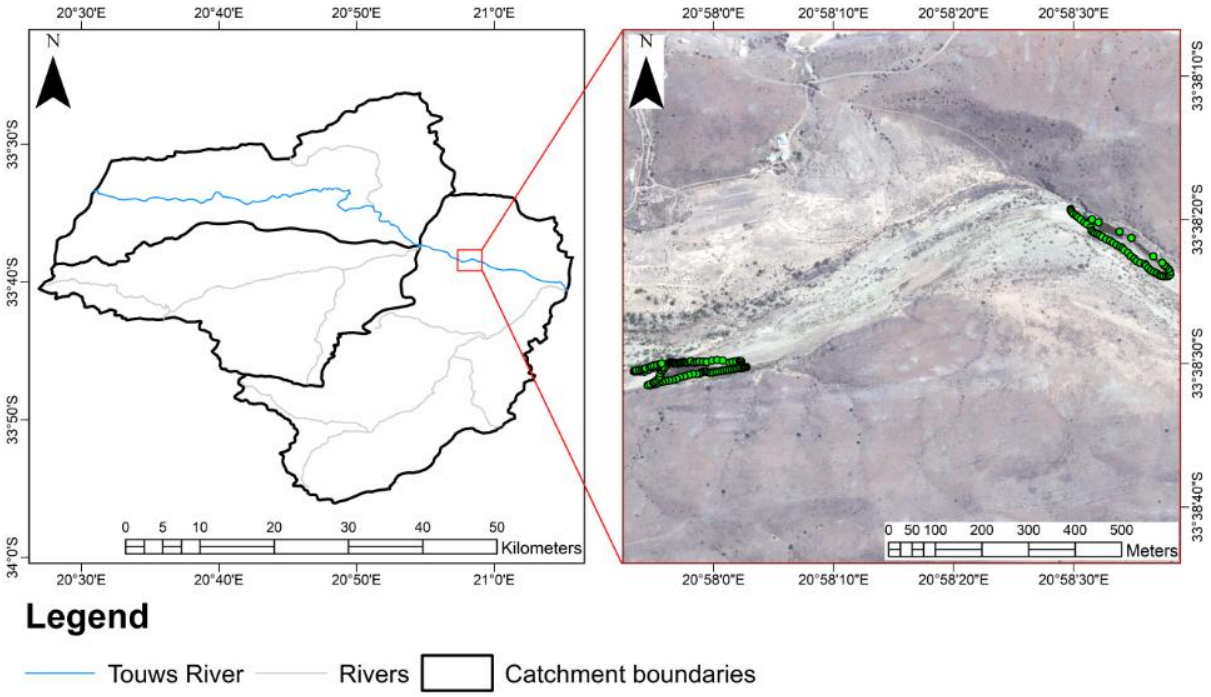

Figure 4.2 Location of the study sight describing the interpolated digitised pools within Touws River near Plathuis from DGPS. Source: WorldView-2 (October 2017)

4.2.2 Data analysis

Image pre-processing

Sentinel-2 datasets were downloaded as TOA reflectance, but the quantification value was increased by a factor of 10 000. Therefore, all bands were divided by a rescaling coefficient of 10 000, to retrieve true TOA reflectance values (Martins et al., 2017). Landsat 8 datasets were converted from radiance to TOA reflectance, to correct for solar angle and earth-sun distance errors (Li et al., 2013). The following formulae from the Landsat 8 Data Users Handbook (USGS, 2016) were used:

$$\rho\lambda' = M_\rho * Q_{cal} + A_\rho \quad (4.1)$$

where $\rho\lambda'$ is the TOA planetary spectral reflectance without correction for solar angle (unitless), M_p is the reflectance multiplicative scaling factor for the band, A_p is the reflectance additive scaling factor for the band, and Q_{cal} is the pixel value in digital numbers (DN).

$$\rho_\lambda = \frac{\rho\lambda'}{\sin(\theta)} \quad (4.2)$$

where $\rho\lambda$ is the TOA planetary reflectance (unitless), and θ is the solar elevation angle.

http://etd.uwc.ac.za/

The Dark Object Subtraction 1 (DOS1) atmospheric correction technique was applied to the Sentinel-2 and Landsat 8 TOA reflectance products to remove atmospheric effects (Song et al., 2001; Masocha et al., 2018). A separate atmospheric correction method was applied to Sentinel-2, using the Sen2Cor processor (ESA, 2015) in the Sentinel Application Platform (SNAP). This process develops a Sentinel-2 L2A Bottom-of-Atmosphere (BOA) reflectance product (Novelli et al., 2016). This was done to determine whether the newly-developed atmospheric correction method for Sentinel-2 is more optimal than the simpler DOS1 atmospheric correction method.

The bands highlighted in Tables 4.3 and 4.4 were rescaled to the same spatial resolution. All Sentinel-2 bands used in this study were resampled from a 20 m to a 10 m spatial resolution (Table 4.3). All Landsat 8 bands were pan-sharpened from a 30 m to a 15 m spatial resolution (Table 4.4). Bands in bold were excluded from this study, as they were not required for further processing. Five remotely-sensed datasets were pre-processed. This included one TOA reflectance Sentinel-2 product, one TOA reflectance Landsat 8 product, one DOS1 atmospherically-corrected Sentinel-2 product, one DOS1 atmospherically-corrected Landsat 8 product and one Sen2Cor atmospherically-corrected Sentinel-2 product.

Table 4.3 Specifications of Sentinel-2 MSI satellite bands with their centre wavelengths and spatial resolutions. Bands in bold were excluded from this study

UNIVERSITY of the
WESTERN CAPE

Sentinel-2 MSI			
Spectral band	Band name	Wavelength (μm)	Resolution (m)
B1	**Aerosol detection**	**0.443**	**60**
B2	Blue	0.490	10
B3	Green	0.560	10
B4	Red	0.665	10
B5	**Vegetation Red Edge**	**0.705**	**20**
B6	**Vegetation Red Edge**	**0.740**	**20**
B7	**Vegetation Red Edge**	**0.783**	**20**
B8	NIR	0.842	10
B8a	**Vegetation Red Edge**	**0.865**	**20**
B9	**Water Vapour**	**0.945**	**60**
B10	**Cirrus (SWIR)**	**1.380**	**60**
B11	SWIR-1	1.610	20
B12	SWIR-2	2.190	20

http://etd.uwc.ac.za/

Table 4.4 Specifications of Landsat 8-OLI satellite bands with their centre wavelengths and spatial resolutions. Bands in bold were excluded from this study

Landsat 8-OLI			
Spectral band	Band name	Wavelength (μm)	Resolution (m)
B1	**Coastal Aerosol**	**0.443**	**30**
B2	**Blue**	**0.482**	**30**
B3	Green	0.561	30
B4	Red	0.655	30
B5	NIR	0.865	30
B6	SWIR-1	1.609	30
B7	SWIR-2	2.201	30
B8	Panchromatic	0.590	15
B9	**Cirrus**	**1.373**	**30**
B10	**TIR-1**	**10.895**	**100**
B11	**TIR-2**	**12.005**	**100**

Surface water classification

This study assesses the most optimal multiband method for surface water classification in non-perennial rivers for the Western Cape. Based on the methods reviewed in Chapter 2, six multiband methods were selected and tested. The multiband methods used in this study are the NDWI (Mcfeeters, 1996), MNDWI (Xu, 2006), NDVI (Rouse et al., 1973), $AWEI_{sh}$ and $AWEI_{nsh}$ (Feyisa et al., 2014) and the MBWI methods (Wang et al., 2018). Table 4.5 presents the algorithms for the six multiband methods that were used to extract and identify surface water from Sentinel-2 and Landsat 8.

http://etd.uwc.ac.za/

Table 4.5 Multiband methods used to extract surface water bodies from Sentinel-2 MSI and Landsat 8-OLI imagery

Index	Equation	Threshold value	Spatial scale	Reference
NDWI	$NDWI = (B_{green} - B_{NIR})/(B_{green} + B_{NIR})$	NDWI > 0	10 m	McFeeters (1996)
MNDWI	$MNDWI = (B_{green} - B_{SWIR-1})/(B_{green} + B_{SWIR-1})$	MNDWI > 0	Resampled 10 m	Xu (2006)
NDVI	$NDVI = (B_{NIR} - B_{red})/(B_{NIR} + B_{red})$	NDVI < 0	10 m	Rouse et al., (1973)
$AWEI_{sh}$	$AWEI_{sh} = B_{blue} + 2.5 \times B_{green} - 1.5 \times (B_{NIR} + B_{SWIR-1}) - 0.25 \times B_{SWIR-2}$	$AWEI_{sh} > 0$	Resampled 10 m	Feyisa et al., (2014)
$AWEI_{nsh}$	$AWEI_{nsh} = 4 \times (B_{green} - B_{SWIR-1}) - (0.25 \times B_{NIR} + 2.75 \times B_{SWIR-1})$	$AWEI_{nsh} > 0$	Resampled 10 m	Feyisa et al., (2014)
MBWI	$MBWI = 2 \times B_{green} - B_{red} - B_{NIR} - B_{SWIR-1} - B_{SWIR-2})$	MBWI > 0	Resampled 10 m	Wang et al., (2018)

where B_{green} indicates the green band, B_{NIR} indicates the Near-Infrared band, B_{SWIR-1} indicates the first shortwave-infrared band, B_{red} indicates the red band, B_{blue} indicates the blue band and B_{SWIR-2} indicates the second shortwave-infrared band.

UNIVERSITY of the
WESTERN CAPE

Each multiband method was applied to each of the five pre-processed products, as mentioned above. Surface water bodies that were digitised from in-situ measurements and high resolution imagery were used as a mask to extract all pixels within the boundaries of the pools. The buffer technique proposed by Brovelli et al. (2015) was applied to develop a confusion matrix for the accuracy assessments. Pixels within the digitised boundaries were known to have water Pixels within the area of the buffer were known have no water.

Accuracy assessment

A binary confusion matrix was calculated to summarise the processed data and calculate the accuracy statistics. The overall accuracy (Equation 4.3), the producers' accuracy (Equation 4.4), the users' accuracy (Equation 4.5), the allocation disagreement (Equation 4.6) and the quantity disagreement (Equation 4.7) were calculated for each multiband method for the five pre-processed products. The equations were selected based on their viability, to statistically illustrate the degree of accuracy for each classified image, in a simpler and more interpretable manner. The formulae for each calculation are as follows:

http://etd.uwc.ac.za/

$$Overall\ accuracy = \frac{\sum_{i=1}^{m} n_{ii}}{n} \times 100\% \quad (4.3)$$

$$Producers'accuracy = \frac{n_{ii}}{n_{+i}} \quad (4.4)$$

$$Users'accuracy = \frac{n_{ii}}{n_{i+}} \quad (4.5)$$

$$Allocation\ Disagreement = \frac{\sum(2\times\min(\frac{n_{+i}}{n}-\frac{n_{ii}}{n},\frac{n_{i+}}{n}-\frac{n_{ii}}{n}))}{2} \times 100 \quad (4.6)$$

$$Quantity\ Disagreement = \frac{\sum\left|\frac{n_{+i}}{n}-\frac{n_{i+}}{n}\right|}{2} \times 100 \quad (4.7)$$

where n is the total number of testing pixels, m is the number of classes, n_{ii} is the element in the i-th row and the i-th column, n_{i+} is the sum of the class row and n_{+i} is the sum of the class column. The results from the accuracy assessment allowed for the determination of the multiband method (Table 4.4) that most accurately classifies pools in non-perennial rivers.

The reclassified products were interpolated to calculate the estimated surface water area. The Root Mean Square Error (RMSE) was calculated, in this instance, to determine the error the of estimated surface water area of the classified images against the observed surface water area. The formula that was used to calculate the RMSE is as follows:

UNIVERSITY of the
WESTERN CAPE

$$RMSE = \sqrt{\frac{\sum_{i=1}^{n}(a_i-b_i)^2}{n}} \quad (4.8)$$

where a is the observed value dataset, b is the estimated value dataset and n is the number of samples.

4.3 Results

The results illustrate the performance of the different remotely-sensed datasets in classifying surface water, using different pre-processing and classification methods. The classification methods described in Table 4.5 were assessed on the four rivers that are presented in Table 4.2.

http://etd.uwc.ac.za/

4.3.1 Comparison of remotely-sensed datasets for surface water classification

The Nuwejaars River

According to the RQIS of the Department of Water and Sanitation, the Nuwejaars River is classified as a non-perennial river. A reach of the Nuwejaars River was selected to test the ability of remotely-sensed datasets and multiband methods to classify surface water (Figure 4.3). The area outlined in blue on the right-hand image in Figure 4.3 was digitised, with the aid of high resolution aerial photography and it was validated during field reconnaissance visits for the presence of surface water.

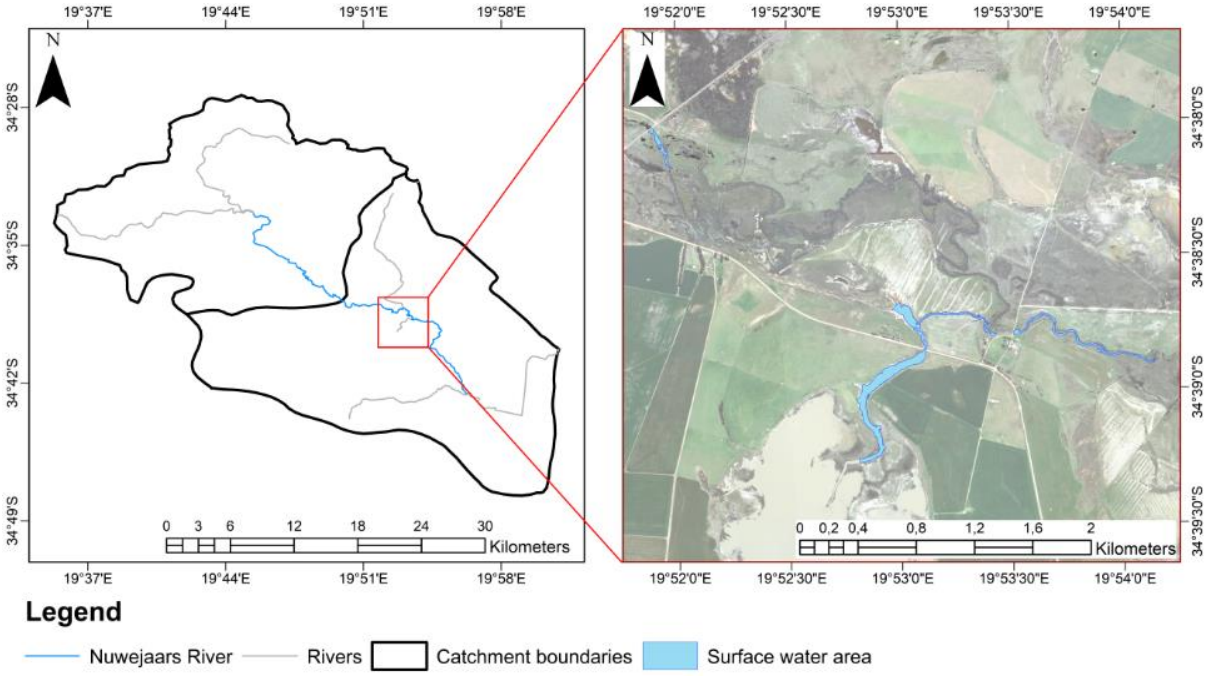

Figure 4.3 Location of study sight along the Nuwejaars River, indicated by blue on the right. Source: Aerial photograph (September 2016)

No cloud-free Landsat 8 imagery was available near the date of capture of the aerial photography during September and October of 2016. Therefore, only Sentinel-2 datasets were assessed, in terms of surface water classification for the study sight along the Nuwejaars River. Figure 4.4 illustrates the performance of each multiband method applied to different pre-processed images. The rows in Figure 4.4 illustrate the different pre-processed remotely-sensed datasets, and the columns illustrate the different multiband methods applied to each pre-processed dataset. The multiband methods applied to Sentinel-2 TOA reflectance datasets and Sen2Cor atmospherically corrected datasets had the highest performance in surface water classification. All of the products successfully detected water in the Voelvlëi Lake, except for

http://etd.uwc.ac.za/

the MBWI in all cases, and the NDWI was applied to the Sentinel-2 DOS1 atmospherically-corrected product. The MNDWI, NDVI and $AWEI_{sh}$ showed the most promising results in classifying surface water in the Nuwejaars River.

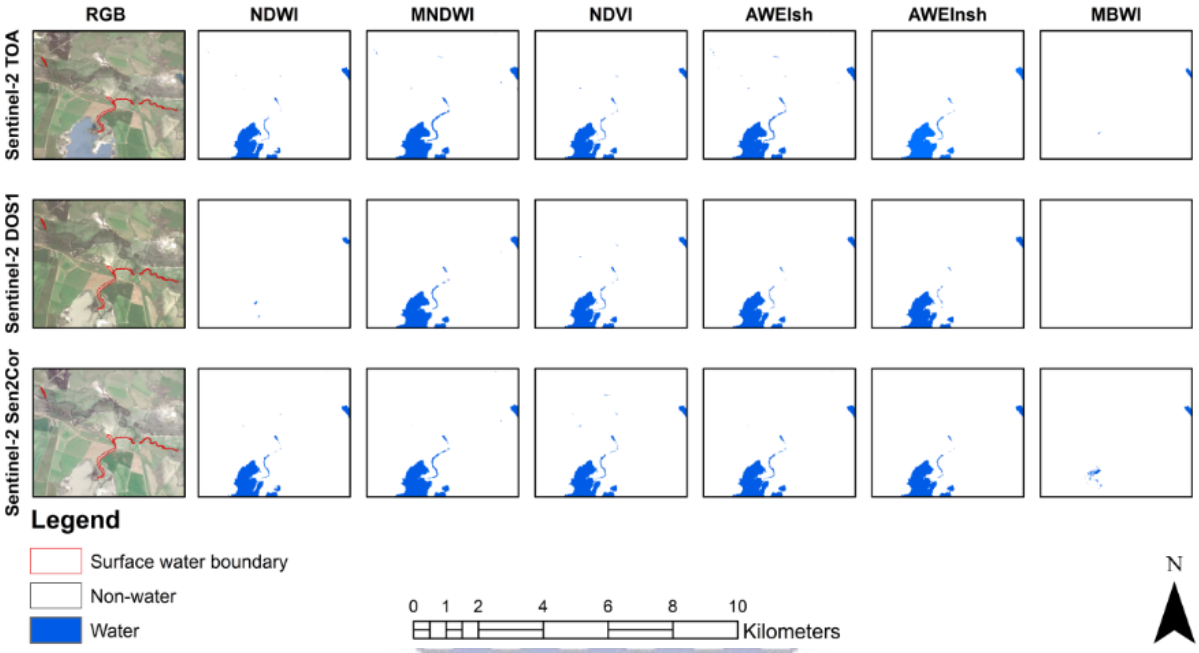

Figure 4.4 Performance of the six multiband methods applied to different pre-processed images of Sentinel-2 in the Nuwejaars River

UNIVERSITY of the
WESTERN CAPE

The Breede River

According to the RQIS of the Department of Water and Sanitation, the Breede River is classified as a perennial river system. However, based on field visits in early 2017, large stretches of the river were dry, with no flow. This shows that the Breede River has non-perennial stretches throughout the river. A reach of the Breede River was selected to assess the performance of the multiband methods applied to remotely-sensed datasets, to classify surface water (Figure 4.5). The reach of the river was selected, based on its accessibility, the availability of high resolution aerial photography and its features of non-perenniality. The area outlined in blue on the right-hand image in Figure 4.5 was digitised, using aerial photography as a reference and the presence of surface water was validated during field reconnaissance visits.

http://etd.uwc.ac.za/

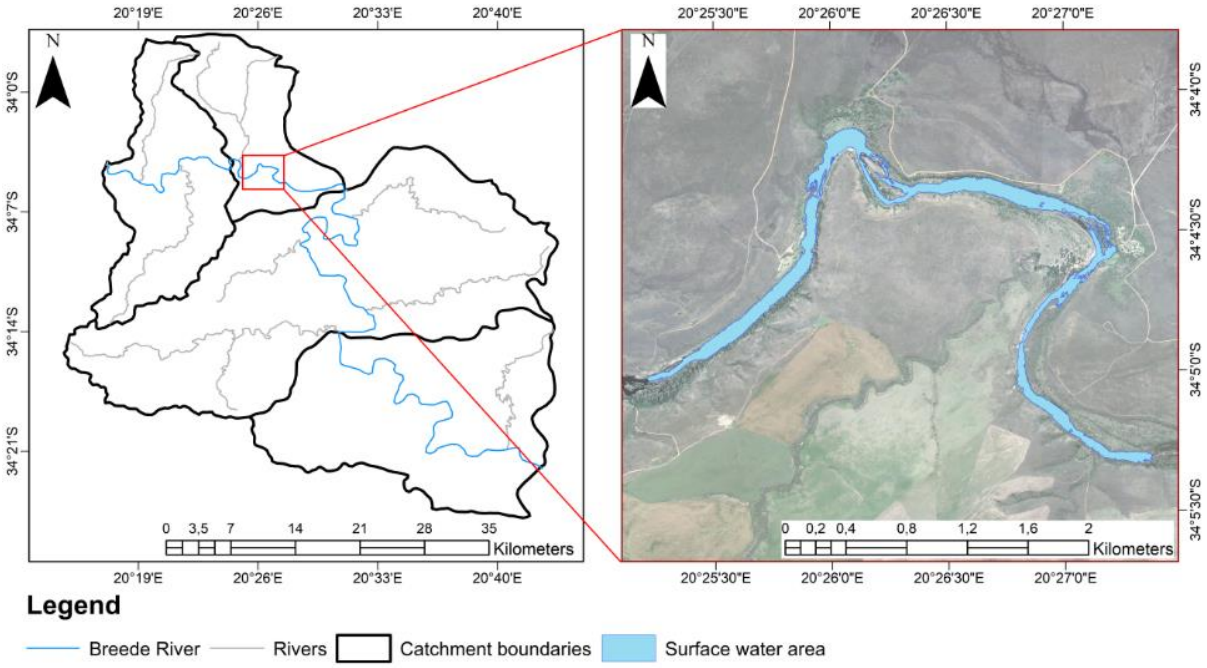

Figure 4.5 Location of study site along the Breede River, which is indicated by blue on the right. Source: Aerial photograph (September 2016)

No cloud-free Landsat 8 imagery was available near the date of capture of the aerial photography during September and October of 2016. Therefore, only Sentinel-2 datasets were used for identifying surface water in the river. Figure 4.6 illustrates the performance of the different multiband methods in classifying surface water, under different pre-processed conditions, for Sentinel-2. The rows in Figure 4.6 illustrate the different pre-processed remotely-sensed datasets, and the columns illustrate the different multiband methods applied to each pre-processed dataset.

Cloud cover was present on the 10th of September 2016 when the Sentinel-2 image was captured, but it did not cover the study site. Figure 4.6 shows that multiband methods applied to the Sentinel-2 TOA reflectance image were most promising in identifying surface water in the Breede River. However, shadows from the clouds in the upper regions of the map were misclassified as water. DOS1 and Sen2Cor atmospheric correction eliminated the effects of cloud shadows, in all circumstances, but many surface water pixels were also eliminated and misclassified as non-water. The NDVI and MBWI applied to the Sentinel-2 TOA reflectance image were the only two methods that misclassified the least number of surface water pixels, while they correctly identified surface water in the Breede River. The MNDWI and $AWEI_{sh}$ seemed to overestimate surface water in the Breede River.

http://etd.uwc.ac.za/

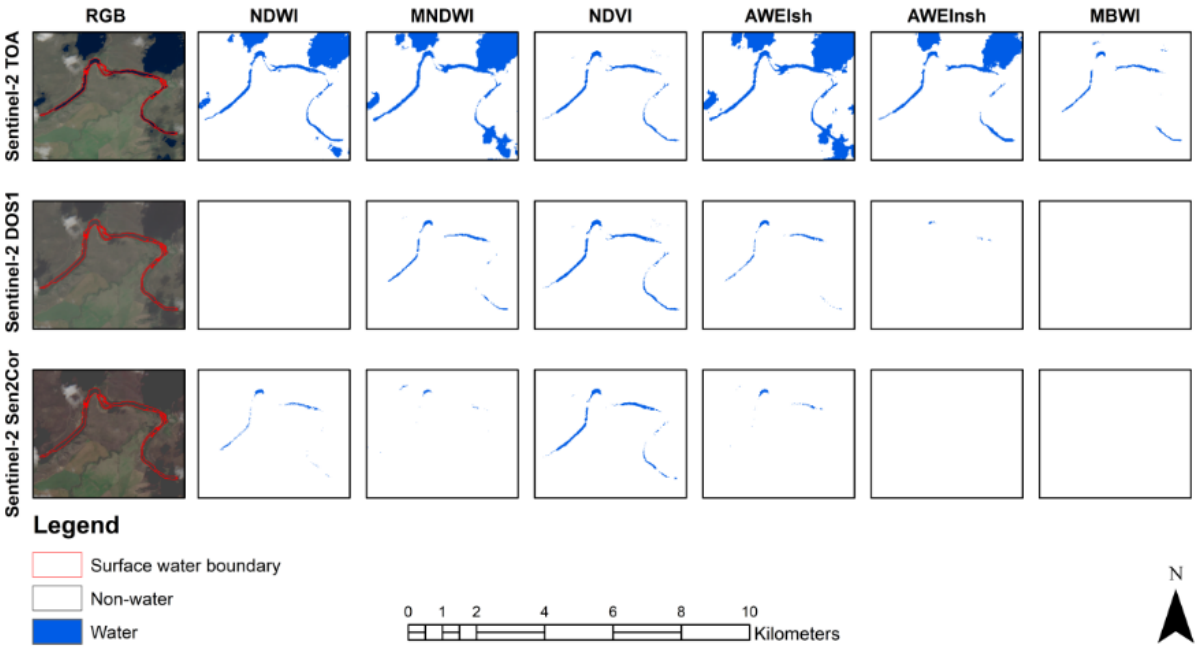

Figure 4.6 Performance of the six multiband methods applied to different pre-processed images of Sentinel-2 in the Breede River

The Touws River

In-situ measurements were taken along the boundaries of two pools in the Touws River in November 2017 (Figure 4.2). DigitalGlobe WorldView-2 imagery was obtained for the same reach of the Touws River on the 17th of October 2017. A total of twelve pools were mapped and digitised, with the aid of in-situ measurements and the high resolution WorldView-2 datasets. The pools varied in size and shape, ranging from 380 – 8 243 m^2.

Figure 4.7 illustrates the performance of surface water classification, using the six multiband methods applied to different pre-processed Sentinel-2 and Landsat 8 datasets. Each blue dot in Figure 4.7 represents a pixel that was correctly classified as water within the boundaries of the pools. Multiband methods applied to the Sentinel-2 and Landsat 8 TOA reflectance images were the most promising in identifying surface water. All multiband methods applied to the Landsat 8 DOS1 atmospherically corrected image showed no surface water detected, with the exception of the NDVI, which correctly classified water in one of the twelve pools. The $AWEI_{nsh}$ and MBWI were unsuccessful in detecting surface water, in all instances. The NDWI and NDVI were the most promising in identifying surface water in the Touws River.

http://etd.uwc.ac.za/

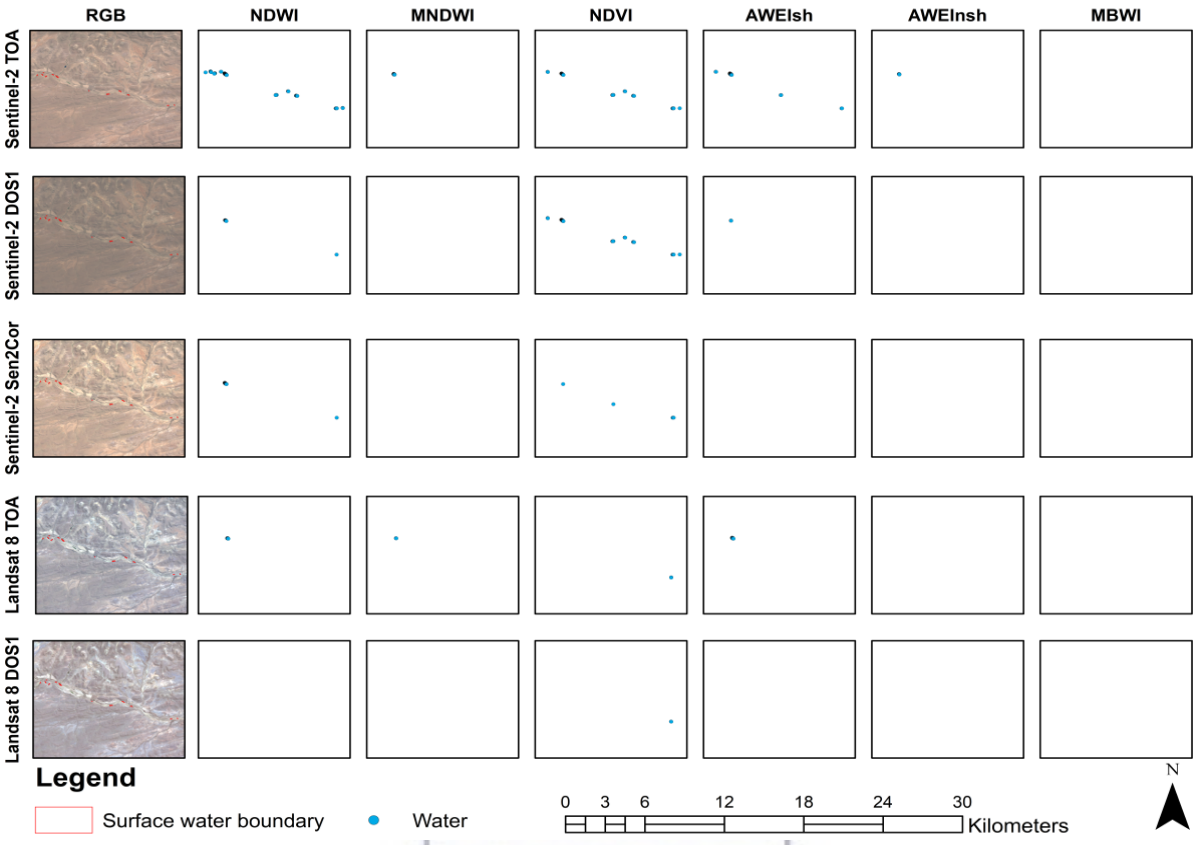

Figure 4.7 Performance of six multiband methods applied to the different pre-processed images of Sentinel-2 and Landsat 8, for the Touws River

UNIVERSITY of the
WESTERN CAPE

The Tankwa River

According to the RQIS of the Department of Water and Sanitation, the Tankwa River is classified as a non-perennial river. The Tankwa River flows through the Tankwa Karoo National Park and drains into the Oudebaaskraal Dam. A reach of the Tankwa River was selected, in order to assess the performance of classification methods in identifying surface water within the river (Figure 4.8), based on the availability of high resolution aerial photography. The area outlined in blue on the right-hand image in Figure 4.8 was digitised, using the aerial photography as reference, and the presence of surface water was validated during reconnaissance visits.

http://etd.uwc.ac.za/

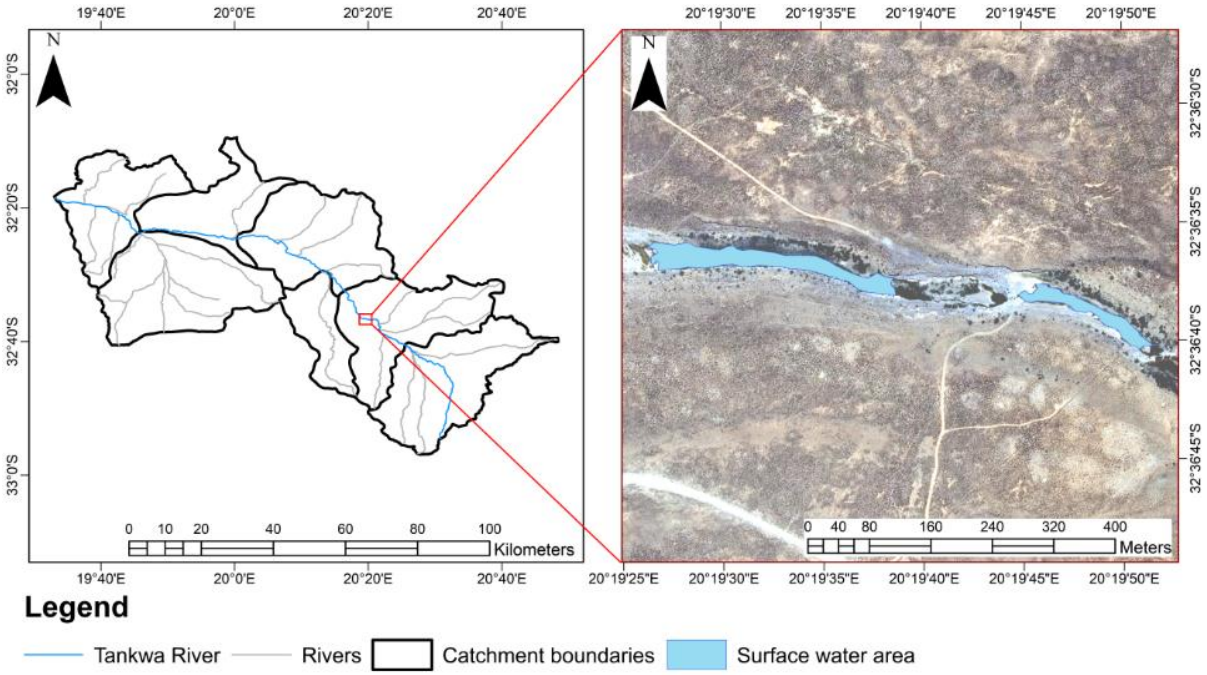

Figure 4.8 Location of study site along the Tankwa River, which is indicated by blue on the right. Source: Aerial photograph (October 2016)

Five pre-processed, remotely-sensed datasets were analysed to assess their performance in identifying surface water in the Tankwa River (Figure 4.9). Figure 4.9 illustrates the performance of each multiband method applied to the Sentinel-2 TOA reflectance product, the Sentinel-2 DOS1 atmospherically-corrected product, the Sentiel-2 Sen2Cor atmospherically-corrected product, the Landsat 8 TOA reflectance product and the Landsat 8 DOS1 atmospherically-corrected product.

Multiband methods applied to the Landsat 8 DOS1 atmospherically-corrected dataset were unsuccessful in classifying surface water. The $AWEI_{nsh}$ and MBWI were unsuccessful in identifying surface water, in all instances. Multiband methods applied to Sentinel-2 TOA reflectance dataset had the best performance in surface water classification. The NDWI, NDVI and $AWEI_{sh}$ were the most successful in identifying surface water along the Tankwa River.

http://etd.uwc.ac.za/

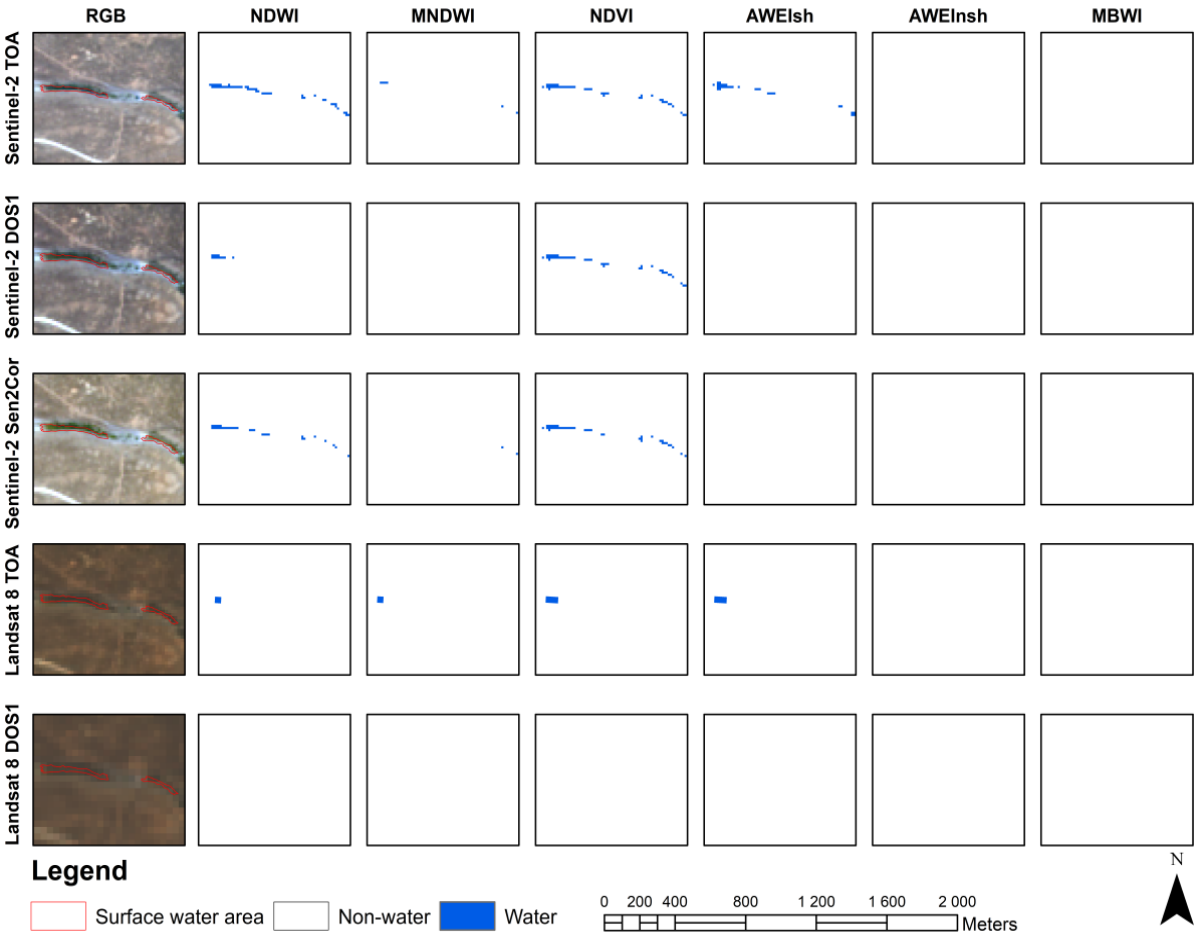

Figure 4.9 Performance of six multiband methods applied to the different pre-processed images of Sentinel-2 and Landsat 8, for the Tankwa River

UNIVERSITY of the
WESTERN CAPE

4.3.2 Accuracy of multiband methods for surface water classification

The Nuwejaars River

The overall accuracy (OA), quantity disagreement (QD), allocation disagreement (AD) producers' accuracy (PA) and users' accuracy (UA) were calculated to describe the performance of the multiband methods applied to different pre-processed, remotely-sensed datasets. Figure 4.10 describes the OA, QD, AD, PA and UA for each multiband method applied to different Sentinel-2 pre-processed datasets. No Landsat 8 datasets were available due to cloud cover, as explained in Section 4.3.1. The OA ranged from 75 – 85% for each multiband method. The MNDWI applied to the Sentinel-2 TOA reflectance image showed the highest OA of 85%, and a PA of 47% (Figure 4.10 a). The QD accounted for the largest amount of overall disagreement for all multiband methods. The PA was low throughout all methods. The MBWI had the lowest OA of 72% and a PA of 0%, in every instance.

http://etd.uwc.ac.za/

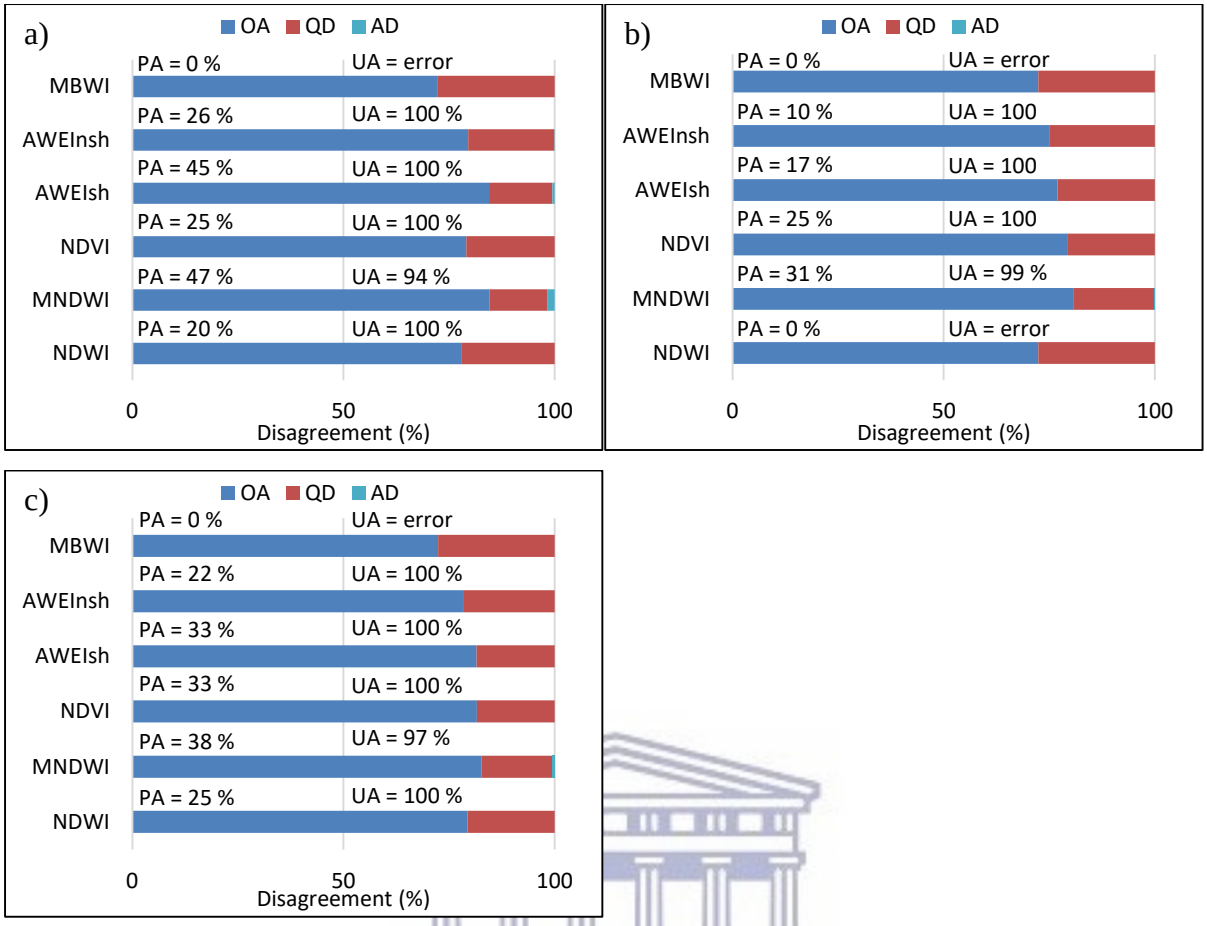

Figure 4.10 OA, QD, AD, PA and UA of the multiband methods for the Nuwejaars River. a) Sentinel-2 TOA reflectance image, b) Sentinel-2 DOS1 image and c) Sentinel-2 Sen2Cor image

UNIVERSITY of the
WESTERN CAPE

http://etd.uwc.ac.za/

The Breede River

No Landsat 8 datasets were available due to cloud cover, as explained in Section 4.3.1. The OA ranged from 53 – 86% for each multiband method. The NDWI applied to the Sentinel-2 TOA reflectance image had the highest OA of 86%, while the $AWEI_{sh}$ applied to the Sentinel-2 TOA reflectance image had the highest PA of 83% (Figure 4.11 a). The QD accounted for the largest amount of overall disagreement for all multiband methods applied to the Sentinel-2 atmospherically-corrected images (Figure 4.11 b and c). The AD accounted for the largest amount of overall disagreement for the MNDWI and $AWEI_{sh}$ for the Sentinel-2 TOA reflectance image (Figure 4.11 a). The NDWI and MBWI in Figure 4.11 (b) and (c) had the lowest OA of 53% and a PA of 0%.

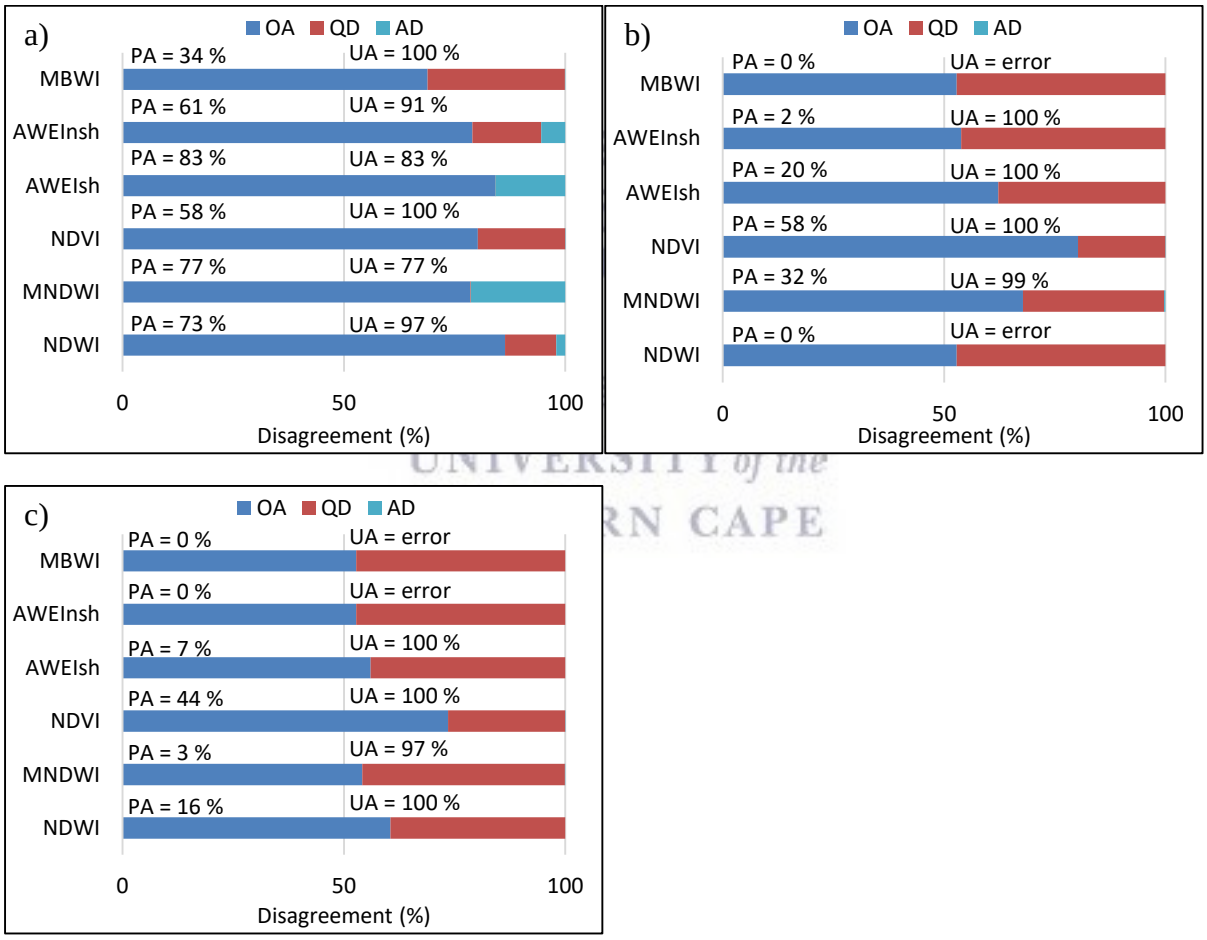

Figure 4.11 OA, QD, AD, PA and UA of the multiband methods for the Breede River. a) Sentinel-2 TOA reflectance image, b) Sentinel-2 DOS1 image and c) Sentinel-2 Sen2Cor image

http://etd.uwc.ac.za/

The Touws River

The OA ranged from 80 – 90% for all multiband methods. The NDWI applied to the Sentinel-2 TOA reflectance image had the highest OA of nearly 90%, and a PA of 34% (Figure 4.12 a). The QD accounted for the largest amount of overall disagreement for all methods. The MBWI had a PA of 0% in every case. The UA was mostly high, except where if the PA was 0 %, the UA was undefined. The lowest UA was 50%, when applying the NDVI to the Landsat 8 TOA (Figure 4.12 d) and the Landsat 8 images (Figure 4.12 e).

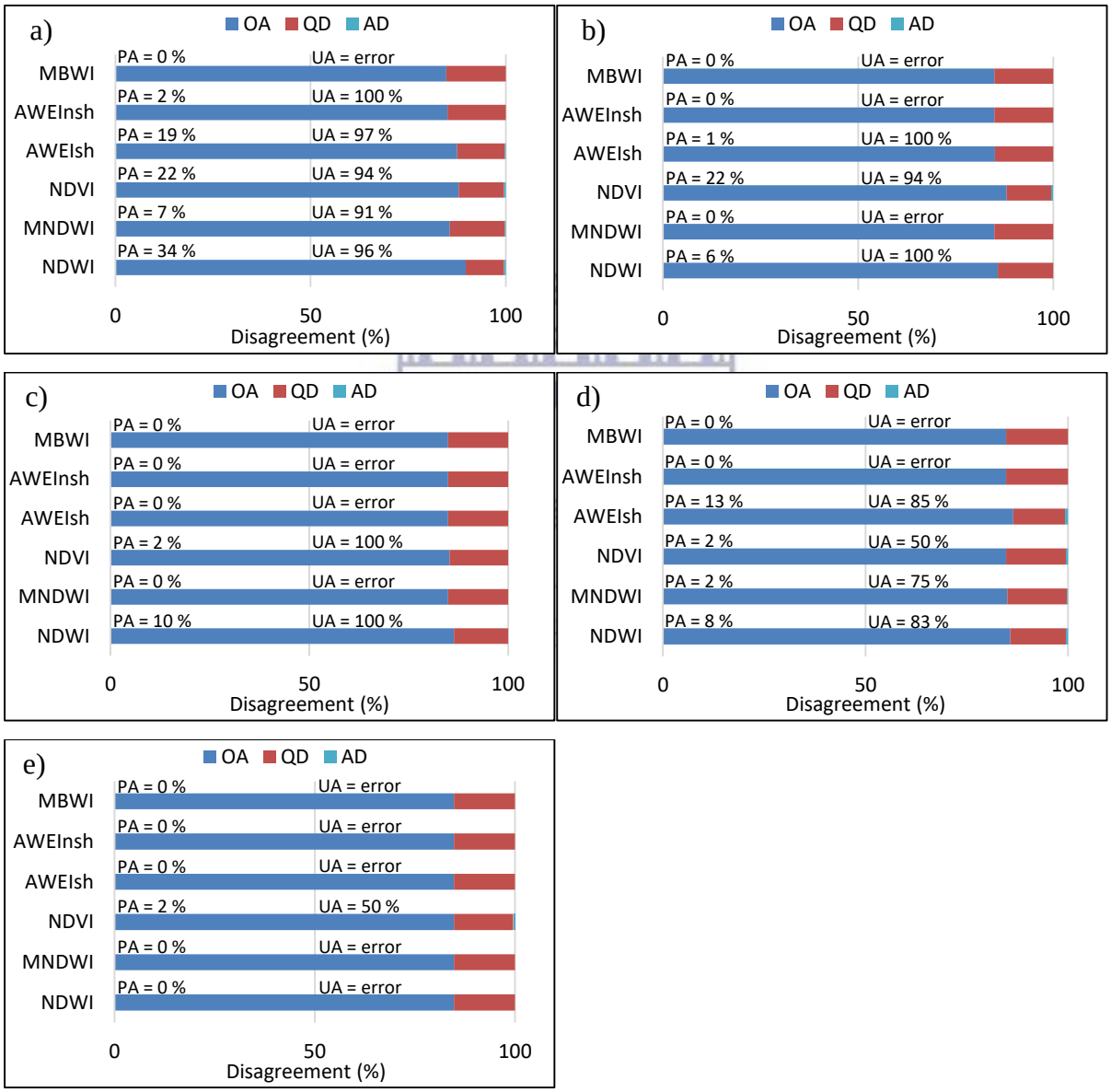

Figure 4.12 OA, QD, AD, PA and UA of the six multiband methods for the Touws River. a) Sentinel-2 TOA reflectance image, b) Sentinel-2 DOS1 image, c) Sentinel-2 Sen2Cor image, d) Landsat 8 TOA reflectance image and e) Landsat 8 DOS1 image

http://etd.uwc.ac.za/

The Tankwa River

The OA ranged from 77 – 86 % for all multiband methods. The NDWI and NDVI applied to the Sentinel-2 TOA reflectance image had the highest OA of 86% (Figure 4.13 a). The NDVI applied to the Sentinel-2 DOS1 atmospherically-corrected image had the highest PA of 40% (Figure 4.13 b). The QD accounted for the largest amount of overall disagreement for all multiband methods. All multiband methods applied to Landsat 8 imagery showed little variation, in terms of OA, PA and UA.

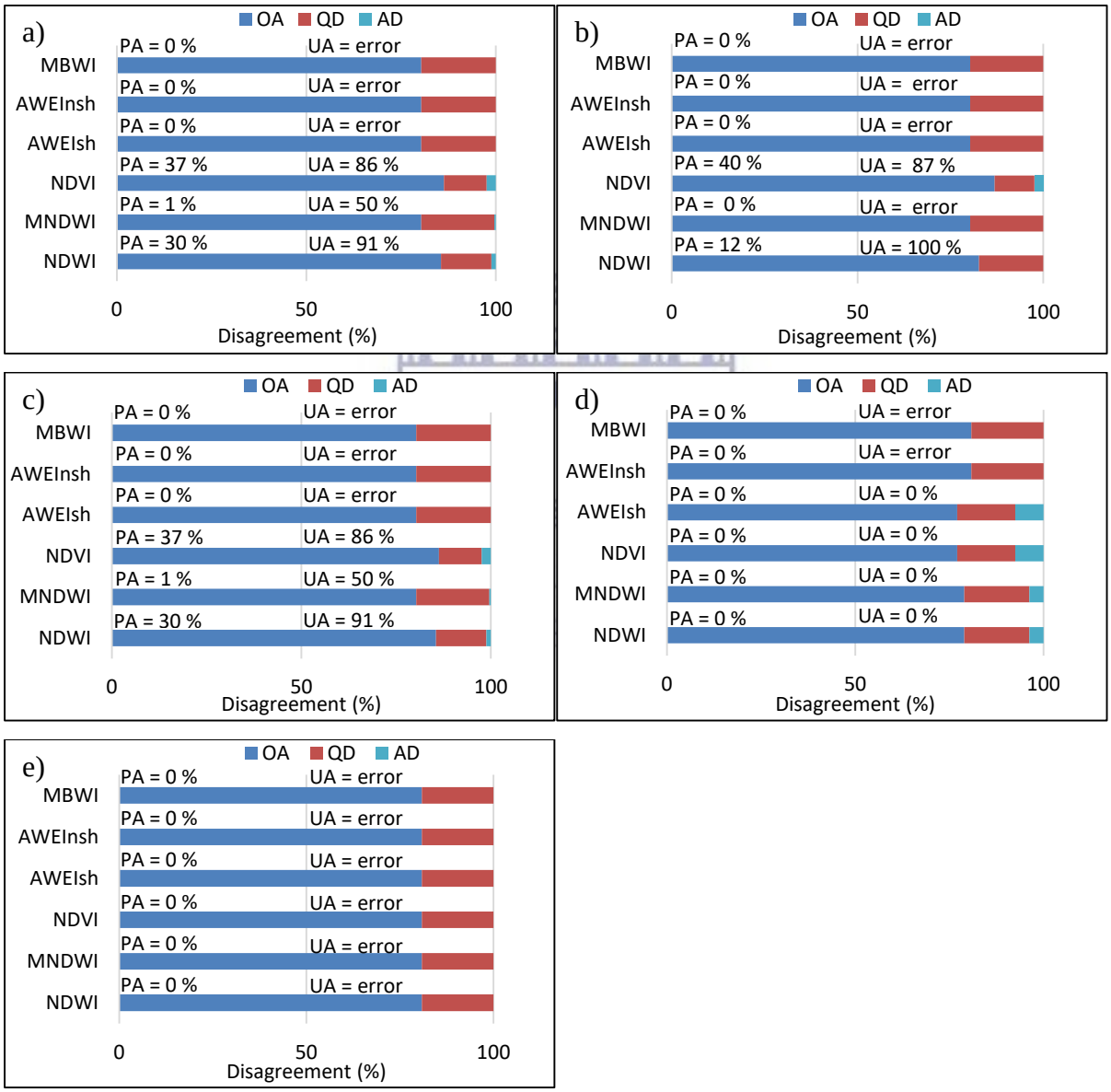

Figure 4.13 OA, QD, AD, PA and UA of the six multiband methods for the Tankwa River. a) Sentinel-2 TOA reflectance image, b) Sentinel-2 DOS1 image, c) Sentinel-2 Sen2Cor image, d) Landsat 8 TOA reflectance image and e) Landsat 8 DOS1 image

http://etd.uwc.ac.za/

Summary of overall accuracy

The variation of the OA for each multiband method applied to different pre-processed remotely-sensed datasets, for the Nuwejaars, Breede, Touws and Tankwa Rivers (Figure 4.14). The (x) in Figure 4.14 shows the mean value for each box-plot. The OA varied between the multiband methods, and the pre-processed datasets. The multiband methods that were applied to the Sentinel-2 TOA reflectance image, Landsat 8 TOA reflectance image and Landsat 8 DOS1 atmospherically-corrected image showed the lowest variability, in terms of the OA. The NDWI that was applied to the Sentinel-2 TOA reflectance dataset had the highest OA average of 85%. The variation of the OA for the Landsat 8 DOS1 atmospherically-corrected dataset was not included, as all multiband methods shared the same average OA value of 83 % and no variation in the OA was shown.

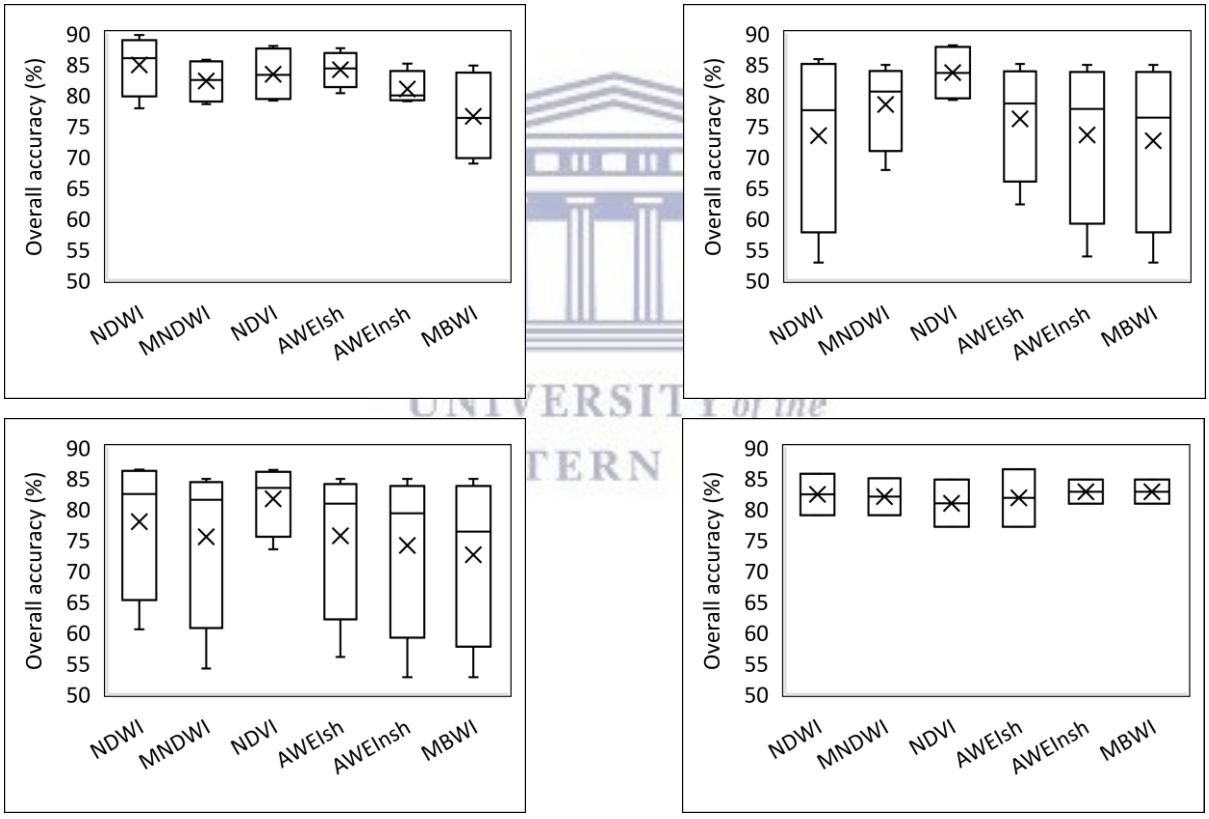

Figure 4.14 OA distribution of classified water. Each box plots shows the location of the 10th, 25th, 50th, 75th, and 90th percentiles using horizontal lines, for the Nuwejaars, Breede, Touws and Tankwa Rivers. a) Sentinel-2 TOA reflectance, b) Sentinel-2 DOS1, c) Sentinel-2 Sen2Cor and d) Landsat 8 TOA reflectance

http://etd.uwc.ac.za/

Comparison of estimated and observed surface water areas

The estimated pool areas from the classified maps were compared to the observed pool areas that were mapped from in-situ measurements and higher resolution datasets (Figure 4.15). A positive relationship was shown for each classification method across all pre-processed images. The results that did not show a positive relationship were excluded. Therefore, the results of the Landsat 8 DOS1 atmospherically-corrected product were excluded. Multiband methods that did not show a positive relationship between the observed and the estimated pool areas on the remaining pre-processed images were also excluded. The estimated surface water area calculated from multiband methods applied to the Sentinel-2 TOA reflectance dataset showed the strongest relationships, with the NDWI having the highest R^2 of 0.7 (Figure 4.15 a). Therefore, the results suggest that using the Sentinel-2 TOA reflectance dataset is the most suitable for image classification and for estimating the pool areas. Despite this, all methods seemed to underestimate the surface area of the pools. This may be attributed to the size of the pools that were analysed.

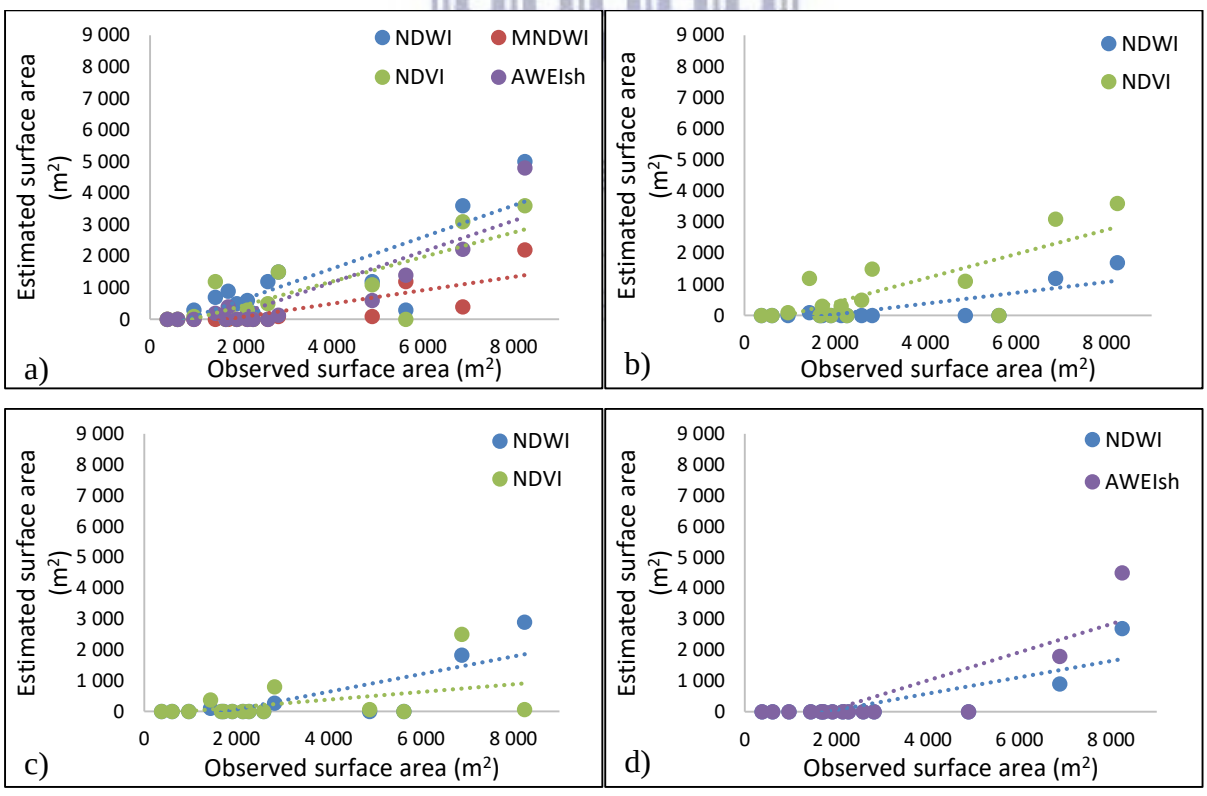

Figure 4.15 Comparison of observed and estimated surface water area of the study areas in the Nuwejaars, Breede, Touws and Tankwa Rivers. a) Sentinel-2 TOA reflectance image, b) Sentinel-2 DOS1 image, c) Sentinel-2 Sen2Cor image, and d) Landsat 8 TOA reflectance image

http://etd.uwc.ac.za/

The Root Mean Square Error (RMSE) was calculated to measure the difference between the observed surface water area and estimated surface water area. The RMSE was calculated for each multiband method, under different pre-processed conditions (Table 4.6). The results show that the NDWI applied to the Sentinel-2 TOA reflectance product had the lowest RMSE of 48.09 m^2. This indicates that the NDWI had the lowest error and highest accuracy, in terms of estimating the surface water area. All multiband methods applied to the Landsat 8 DOS1 atmospherically-corrected image shared the highest RMSE of 59 m^2. The results of the accuracy assessments and RMSE suggest that the most optimal remotely-sensed dataset for surface water classification is the Sentinel-2 TOA reflectance product. The most suitable multiband method that is suggested for surface water classification in non-perennial rivers in the Western Cape is, therefore, the NDWI.

Table 4.6 Calculated RMSE (m^2) for the six multiband methods tested on the different remotely-sensed pre-processed datasets

	NDWI	**MNDWI**	**NDVI**	**$AWEI_{sh}$**	**$AWEI_{nsh}$**	**MBWI**
Sentinel- 2 TOA	48.09	56.95	51.59	51.39	60.55	61.03
Sentinel-2 DOS1	57.82	61.03	51.59	60.75	61.03	61.03
Sentinel-2 Sen2Cor	55.77	61.01	58.31	61.03	61.03	61.03
Landsat 8 TOA	54.96	58.05	57.55	51.83	59.59	59.59
Landsat 8 DOS1	59.59	59.59	59.47	59.59	59.59	59.59

UNIVERSITY of the WESTERN CAPE

4.4 Discussion

Atmospheric correction has been known to be a crucial step for aquatic remote sensing applications (Vanhellemont & Ruddick, 2016). This is done to correct for Rayleigh scattering by air molecules and to correct for the scattering and absorption of light from aerosols. If not undertaken, image classification methods may misclassify different land cover types. Currently, there is no existing multiband method that is able to automatically differentiate surface water from the shadows and low albedo urban surfaces (Sarp & Ozcelik, 2017). The results presented in this chapter demonstrated that when remotely-sensed datasets underwent atmospheric correction, features such as shadows were eliminated during the image classification. However, atmospheric correction also caused a large amount of surface water to be misclassified as non-water. By eliminating the effects of misclassification caused by atmospheric effects and shadows, classified surface water features may also be eliminated.

http://etd.uwc.ac.za/

Accuracies ranged from 52 – 89% across the surface water bodies and pre-processed sensors that were studied. The results presented in this chapter showed a similar trend to the study by Fisher et al. (2016), who compared the surface water reflectance values of different water body types, using Landsat datasets. Two key findings were presented in their results. Firstly, they found that different surface water types show relatively unique reflectance properties. Clear and deep waters have an overall trend of decreasing reflectance values. Dark-green and green waters i.e. water bodies with considerable plant matter, have reflectance peaks in the green band, while brown and dark-brown waters, with high concentrations of sediments showed reflectance peaks in the red band. The different surface water bodies selected in this study ranged from clear-deep water, green water, dark-green water, brown water and dark-brown water (Appendix 4.1). This suggests that the accuracy of the multiband methods will vary, depending on the water feature studied. Secondly, the study found that each multiband method produced different errors for different water and non-water types, but accurately classified pure water pixels. Therefore, accuracies may vary, depending on the background colour, river bed or plants and the classification technique applied.

In this study, the results showed that the NDWI, NDVI and $AWEI_{sh}$ were the most suitable for classifying surface water in non-perennial rivers, when applied to TOA reflectance imagery. The NDWI maintained the highest average OA across all study sites, with little variation in accuracy. Studies by Rokni et al. (2014), Sisay (2016), Sarp & Ozcelik (2017) and Zhou et al. (2017) all showed that the NDWI and $AWEI_{sh}$ were the most suitable for surface water classification across various regions. When multiband methods were applied to the Sentinel-2 atmospherically-corrected imagery in this study, the NDVI was shown to be the most successful. Duggin & Piwninski (1984), Hadjimiysis et al. (2010), Agapiou et al. (2011) and Nguyen et al. (2015) all showed an 18 % increase in accuracy, when using the NDVI for image classification after atmospheric correction. The results of this study regarding the accuracy of the NDVI, when applied to atmospherically-corrected datasets were consistent with the above-mentioned studies. However, the NDVI was still unsuccessful when applied to Landsat 8 DOS1 atmospherically-corrected imagery. Sharma et al. (2015) found that the NDWI performed relatively well, based on its robustness in surface water classification on a global scale, when using MODIS. In arid regions, the study found that the MNDWI and AWEI were unable to correctly explain the variations in surface water cover. The Western Cape is considered as a predominantly arid to semi-arid region, which may

UNIVERSITY of the WESTERN CAPE

http://etd.uwc.ac.za/

explain the reason for the MNDWI and AWEI not performing as accurately as the NDWI, in some cases.

The accuracy of the classified maps was greatly increased by implementing a second variable of non-water pixels. Sader et al. (1995), Boudewyn et al. (2000) and Smith et al. (2002) suggested that the more variables included in image classification, the more accurate the classified image. The results in this study showed that by including the second variable, the OA greatly increased for the classified images. Despite this, the OA in this study did not exceed 89% across all the study areas. Wynne et al. (2000) discovered that, even in a simple binary classification, it is difficult to exceed an OA of 85% on a per pixel basis. This result is limited by only focusing on the reflectance of different features and not taking into account other sources of information, such as digital elevation models and soils maps. With the OA not exceeding 89%, this may be explained by the fact that only two variables were considered, and with the addition of more variables, the accuracy may improve. Across all accuracy assessment results, the PA was significantly lower than the UA. The PA illustrates the probability that a particular land cover type of an area on the ground is correctly classified. There was a lower chance that water pixels were correctly classified, due to the size, shape and depth of the pools. The UA illustrates its reliability and that the class on the map will be present on the ground. The UA values were considerably higher. This may be due to the fact that more pixels in the classified map represented non-water, rather than water. These results were also seen in Fisher et al. (2016), where PA values were lower than the UA values.

UNIVERSITY of the
WESTERN CAPE

The estimated surface water area of the water bodies was assessed on their accuracy by using the RMSE to compare the observed surface water area, from the reference datasets against the estimated surface water area, from the classified images. The results in this study showed that the NDWI had the lowest RMSE, when applied to the Sentinel-2 TOA reflectance datasets across all the study sites. Sarp & Ozcelik (2017) estimated the surface water area of a lake in Turkey and found that the NDWI performed significantly better than all other methods, with a RMSE ranging from 52 – 62 m^2. The results of this study agreed with Sarp & Ozcelik (2017) that the NDWI showed more promising results in accurately estimating surface water area. A recent study by Ogilvie et al. (2018) used Sentinel-2 imagery to monitor small surface water bodies in northern Africa. By replacing Landsat 8 with Sentinel-2, the RMSE decreased significantly, when using the multiband methods for surface water classification. The studies by Yamazaki et al. (2015), Du et al. (2016) and Ogilvie et al.

http://etd.uwc.ac.za/

(2018) showed that an increase in spatial resolution reduced the RMSE, which was also seen in the results presented in this chapter. The lowest RMSE for Sentinel-2 was 48.09 m^2, while this was 51.83 m^2 for Landsat 8.

4.5 Summary

The accuracy of the classified maps varied, depending on the sensor used, the pre-processing steps undertaken, the multiband method applied and the area of study. The overall accuracies ranged from 52 – 89% across all multiband methods applied to the different pre-processed datasets. Despite Landsat 8 datasets being pan-sharpened to 15 m spatial resolution, Sentinel-2 was more superior in identifying surface water. All multiband methods maintained a relatively high accuracy in classifying surface water; however, some were more successful. Multiband methods that were applied to the Sentinel-2 TOA reflectance datasets maintained the highest accuracy across all regions, with an average OA of 82%. Of those values, the NDWI maintained the highest accuracy, with an average OA of 85% and lowest RMSE of 48.09 m^2. Cloud cover and shadows had a significant impact in the misclassification of surface water pixels, despite the cloud-masking datasets available from the Sentinel-2 data. The NDWI, when applied to Sentinel-2 TOA reflectance datasets, was shown to be the most suitable for surface water mapping in non-perennial rivers in the Western Cape. The Sentinel-2 TOA reflectance dataset and NDWI were used to monitor the surface water availability in selected non-perennial rivers from 2016 – 2017.

UNIVERSITY of the
WESTERN CAPE

http://etd.uwc.ac.za/

5. ESTIMATION OF SURFACE WATER AVAILABILITY IN POOLS

5.1 Introduction

Long-term surface water monitoring provides an insight into the availability of freshwater resources. The use of multi-temporal remote sensing datasets can provide fast, accurate and cost-effective estimations of surface water availability for water resources management. This chapter explores the potential of using Sentinel-2 remotely-sensed datasets for the long-term monitoring of surface water in non-perennial rivers, and for addressing the second objective of this study, which is to describe the spatial and temporal changes of pools along non-perennial rivers, using remotely-sensed datasets. The dataset and classification method applied in this study were selected, based on the results in the previous chapter. The Sentinel-2 TOA reflectance product was selected as the dataset, and the NDWI was selected as the classification method that most accurately identifies surface water in non-perennial rivers.

5.2 Materials and Methods

The steps that were undertaken are outlined in Figure 4.1. Once the most suitable remotely-sensed dataset and multiband method had been selected, images covering a two-year period were downloaded and reclassified to illustrate water vs. non-water pixels through binary classification. All reclassified images were then layer-stacked to produce a summary layer and to illustrate surface water occurrence and recurrence from 2016 – 2017. A DEM was used to generate a hillslope for a shadow masking layer and it was overlain above the summary layer to remove any shadow pixels that had been misclassified as water pixels. The reclassified maps were then interpolated to calculate the changes in the pool areas, and a hydroperiod classification system, based on the work by Montgomery et al. (2018) was undertaken. The rivers selected for monitoring pool dynamics were the same rivers that were assessed in Chapter 4, namely the Nuwejaars, Breede, Touws and Tankwa Rivers.

UNIVERSITY of the WESTERN CAPE
http://etd.uwc.ac.za/

5.2.1 Data collection

Remote sensing data

Sentinel-2 data was downloaded via the European Spaces Agency's Copernicus Open Access Hub (https://scihub.copernicus.eu/), as Level-1C radiometrically- and geometrically-calibrated TOA reflectance products (ESA, 2015). All available cloud-free datasets were downloaded over a two-year period, from January 2016 to December 2017, for each river of study. A total of eleven images were available for the Nuwejaars River, fourteen for the Breede River, twenty for the Touws River and thirteen for the Tankwa River (Table 5.1). Equal intervals over the two years were established for each river to achieve consistency and to avoid bias for certain months or seasons i.e. more images are available in the summer months, due to less cloud cover. If all the available cloud-free imagery were used, there would be inconsistency in the mapping of surface water recurrence during different seasons of the year.

Table 5.1 Dates of available cloud-free Sentinel-2 satellite images for the rivers between 2016 and 2017

Nuwejaars River	Breede River	Touws River	Tankwa River
2016/02/06	2016/01/04	2016/01/04	2016/02/06
2016/04/06	2016/03/04	2016/02/06	2016/04/06
2016/06/05	2016/04/26	2016/03/04	2016/06/05
2016/08/04	2016/06/22	2016/04/26	2016/08/04
2016/10/13	2016/08/11	2016/06/05	2016/10/03
2016/12/22	2016/10/03	2016/07/02	2016/12/02
2017/03/02	2016/12/02	2016/08/01	2017/01/31
2017/05/21	2017/01/18	2016/09/23	2017/03/22
2017/08/09	2017/03/19	2016/10/30	2017/05/21
2017/10/28	2017/05/08	2016/12/02	2017/07/20
2017/12/27	2017/07/07	2017/01/08	2017/09/18
	2017/09/03	2017/02/17	2017/11/12
	2017/10/28	2017/03/29	2017/12/22
	2017/12/27	2017/05/21	
		2017/06/30	
		2017/08/06	
		2017/09/10	
		2017/10/13	
		2017/11/12	
		2017/12/19	

http://etd.uwc.ac.za/

Meteorological data

The daily rainfall and daily temperature data were obtained for selected weather stations from the South African Weather Services (SAWS) and the Agricultural Research Council (ARC). Data were collected from the 1st of January 2016 to the 31st of December 2017 from weather stations near the selected rivers. The daily rainfall and temperature values were used to correlate to the surface water area changes in the non-perennial rivers, in order to improve the understanding of their spatio-temporal dynamics and influences. A list of the weather stations used is shown in Appendix 5.1, together with their names and co-ordinates.

5.2.2 Remotely-sensed data analysis

The NDWI was applied to each image through batch processing in ArcMap. The classified images were then reclassified to create a binary image that illustrated the water and non-water pixels. Boolean logic was used to reclassify the images. The water pixels were given a weighted value of one to ensure that when the reclassified images were layer stacked, water occurrence and recurrence could be easily identified. All reclassified images for each river were then layer-stacked, to create a summary layer. This was undertaken to illustrate the permanence of surface water within the non-perennial rivers.

The next step was to eliminate the effects of shadows that cause the misclassification of surface water. A 30 m DEM was used to minimise the effects of mountainous shadows. A hillshade was created, using the azimuth and altitude values from the metadata of Sentinel-2. The DEM was resampled to 10 m to match the spatial resolution of Sentinel-2, using the nearest neighbour technique. A shadow mask was developed from the hillshade to remove misclassified pixels, without eliminating or altering the true water pixels. Certain study areas had to be eliminated, due to the location of surface water bodies below a mountain/hill drop and those that were constantly under shadow (Appendix 5.2).

The next step involved interpolating the reclassified maps to obtain the surface water area changes in the non-perennial rivers. This was done in order to estimate the variability of surface water over a period of two years. Surface water area estimates were compared to the daily mean rainfall and temperature records from weather stations within the proximity of pools, to better understand the variations of surface water area change.

The final step involved developing a hydroperiod of the surface water present in the non-perennial rivers i.e. the presence and duration of open water for a given period of time. The

UNIVERSITY of the WESTERN CAPE
http://etd.uwc.ac.za/

reclassified maps were then summarised into a single frequency map. Surface water permanence was measured using an 'equal-frequency' routine on the number of images captured for each river per year, based on the methodology used by Montgomery et al. (2018). An unclassified pixel frequency map was developed from this, illustrating the number of times that a pixel is identified as water. The next step involved classifying the surface water permanence map into a surface water hydroperiod map, based on the classification system in Table 2.3. one to two months represented temporary water (Class II), three to four months represented seasonal water (Class III), and five months or more represented semi-permanent/permanent water (Classes IV and V). The resulting product illustrated a summary hydroperiod map of surface water permanence in the non-perennial rivers of study.

5.3 Results

The results presented in this chapter address the second objective of this study, namely, to describe the spatial and temporal changes of surface water along non-perennial rivers, using remotely sensed datasets. The results quantify the spatial and temporal variability of pools within selected non-perennial rivers, using the appropriate methods assessed in Chapter 4. The regions of interest along the Nuwejaars, Breede, Touws and Tankwa Rivers were assessed, to better understand the surface water availability. The results were compared to the daily mean rainfall and daily mean temperature to provide a better understanding for the seasonal variation of surface water availability in the non-perennial rivers.

UNIVERSITY of the
WESTERN CAPE

5.3.1 Mapping surface water recurrence in non-perennial rivers

The Nuwejaars River

It is challenging to map the occurrence of surface water along an entire river due to its varying width and length. Therefore, regions of interest were selected along the river to map the spatial and temporal variability of a number of pools. The frequency of water occurrence was analysed in selected regions of the Nuwejaars River over two years (Figure 5.1). The location of the pools that were examined are shown by the coordinates indicated on the border of the map. The frequency of surface water occurrence was calculated, based on the number of available cloud-free images. Surface water that was identified in all of the images suggest water was present 100% of the time, shown by the darker blue. Surface water identified in one of the images suggest water was present 9% of the time, shown by the lighter blue.

http://etd.uwc.ac.za/

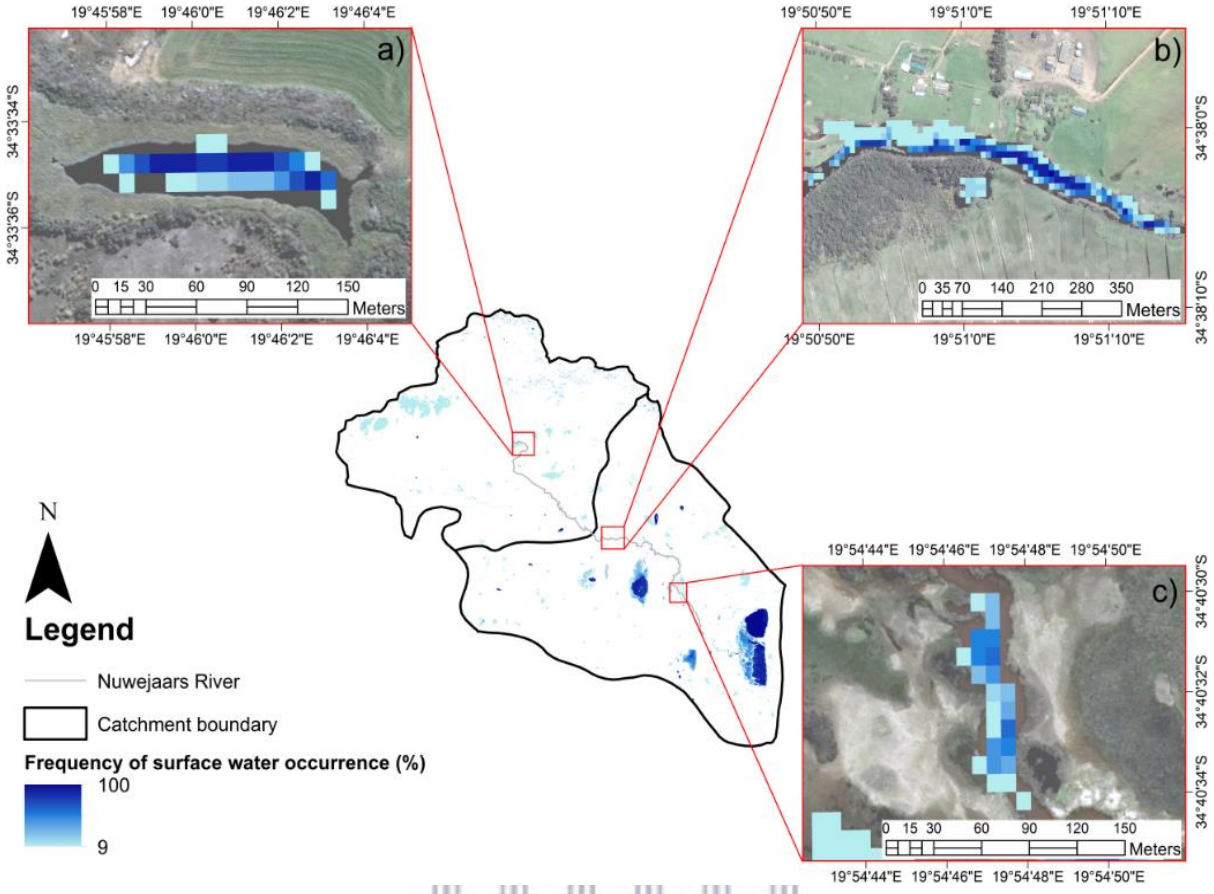

Figure 5.1 Frequency of surface water recurrence within the Heuningnes Catchment and Nuwejaars River. (a) illustrates a pool in the upper part of the Nuwejaars River, (b) illustrates a pool in the middle part and (c) illustrates a pool in the lower part. Source: Aerial photography

UNIVERSITY of the
WESTERN CAPE

The variation in pool area over two years was analysed along the Nuwejaars River (Figure 5.2). The variations in pool sizes suggest that they followed the natural seasonal changes, with the pool size decreasing during the summer months, while they increased during the winter months. The maximum area estimated for Pool (a) was 1 672 m^2 on the 5th of June 2016 (Figure 5.2). The estimated pool area then decreased to 0 m^2 on the 22nd of December 2016, and increased again in 2017 (Figure 5.2). The estimated area for Pool (b) and Pool (c) followed a similar pattern. The maximum pool area for Pool (b) was 20 718 m^2, recorded on the 4th of August 2016, and then decreased during the summer of late 2016 and early 2017. The maximum pool area for Pool (c) was estimated at 2 025 m^2 on the 4th of August 2016 and decreased to 0 m^2 from December 2016 to May 2017 (Figure 5.2). The results suggest that pool area decreased from 2016 to 2017 and that 2017 was a dry year.

http://etd.uwc.ac.za/

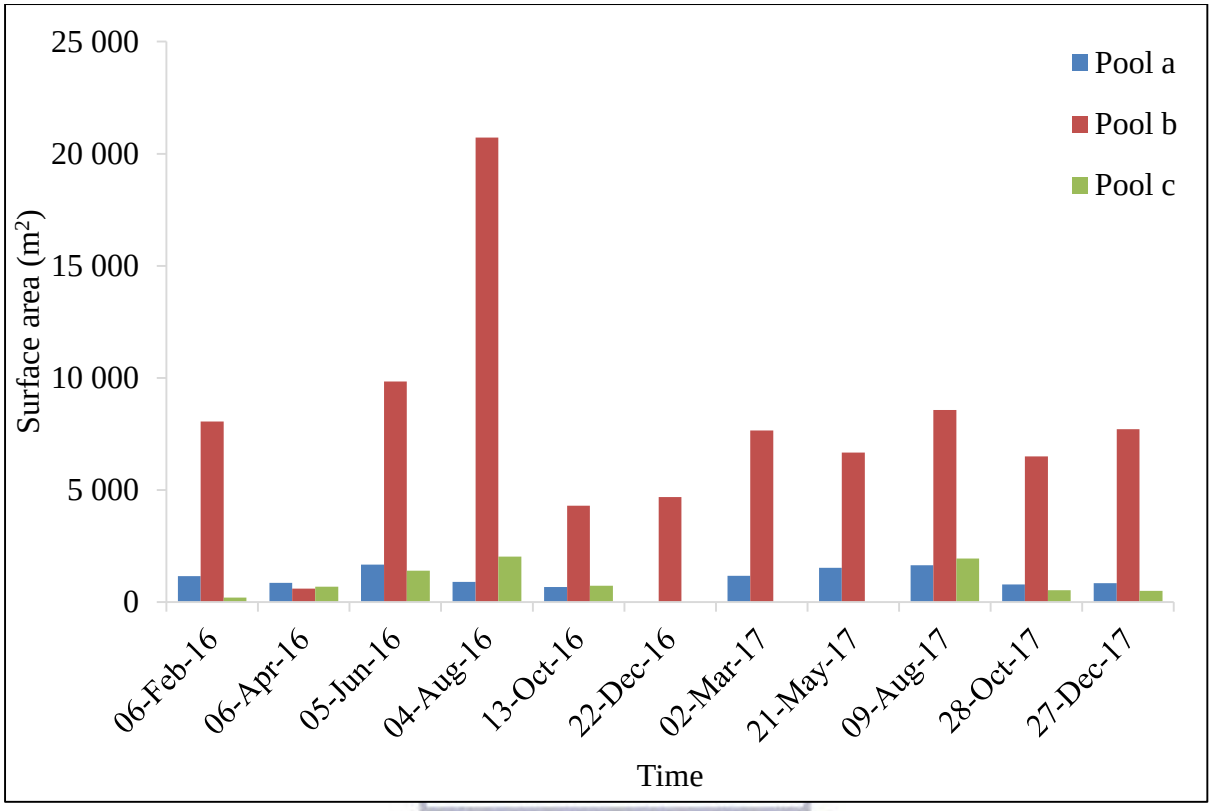

Figure 5.2 Surface water area estimates over a two-year period of selected regions within the Nuwejaars River. Pool (a) illustrates a pool in the upper part of the Nuwejaars River, (b) illustrates a pool in the middle part and (c) illustrates a pool in the lower part

UNIVERSITY of the
WESTERN CAPE

The Breede River

Regions of interest along the Breede River channel were selected to illustrate the spatial and temporal variability of a small number of pools. This was undertaken, as it is challenging to map the occurrence and recurrence of surface water along the entire stretch of the river. The frequency of water occurrence was analysed in the regions of interest for the Breede River over two years (Figure 5.3). The location of the pools is shown by the coordinates indicated along the border of the map. During the period analysed, based on the number of images, the frequency of the occurrence of water was calculated. The water identified in all fourteen images over the two years suggested that water was present 100% of the time, which is shown by the darker blue. The water identified in only one of the images suggested a water presence for 7% of the time, as shown by the lighter blue.

http://etd.uwc.ac.za/

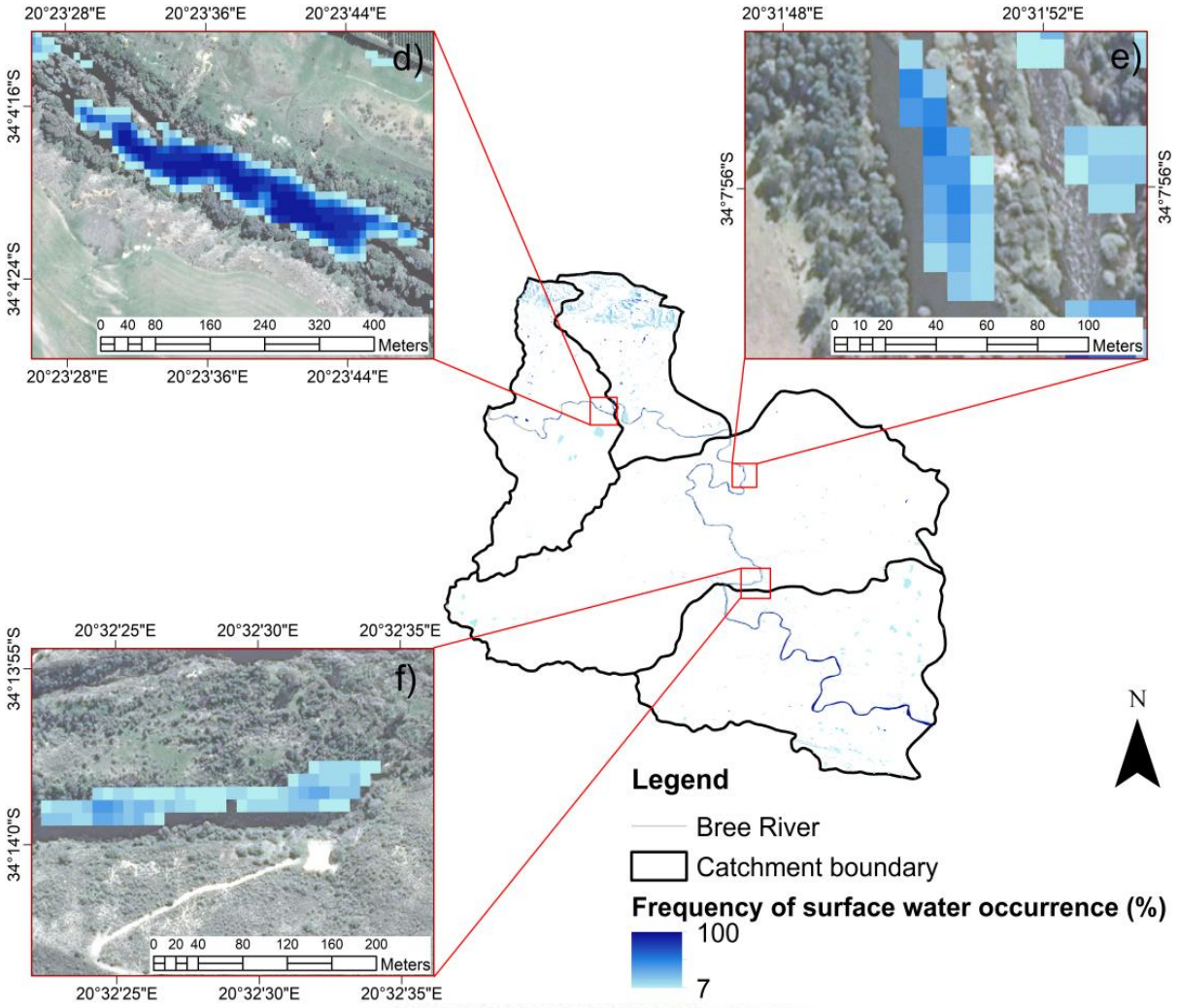

UNIVERSITY of the
WESTERN CAPE

Figure 5.3 Frequency of surface water recurrence within the Breede River. (d) Illustrates a pool in the upper part of the Breede River, (e) illustrates a pool in the middle part and (f) illustrates a pool in the lower part. Source: Aerial photography

The variation in the pool area over two years was analysed along the Breede River (Figure 5.4). The variations in pool sizes suggest that they followed the natural seasonal changes, with the pool size decreasing during the summer months, while it increased during winter months. On the 3rd of October 2016, no surface water was identified in any of the pools. This suggests that the Sentinel-2 failed to identify surface water on that day and that it was not a case of water drying up. The maximum area estimated for Pool (d) was 25 449 m^2 on the 22nd of June 2016 (Figure 5.4). The estimated pool area then decreased to a minimum of 9 112 m^2 on the 27th of December 2017, excluding the 0 m^2 estimated on the 3rd of October 2016. The estimated area for Pools (e) and (f) were significantly smaller. The maximum pool area for Pool (e) was 1 967 m^2, recorded on the 22nd of June 2016. During 2017, Pool (e) decreased to a minimum of 137 m^2 on the 28th of October 2017. The maximum pool area for Pool (f) was

http://etd.uwc.ac.za/

estimated at 6 045 m^2 on the 22nd of June 2016. During 2017, Pool (f) decreased to a minimum of 0 m^2 on the 3rd of September 2017 (Figure 5.4). The results suggest that pool area in the Breede River also decreased from 2016 to 2017.

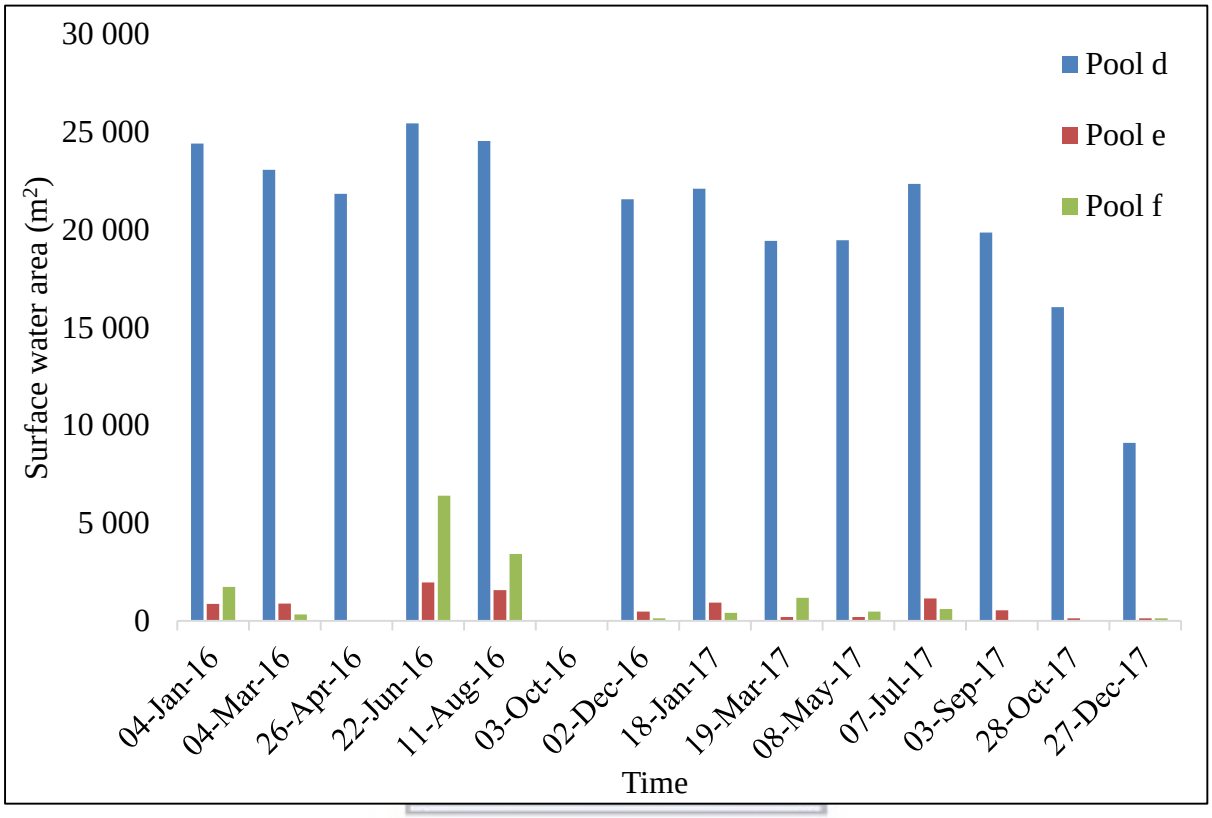

Figure 5.4 Surface water area estimates over a two-year period of selected regions within the Breede River. (d) illustrates a pool in the upper part of the Breede River, (e) illustrates a pool in the middle part and (f) illustrates a pool in the lower part

UNIVERSITY of the
WESTERN CAPE

The Touws River

Regions of interest along the Touws River channel were selected to describe the spatial and temporal variability of a small number of pools, due to the challenge of mapping surface water along the entire stretch of the river. The frequency of water occurrence was analysed in the regions of interest for the Touws River over two years (Figure 5.5). The location of the pools is shown by the coordinates indicated along the border of the map. The frequency of surface water occurrence was calculated, based on the number of available cloud-free images. Water identified in all twenty images over the two years suggested a water presence 100% of the time, which is shown by the darker blue. Water identified in only one of the images suggested a water presence for 5% of the time, as shown by the lighter blue. The large

http://etd.uwc.ac.za/

regions of shadow were misclassified as water, despite the shadow mask that was generated by the DEM in the catchment. This is because the Touws River Catchment area is situated in a mountainous region of the Western Cape.

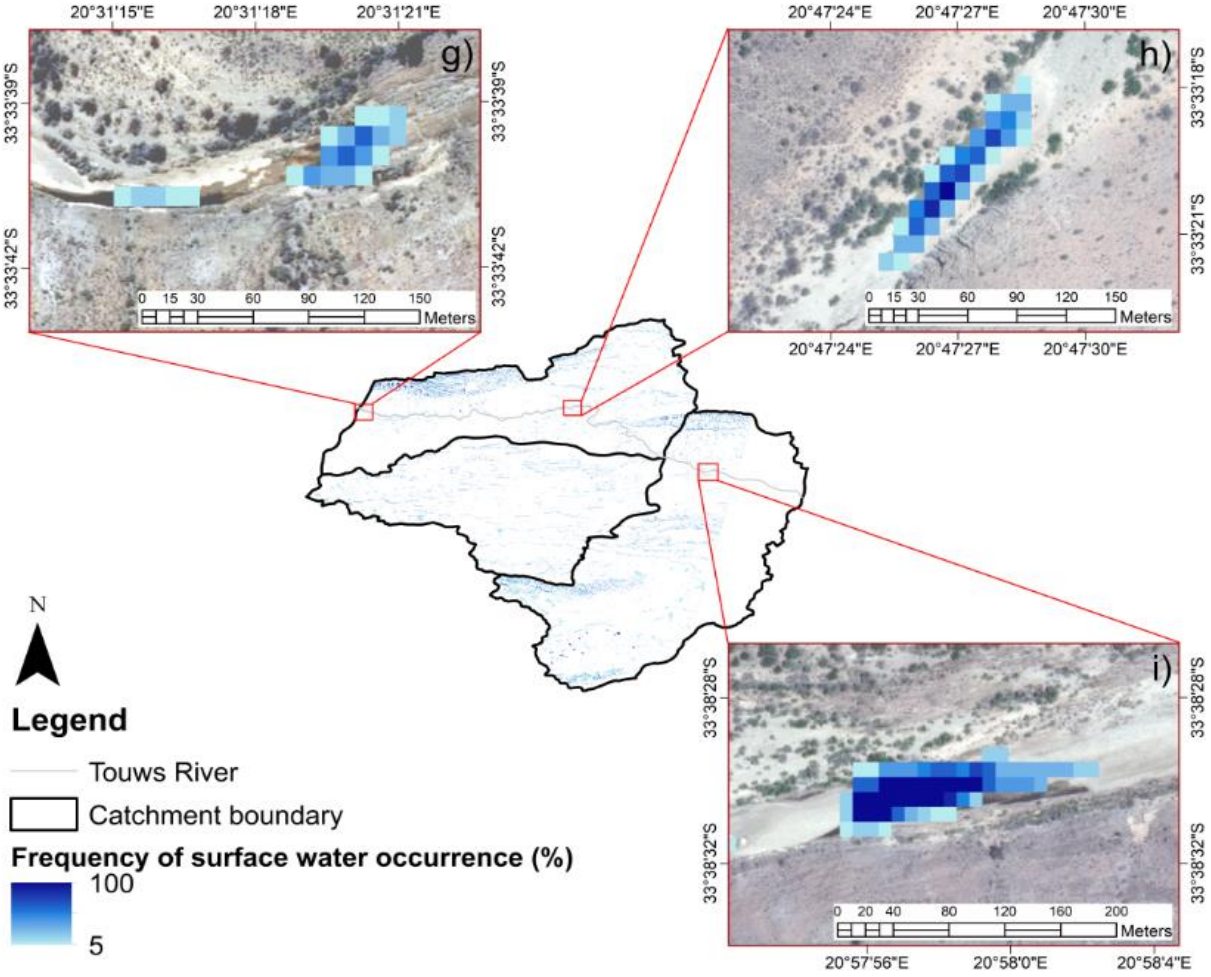

Figure 5.5 Frequency of surface water recurrence within the Touws River. (g) illustrates a pool in the upper part of the Touws River, (i) illustrates a pool in the middle part and (h) illustrates a pool in the lower part. Source: WorldView-2

The variation in the pool area over two years was analysed along the Touws River (Figure 5.6). The maximum area estimated for Pool (g) was 1 681 m^2 on the 2nd of July 2016 (Figure 5.6). The estimated pool area then decreased to 0 m^2 from the 23rd of September 2016 to the 8th of January 2017, and again from the 10th of September 2017 to the 19th of December 2017. The pool area was significantly smaller in the Touws River than in the Nuwejaars and Breede Rivers. With the Touws River Catchment being an arid catchment, the results suggest that Pool (g) dried up during the summer months and filled up again during the winter months. The maximum pool area for Pool (h) was 2 651 m^2, recorded on the 21st of May 2017 (Figure

http://etd.uwc.ac.za/

5.6). The pool surface area was estimated at 0 m^2 from the 1st of August 2016 to the 17th of February 2017, suggesting that the pool dried up or was too small to be identified by Sentinel-2. The maximum pool area for Pool (i) was estimated at 4 216 m^2 on the 1st of August 2016. No surface water was identified in Pool (i) from the 29th of March 2017 to the 21st of May 2017 (Figure 5.6). Overall, the pools analysed in the Touws River suggest that the pool area also decreased from 2016 to 2017.

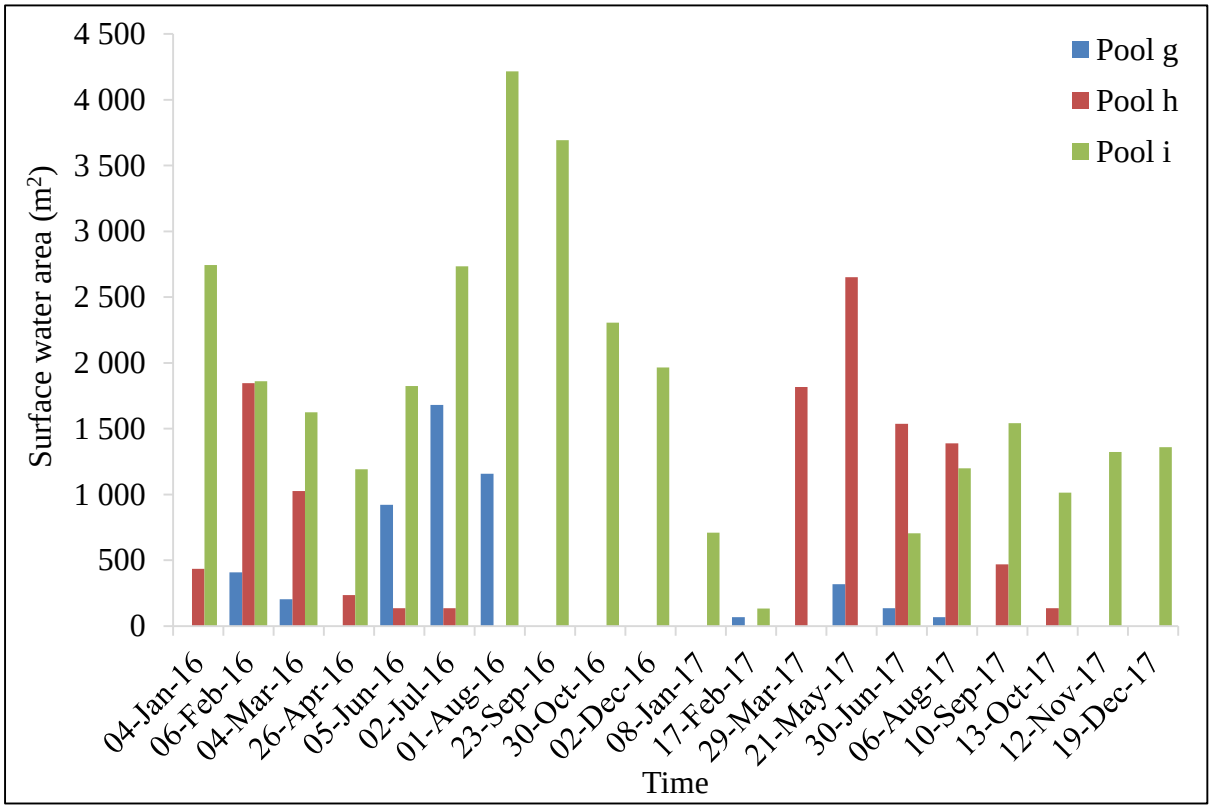

Figure 5.6 Surface water area estimates over a two-year period of selected regions within the Touws River. (g) illustrates a pool in the upper part of the Touws River, (h) illustrates a pool in the middle part and (i) illustrates a pool in the lower part

The Tankwa River

Regions of interest along the Touws River channel were selected to describe the spatial and temporal variability of a small number of pools, due to the challenge of mapping surface water along the entire stretch of the river. The frequency of water occurrence was analysed in the regions of interest for the Touws River over two years (Figure 5.7). The locations of the pools are shown by the coordinates indicated along the border of the map. The frequency of surface water occurrence was calculated, based on the number of available cloud-free images.

http://etd.uwc.ac.za/

The water identified in all thirteen images over the two years suggested a water presence for 100% of the time, which is shown by the darker blue. The water identified in only one of the images suggested a presence of surface water 8% of the time, shown by the lighter blue. A large region on the western side of the Tankwa Karoo Catchment showed a presence of surface water on the 21st of May 2017 (Figure 5.7). The results suggest either a misclassification of surface water from the Sentinel-2, or the surface water and soil moisture may have been present at the time when the image was captured after a rainfall event.

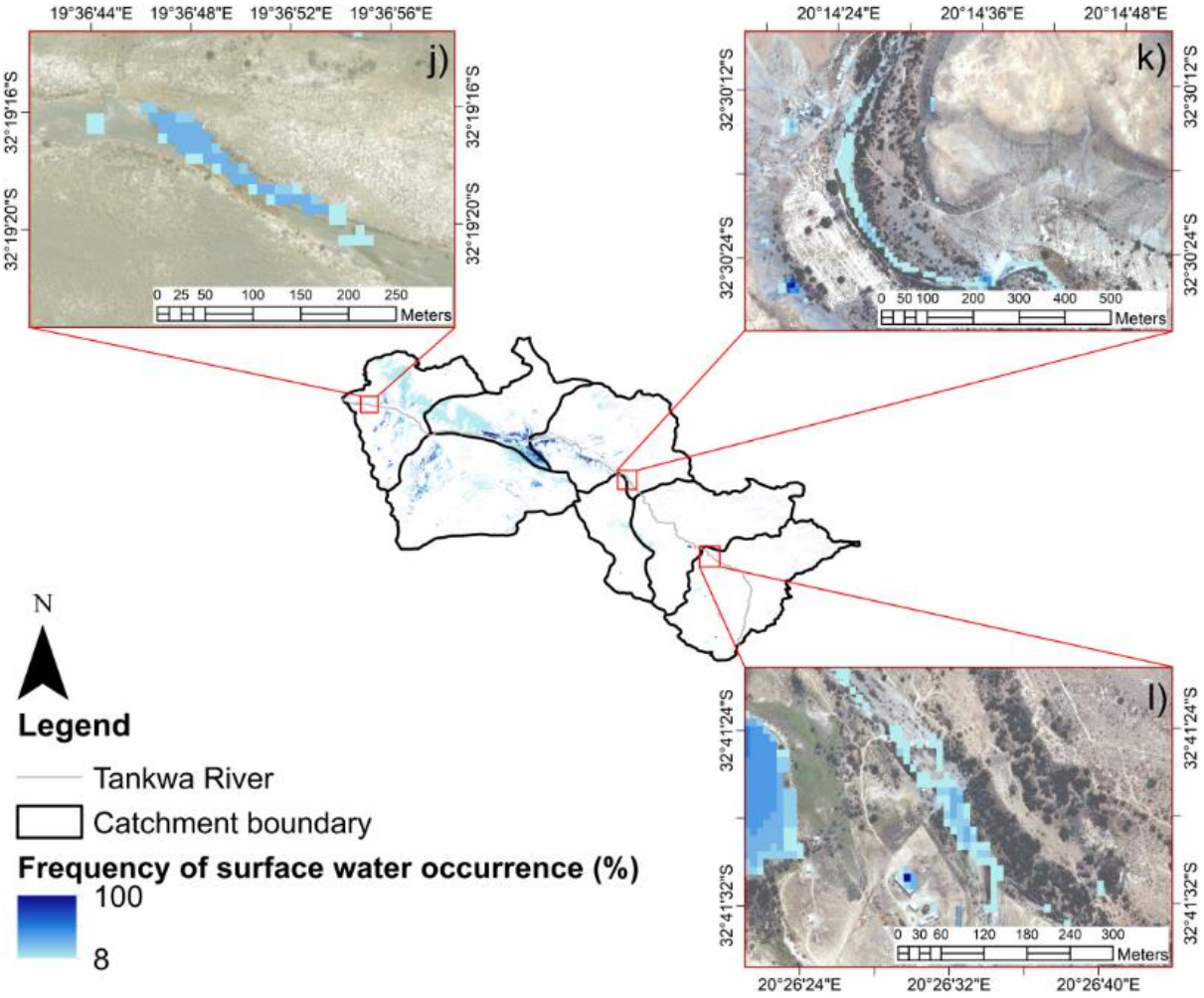

Figure 5.7 Frequency of surface water recurrence within the Tankwa River. (j) illustrates a pool in the upper part of the Tankwa River, (k) illustrates a pool in the middle part and (l) illustrates a pool in the lower part. Source: Aerial photography

http://etd.uwc.ac.za/

The variation in pool area over two years was analysed along the Tankwa River (Figure 5.8). The maximum area estimated for Pool (j) was 7 269 m^2 on the 4th of August 2016. No surface water was identified from the 2nd of December 2016 to the 22nd of December 2017. This suggests that either Sentinel-2 could not identify the surface water from that time, or the pool dried up. The maximum pool area for Pool (k) was 10 756 m^2, on the 4th of August 2016 (Figure 5.8). No surface water was identified on the 31st of January 2017 and from the 21st of May to the 22nd of December 2017. The maximum pool area for Pool (l) was estimated at 4 397 m^2 on the 6th of February 2016. No surface water was identified in Pool (l) on the 3rd of October 2016 to the 31st of January 2017 and from the 21st of May 2017 to the 22nd of December 2017 (Figure 5.8). No surface water was identified in any of the pools from the 21st of May 2017 to the 22nd of December 2017. This suggests that the pools either dried up completely, as the Tankwa Karoo is considered to be a very arid region, or they were too small to be identified by the Sentinel-2 satellite. Overall, the pools analysed in the Tankwa River suggest that the pool area also decreased from 2016 to 2017.

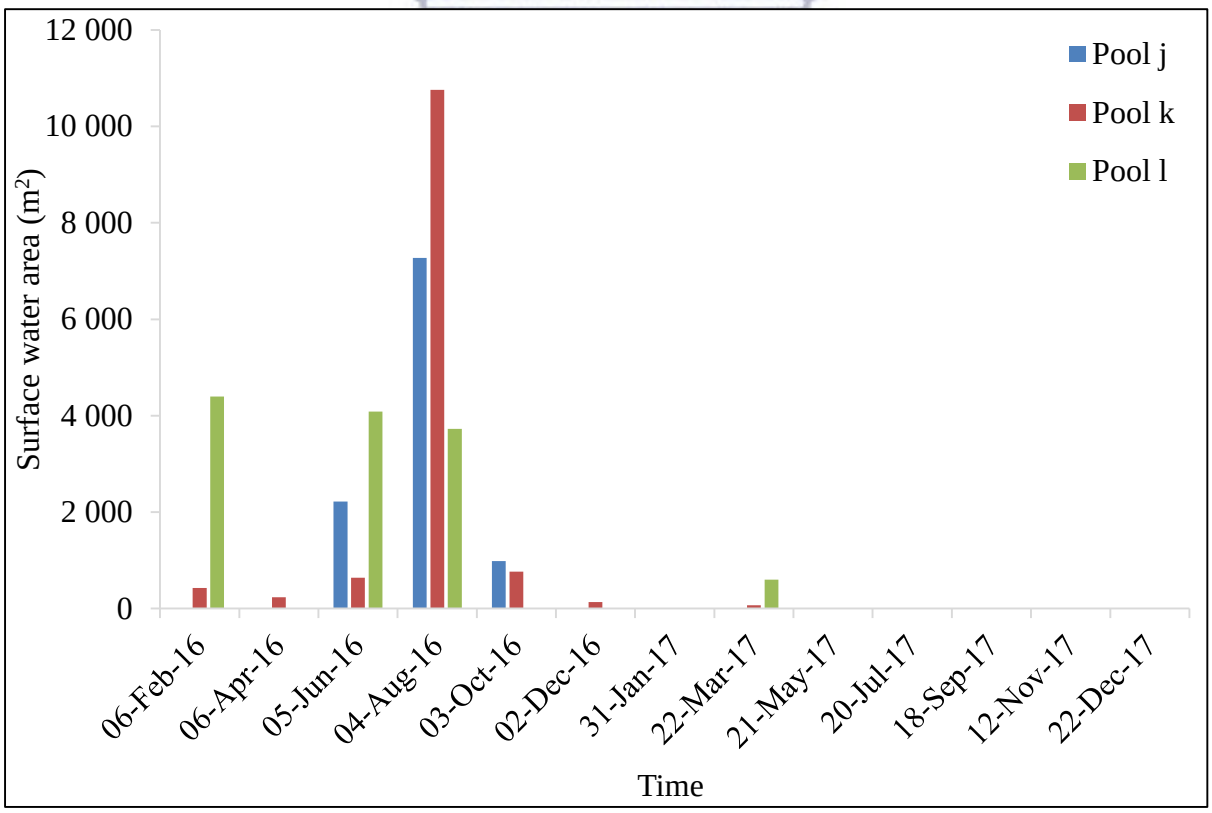

Figure 5.8 Surface water area estimates over a two-year period of selected regions within the Tankwa River. (j) illustrates a pool in the upper part of the Tankwa River, (k) illustrates a pool in the middle part and (l) illustrates a pool in the lower part

http://etd.uwc.ac.za/

5.3.2 Comparison of surface water area change with daily mean rainfall and temperature

The Nuwejaars River

The daily mean rainfall and temperature were compared to the estimated surface water area for selected regions of interest along the Nuwejaars River (Figure 5.9). High rainfall occurrences were followed by increases in estimated surface water area. This is most notably shown during July 2016 in Figure 5.9 (b). The inundated areas decreased during periods of low and no rainfall. This is seen from November 2016 to January 2017, where low rainfall was recorded, followed by no surface water identified (Figure 5.9 a and c). Figure 5.9 (c) showed a weak relationship between the daily mean rainfall and the water area from December 2016 to May 2017. The surface water area decreased during summer, a period with high evaporation rates, as indicated by the notable temperature changes in Figure 5.9 (b). However, an exception is seen from December 2016 to May 2017 in Figure 5.9 (c), where surface water was not identified in Pool (c). This may have been due to the pool drying up, or Sentinel-2 being unable to classify surface water in the pool, as it was too small.

UNIVERSITY of the
WESTERN CAPE

http://etd.uwc.ac.za/

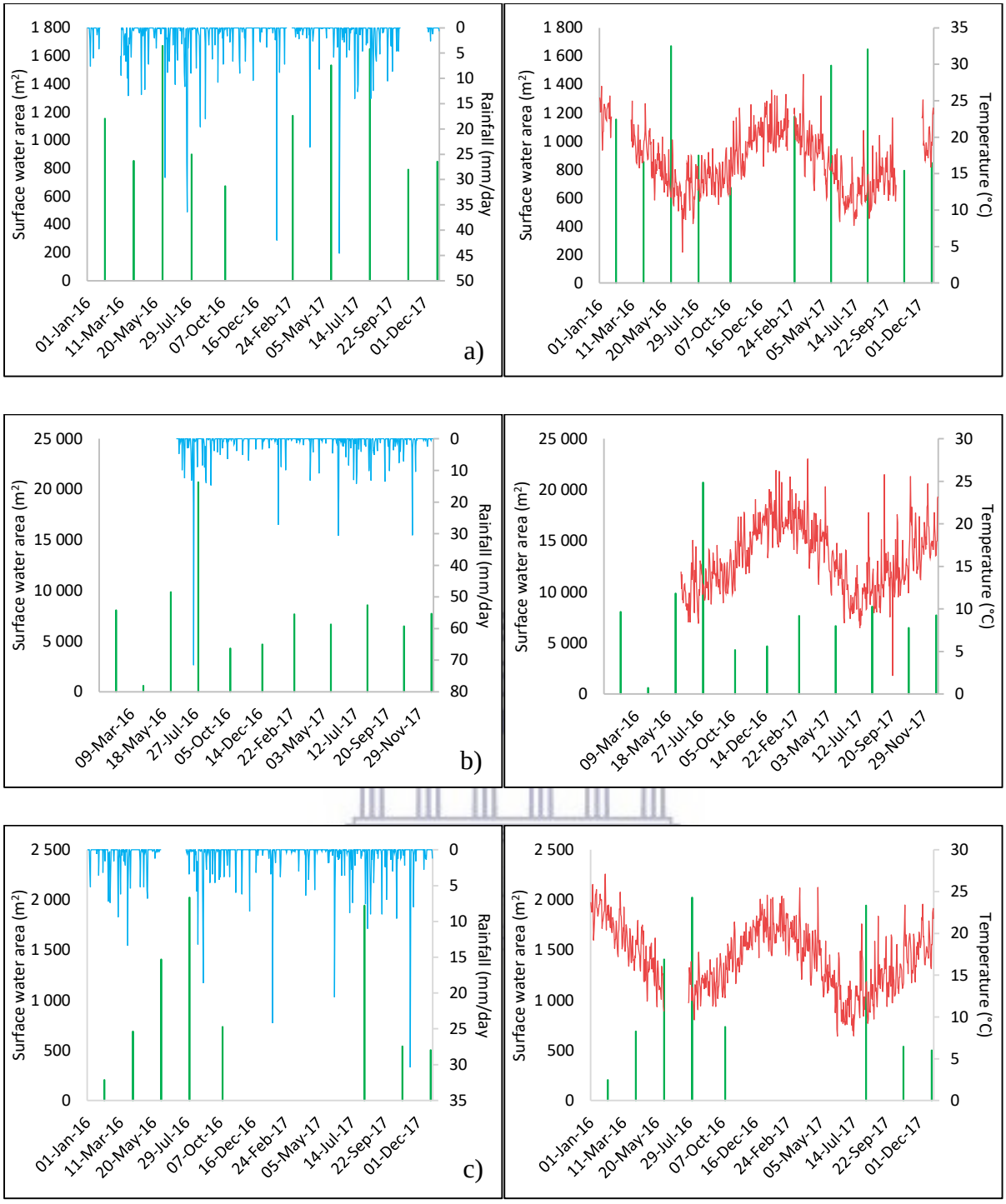

Figure 5.9 Comparison of daily mean rainfall (blue) and temperature (red) to estimated surface water area (green) change of Pool (a), Pool (b) and Pool (c) from 2016 to 2017 in the Nuwejaars River

http://etd.uwc.ac.za/

The Breede River

The daily mean rainfall and temperature were compared to the estimated surface water area for the selected regions of interest along the Breede River (Figure 5.10). No significant relationship was shown between the estimated surface water areas and the rainfall. For example, in April 2016, no water was identified in Pool (e), despite previous rainfall. The daily mean temperature showed a strong relationship to surface water area change in all regions of interest along the Breede River. Higher temperatures were associated with low pool area estimates, while lower temperatures were associated with larger pool area estimates, although, the Western Cape receives larger amounts of rainfall during winter and the pool area is expected to increase during this time. Higher temperatures are associated with higher rates of evaporation, while lower temperatures are associated with lower rates of evaporation, which means that less water is lost through evaporation during winter.

UNIVERSITY of the
WESTERN CAPE

http://etd.uwc.ac.za/

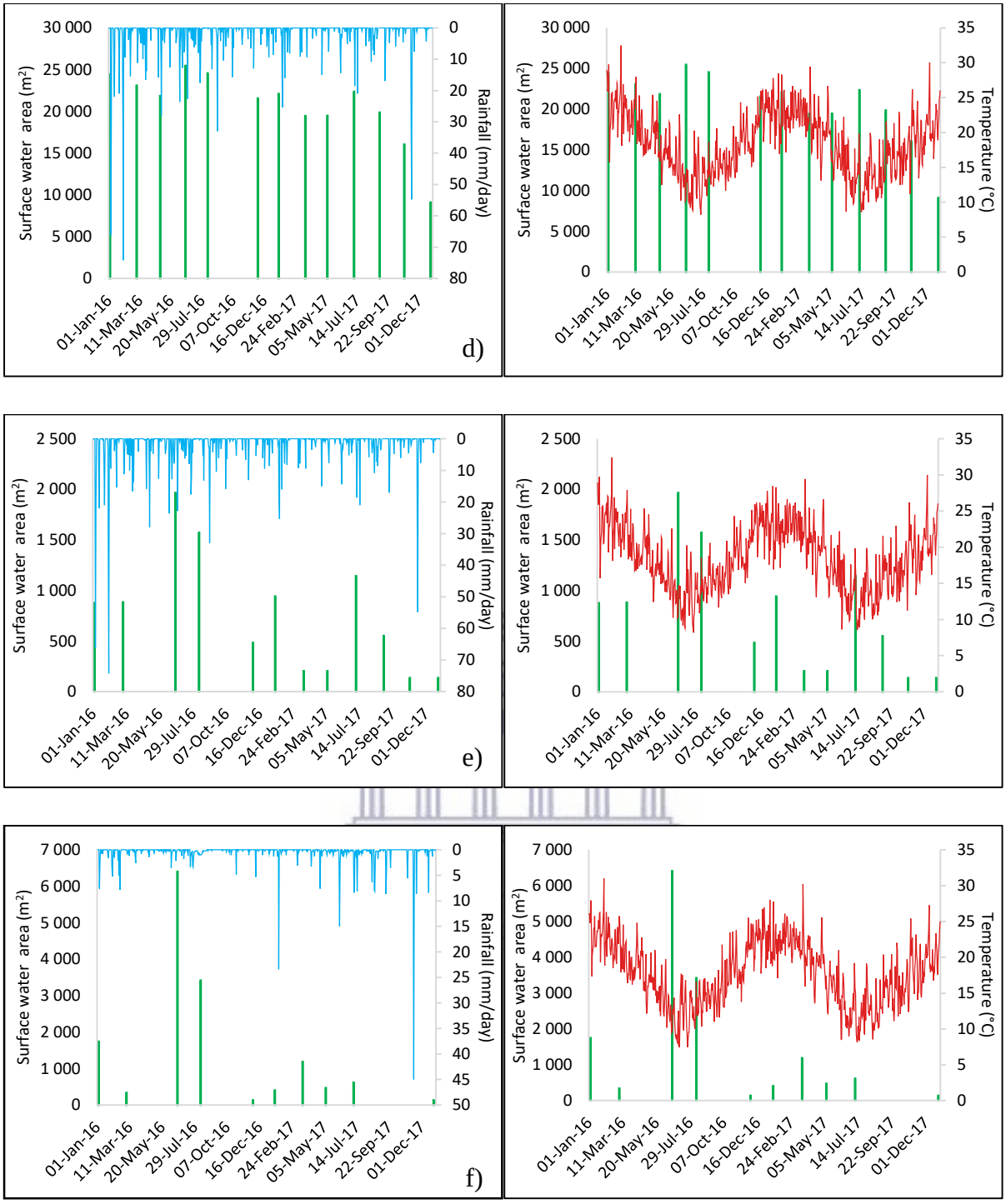

Figure 5.10 Comparison of daily mean rainfall (blue) and temperature (red) to estimated surface water area (green) change of Pool (a), Pool (b) and Pool (c) from 2016 to 2017 in the Breede River

http://etd.uwc.ac.za/

The Touws River

A strong relationship between the estimated surface water area and rainfall was seen across the pools along the Touws River (Figure 5.11). Pool area estimates increased after periods of high rainfall, and smaller surface water area estimates, to no surface water, was identified after periods of no rainfall. The only instance where the rainfall and estimated pool area did not show a strong relationship was from June to October 2016 in Figure 5.11 (i), where consistent rainfall was recorded, but the estimated pool area decreased. This was seen again in May 2017, where a low rainfall was recorded, but the pool surface area increased. A strong relationship was seen between the pool area change and temperature change over the two years. High temperatures resulted in a high rate of evaporation; therefore, the pool size was expected to decrease during higher temperatures. This was seen throughout the pools in the Touws River, during the summer period of 2016 and 2017.

UNIVERSITY of the
WESTERN CAPE

http://etd.uwc.ac.za/

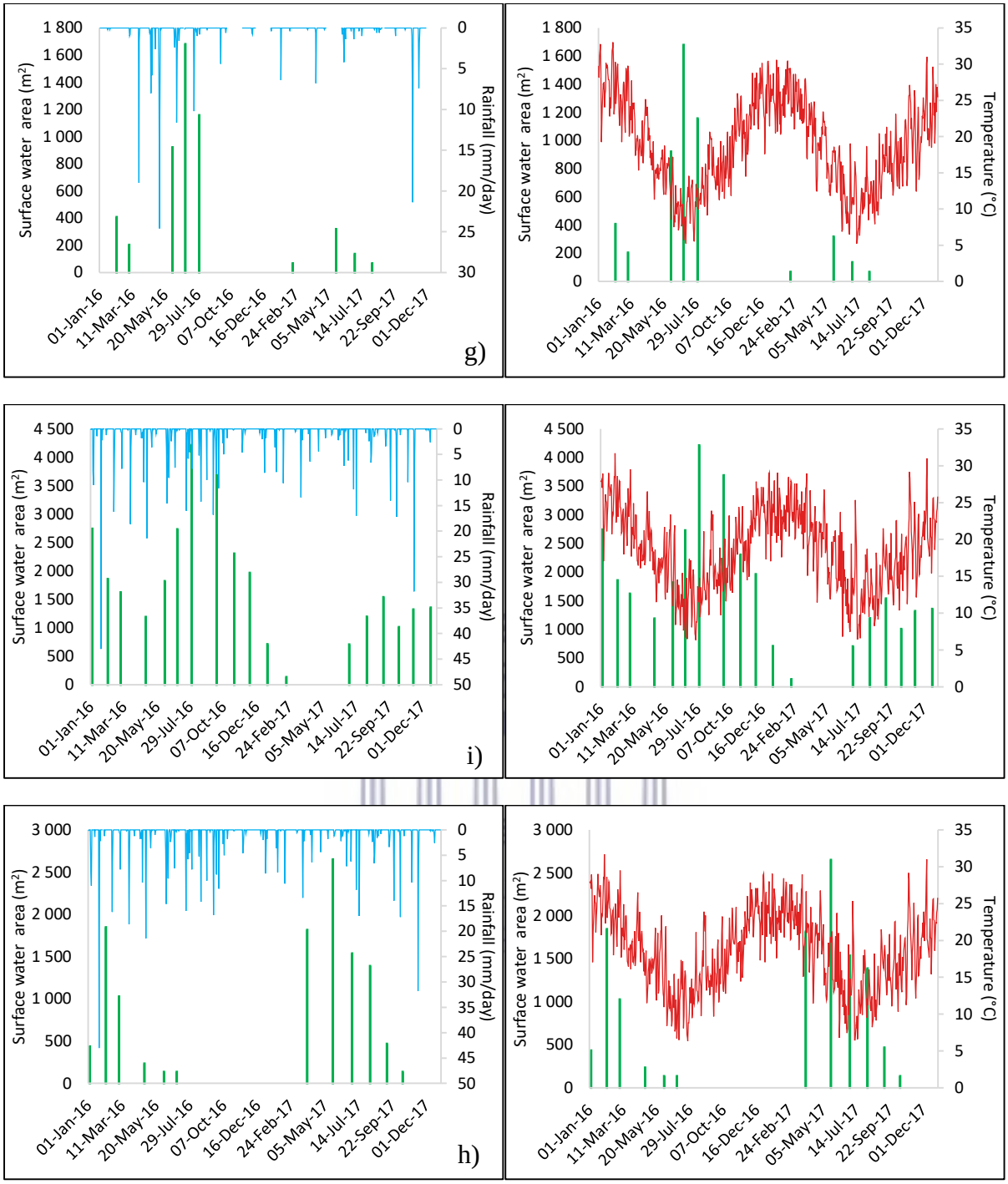

Figure 5.11 Comparison of daily mean rainfall (blue) and temperature (red) to estimated surface water area (green) change of Pool (a), Pool (b) and Pool (c) from 2016 to 2017 in the Touws River

http://etd.uwc.ac.za/

The Tankwa River

Figure 5.12 describes the relationship between the daily mean rainfall and estimated surface water area of selected pools in the Tankwa River. A strong relationship was seen between the rainfall and estimated surface water area in 2016 for Pool (j) and (k). The estimated surface water area for Pool (k) had a maximum surface area of 10 756 m^2 on the 4th of August 2016, after a three-day rainfall period from the 1st to the 3rd of August 2016. From April to December of 2017, no surface water was identified in any of the pools, despite the occurrence of rainfall. A strong relationship between the temperature and estimated surface water area was shown in Pools (j) and (k). Large pool area estimates were seen from June to September 2016 during low temperatures, with some days reaching temperatures of less than 0 °C. This was attributed to the low rate of evaporation during winter. There was no relationship between temperature and the estimated surface water area for Pool (l).

UNIVERSITY of the
WESTERN CAPE

http://etd.uwc.ac.za/

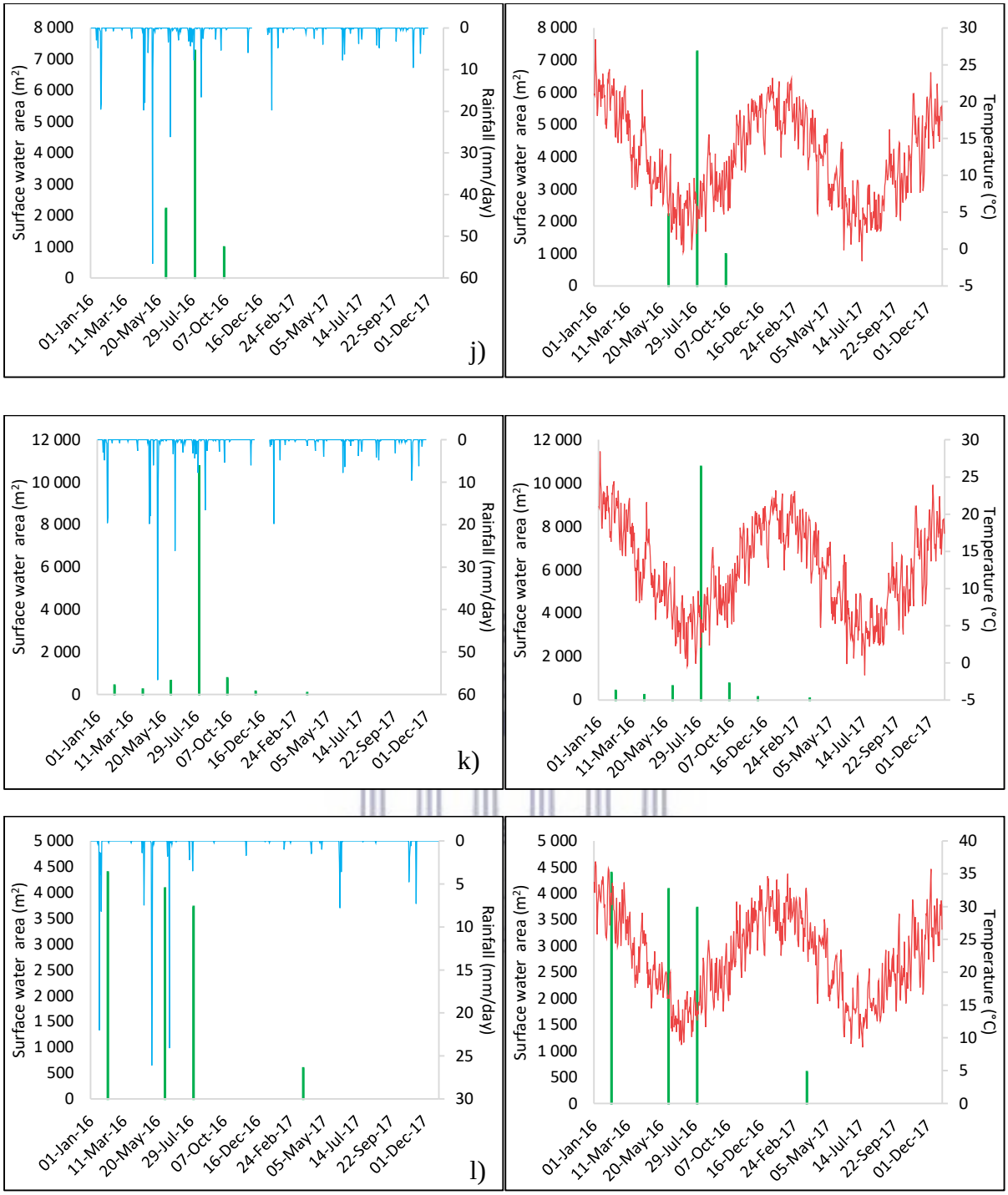

Figure 5.12 Comparison of daily mean rainfall (blue) and temperature (red) to estimated surface water area (green) change of Pool (j), Pool (k) and Pool (l) from 2016 to 2017 in the Tankwa River

http://etd.uwc.ac.za/

5.3.3 Hydroperiod mapping of pools

The hydroperiod for one pool in the Nuwejaars, Breede, Touws and Tankwa Rivers were assessed over a two-year period from 2016 to 2017 (Figure 5.13). This was done to determine the suitability for assessing the hydroperiod of pools in non-perennial rivers. The pool area of each hydroperiod for the pools assessed varied amongst the rivers (Figure 5.13). An overall decrease in pool area was shown for each hydroperiod in the different regions of interest. Pool (b) in the Nuwejaars River and Pool (k) in the Tankwa River showed the largest hydroperiod for temporary surface water in 2016. Pool (d) in the Breede River showed the largest hydroperiod for permanent surface water in 2016 and 2017. Pool (d) also maintained most of its water in 2016 and 2017, suggesting that this pool is permanent and not a temporary pool, as seen in Pool (k) in the Tankwa River. Pool (i) in the Touws River showed a similar pattern to Pool (d) in the Breede River. Pool (i) maintained a relatively stable surface water area across all three hydroperiods from 2016 to 2017. The overall decrease in pool area from 2016 to 2017, for each pool analysed in Figure 5.13, suggests that the pools were affected by the dry year experienced in 2017 in the Western Cape.

UNIVERSITY of the
WESTERN CAPE

http://etd.uwc.ac.za/

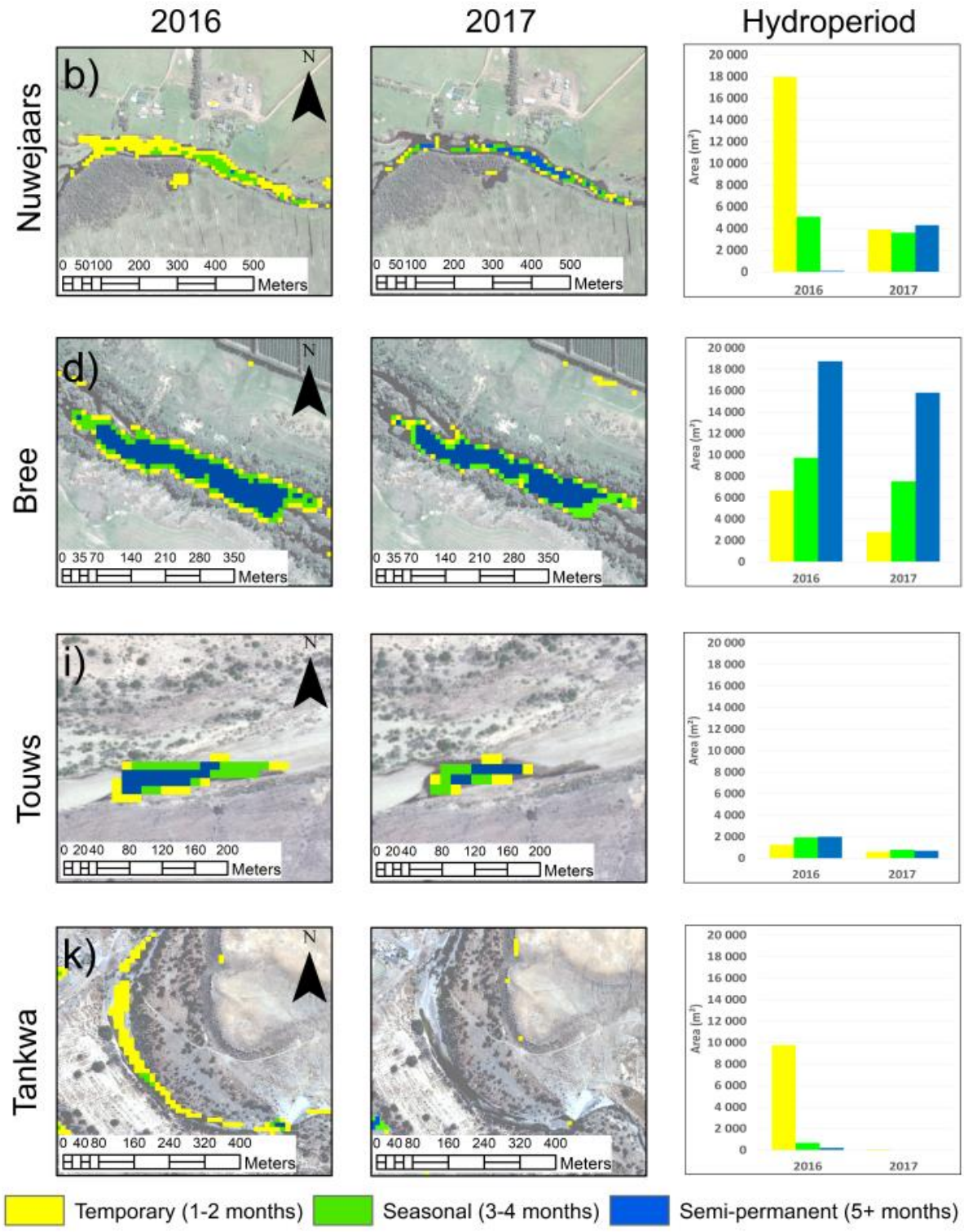

Figure 5.13 Hydroperiod of pools in the Nuwejaars, Breede, Touws and Tankwa Rivers for 2016 and 2017. Pool (b) in the Nuwejaars River, Pool (d) in the Breede River, Pool (i) in the Touws River and Pool (k) in the Tankwa River

http://etd.uwc.ac.za/

5.4 Discussion

Sentinel-2 provides a fine spatial resolution multispectral dataset for improved the monitoring of surface water in non-perennial rivers. The NDWI multiband method is capable of detecting surface water bodies in non-perennial rivers. Monitoring the change of the surface water of small pools was accurate when applying Sentinel-2 datasets. Ogilvie et al. (2018) highlighted the opportunity for using remote sensing in small-scale hydrology, by using next generation optical sensors. Du et al. (2016) took advantage of the Sentinel-2 sensor's capability to accurately delineate water bodies in Italy, by also using the NDWI multiband method and the TOA reflectance datasets.

The changes in the surface areas of the pools in the non-perennial rivers was significant. Many pools decreased in size or dried up, due to evaporation and lack of rainfall. A similar result was seen in the study by Haas et al. (2009) in sub-Saharan Africa, where a time series analysis of surface water, using optical remote sensing data, was developed between 1999 and 2007. Their study illustrated that most of the variable water bodies were only identified in a Temporary-Surface-Water-Body map. Using less frequent remote sensing datasets would cause most temporary water features to go unidentified in the short term. This was seen in regions of the Tankwa River, where brief but large amounts of rainfall occur; however, high temperatures resulted in a high rate of evaporation and the pools would only be present for a brief period of time.

UNIVERSITY of the
WESTERN CAPE

The accuracy of identifying surface water is affected by background areas with low albedo surfaces, such as shadows, clouds and buildings (Sarp & Ozcelik, 2017). In many cases, the presence of shadows caused a misclassification, most notably in the Touws River Catchment, where mountain shadows were misclassified as water. This is a continuing limitation when classifying features that are based on their spectral properties.

Surface water area changes did not show a good relationship to rainfall across all pools. Omute et al. (2012) compared monthly mean water levels of Lake Victoria to rainfall and found an association between the rainfall and changes in Lake Victoria. The study showed the potential of using an NDVI to illustrate the expected natural trends of the changes in the lake's water level. However, this was not the case in this study, where each pool varied in terms of change in surface area. A different result was seen when comparing pool area change to temperature. During the summer months, evaporation rates are high and it is

http://etd.uwc.ac.za/

expected that the pool area would decrease. This was shown in all the pools that were analysed.

The hydroperiod of the pools was heavily influenced by short-term rainfall events. This was also shown in Montgomery et al. (2018), where the daily rainfall and monthly average temperature were compared to the estimated surface water area of wetlands in Canada. Their study found that the wetland surface water changed dynamically, and it corresponded to rainfall that occurred seasonally or annually. This was also seen for the pools in the Touws and Tankwa Rivers where the pool area dynamics changed significantly, as a response to seasonal rainfall.

Pools in the Nuwejaars and Breede Rivers showed more semi-permanent hydroperiods, which was a similar pattern to the hydroperiods of the wetlands analysed in Montgomery et al. (2018). Pools in the Touws and Tankwa Rivers showed more seasonal and temporary hydroperiods. This may be attributed to the Touws and Tankwa regions being extremely arid and having less frequent rainfall events. The pools in the Touws and Tankwa Rivers seemed to follow a similar pattern to the hydroperiods of the Prairie potholes in Canada, which were assessed by Montgomery et al. (2018), with surface water often only present for 1 – 2 months in a year.

One other significant find was in the Nuwejaars and Tankwa Rivers for 2016. The hydroperiod for the pools analysed in these rivers were significant in terms of the temporary surface water. This was described by Haas et al. (2009) in a study that mapped temporary surface water bodies in sub-Saharan Africa. The map was comprised of small temporary water bodies that were not referenced in prior datasets. The pools mapped in this study have also not been documented in any prior datasets, which can be used as a reference for future studies.

UNIVERSITY of the
WESTERN CAPE

5.5 Summary

The Nuwejaars, Breede, Touws and Tankwa Rivers were selected to assess the spatio-temporal changes of pool size variation over a period of two years, using Sentinel-2 satellite imagery. The estimated surface water area changes across the four rivers ranged from 0 – 25 449 m^2. The Nuwejaars and Breede Rivers showed the largest surface water area estimates from 2016 – 2017. The Touws and Tankwa Rivers showed smaller surface water area estimates. This may be attributed to their location, as they are in a more arid region. The

http://etd.uwc.ac.za/

surface water area decreased across all regions of interest in the four rivers, suggesting that a lower amount of rainfall and a higher rate of evaporation had occurred in 2017. The surface water area changes were compared to the daily mean rainfall and temperature from 2016 to 2017. A strong relationship was found between the surface water area and temperature changes. High temperatures often result in a higher rate of evaporation, suggesting a decrease in pool size. This was seen across all the pools that were assessed across the four rivers. Similarly, lower temperatures often result in a lower rate of evaporation, suggesting minimal or no decrease in the surface water area. This was also seen across the pools in the four rivers. Rainfall did not show a strong relationship to surface water area change across the pools. However, a good relationship was seen in the Nuwejaars, Tankwa and Touws Rivers where, after large rainfall events were recorded, an increase in the estimated surface water area of the pools was observed. The hydroperiod analysis of the pools suggests that a time-series of surface water recurrence can be used to determine the hydroperiod and permanence of pools in non-perennial rivers. The temporary hydroperiod class seemed to be the most variable, notably in the Nuwejaars and Tankwa Rivers.

UNIVERSITY of the
WESTERN CAPE

http://etd.uwc.ac.za/

6. CONCLUSION AND RECOMMENDATIONS

This study explored the potential use of remotely-sensed data for monitoring surface water in non-perennial rivers. Landsat 8-OLI and Sentinel-2 MSI were selected as the potential datasets to map and monitor pools in non-perennial rivers in the Western Cape. The first objective of this study was to assess a suitable method for mapping and monitoring pools in non-perennial rivers. Based on the literature reviewed, two atmospheric correction methods were selected, as well as six multiband methods, to assess the most suitable approach for mapping and monitoring surface water in non-perennial rivers. Sentinel-2 largely outperformed Landsat 8 when assessing the accuracy of surface water classification of small pools in non-perennial rivers. The NDWI applied to the Sentinel-2 TOA reflectance product was found to be the most suitable approach for identifying and monitoring pools in non-perennial rivers in the Western Cape. However, the presence of clouds and shadows were a major concern, when obtaining the number of available datasets.

The second objective of this study was to determine the spatio-temporal variability of pools within major non-perennial rivers. The Nuwejaars, Breede, Touws and Tankwa Rivers were selected, based on the criteria discussed in Chapter 3. The NDWI was applied to Sentinel-2 datasets to monitor the spatio-temporal variation of pool size in the rivers over a two-year period. The results showed that the area of pools varied seasonally. A strong relationship was found, in most cases, between estimated pool area and daily mean rainfall. In some instances, a high occurrence of rainfall was followed by increases in the pool area, while low periods of rainfall, coupled with high temperatures, showed decreases in the pool area. This suggests that climatic and seasonal changes have a major influence on the dynamics of the pools in non-perennial rivers.

The use of remote sensing to monitor non-perennial rivers does not replace in-situ measurements, but rather, it adds valuable information. These results can further be used for more extensive analyses on surface water monitoring in non-perennial rivers and to increase the reliability of the results. The results also helped to prove the extensive reliability of using easily-accessible and cost-efficient ancillary validated data as a surrogate for field visits, when necessary.

UNIVERSITY of the WESTERN CAPE
http://etd.uwc.ac.za/

6.1 Recommendations

Optical remote sensing datasets have been a primary resource in remote sensing for many years. The continuous development of remote sensing technology supports the need for consistent evaluations and assessments, to determine its reliability.

As new satellites are being launched more frequently, the potential for using multi-datasets is becoming more viable and realistic, with shorter return periods and higher spatial resolutions. However, optical remote sensing datasets have their limitations and there is a need for future studies to test the potential of integrating optical and radar sensors for monitoring non-perennial rivers. This could fill the gaps caused by cloud cover and other factors. The recently-launched Sentinel-1 synthetic-aperture radar (SAR) has the potential to be used concurrently with Sentinel-2 providing more frequent and more accurate results for surface water monitoring.

Installations of piezometers to measure groundwater levels may be suitable to measure the gains and losses of pool water to groundwater systems, and this information may help in understanding the pool dynamics.

The use of drone technology is also becoming a more realistic and cost-effective approach. With technology continuously improving, estimating the river discharges from remote sensing is becoming a more viable option.

UNIVERSITY of the
WESTERN CAPE

The results found in this study suggest that Landsat 8 is not a suitable dataset for the surface water monitoring of pools in non-perennial rivers. For the long-term monitoring of pool dynamics, it is recommended that Sentinel-2 be the primary dataset. The results also suggest that the use of atmospheric correction has the potential to eliminate the misclassification of surface water from clouds and shadows, but at the cost of also eliminating key water pixels. It is recommended that atmospheric correction only be used when monitoring larger surface water bodies in regions where shadows and/or clouds play a major factor in misclassification.

What is certain is that, with the rapid development of technology and sciences, scientists and researchers are getting closer to better understanding all aspects of the natural environment, not just from a water resources perspective.

http://etd.uwc.ac.za/

REFERENCES

Acharya, T. D., Lee, D. H., Yang, I. T., & Lee, J. K. (2016). Identification of water bodies in a Landsat 8 OLI image using a J48 decision tree. *Sensors (Switzerland)*, *16*(7), 1–16. https://doi.org/10.3390/s16071075

Acreman, M. C., & Dunbar, M. J. (2004). Defining environmental river flow requirements – a review. *Hydrology and Earth System Sciences*, *8*(5), 861–876. https://doi.org/10.5194/hess-8-861-2004

Avisse, N., Tilmant, A., François Müller, M., & Zhang, H. (2017). Monitoring small reservoirs' storage with satellite remote sensing in inaccessible areas. *Hydrology and Earth System Sciences*, *21*(12), 6445–6459. https://doi.org/10.5194/hess-21-6445-2017

Berhanu, B., Seleshi, Y., Demisse, S. S., & Melesse, A. M. (2015). Flow regime classification and hydrological characterization: A case study of Ethiopian rivers. *Water (Switzerland)*, *7*(6), 3149–3165. https://doi.org/10.3390/w7063149

Boudewyn, P., Seemann, D., Wulder, M. A., & Magnussen, S. (2000). The Effects of Polygon Boundary Pixels on Image Classification Accuracy. *Symposium A Quarterly Journal In Modern Foreign Literatures*.

Brovelli, M., Molinari, M., Hussein, E., Chen, J., & Li, R. (2015). The First Comprehensive Accuracy Assessment of GlobeLand30 at a National Level: Methodology and Results. *Remote Sensing*, *7*(4), 4191–4212. https://doi.org/10.3390/rs70404191

Buddemeier, W., deNoyelles, F. J., Egbert, S., Sleezer, O., Young, D. P., Zhan, X., Andereck, Z., Houts, M., Mosiman, B., Taylor, P., Vopata, J., Wilson, W., Renwick, W H., Smith, S. V. (2002). Detection and Characterization of Small Water Bodies. Technical Report. 23pp.

Changwony, C., Sichangi, A. W., & Murimi Ngigi, M. (2017). Using GIS and Remote Sensing in Assessment of Water Scarcity in Nakuru County, Kenya. *Advances in Remote Sensing*, *06*(01), 88–102. https://doi.org/10.4236/ars.2017.61007

Chavez, P. S. (1996). Image-Based Atmospheric Corrections - Revisited and Improved. Photogrammetric Engineering & Remote Sensing, Vol. 62, No. 9, pp. 1025-1036

UNIVERSITY of the WESTERN CAPE

http://etd.uwc.ac.za/

Chemura, A., Mutanga, O., & Dube, T. (2017). Separability of coffee leaf rust infection levels with machine learning methods at Sentinel-2 MSI spectral resolutions. *Precision Agriculture*, *18*(5), 859–881. https://doi.org/10.1007/s11119-016-9495-0

Congalton, R. G., Oderwald, R. G., & Mead, R. A. (1983). Assessing Landsat Classification ACongalton, R. G., Oderwald, R. G., & Mead, R. A. (1983). Assessing Landsat Classification Accuracy Using Discrete Multivariate Analysis Statistical Techniques. Photogrammetric Engineering and Remote Sensing, 49(No. 12), 1. *Photogrammetric Engineering and Remote Sensing*, *49*(No. 12), 1671–1678.

Du, Y., Zhang, Y., Ling, F., Wang, Q., Li, W., & Li, X. (2016). Water bodies' mapping from Sentinel-2 imagery with Modified Normalized Difference Water Index at 10-m spatial resolution produced by sharpening the SWIR band. *Remote Sensing*, *8*(4). https://doi.org/10.3390/rs8040354

ESA. (2015). Sentinel-2 User Handbook, (1), 1–64. https://doi.org/10.13128/REA-22658

Eliasson, J. (2015). The rising pressure of global water shortages. *Nature*, *517*(7532), 6. https://doi.org/10.1038/517006a

Feyisa, G. L., Meilby, H., Fensholt, R., & Proud, S. R. (2014). Automated Water Extraction Index: A new technique for surface water mapping using Landsat imagery. *Remote Sensing of Environment*, *140*, 23–35. https://doi.org/10.1016/j.rse.2013.08.029

Fisher, A., Flood, N., & Danaher, T. (2016). Comparing Landsat water index methods for automated water classification in eastern Australia. *Remote Sensing of Environment*, *175*, 167–182. https://doi.org/10.1016/j.rse.2015.12.055

Frazier, P. S., & Page, K. J. (2000). Water Body Detection and Delineation with Landsat TM Data. *Photogrammetric Engineering & Remote Sensing*, *66*(12), 1461–1467. https://doi.org/0099-1112I0OI6612-1461$3.00/0

Gilabert, M. A., Conese, C., & Maselli, F. (1994). An atmospheric correction method for the automatic retrieval of surface reflectances from TM images. *International Journal of Remote Sensing*, *15*(10), 2065–2086. https://doi.org/10.1080/01431169408954228

UNIVERSITY of the WESTERN CAPE

http://etd.uwc.ac.za/

Haas, E. M., Bartholomé, E., & Combal, B. (2009). Time series analysis of optical remote sensing data for the mapping of temporary surface water bodies in sub-Saharan western Africa. *Journal of Hydrology*, *370*(1–4), 52–63. https://doi.org/10.1016/j.jhydrol.2009.02.052

Hughes, D. A. (2005). Hydrological issues associated with the determination of environmental water requirements of ephemeral rivers. *River Research and Applications*, *21*(8), 899–908. https://doi.org/10.1002/rra.857

Hughes, D. A., Desai, A. Y., Birkhead, A. L., & Louw, D. (2014). A new approach to rapid, desktop-level, environmental flow assessments for rivers in South Africa. *Hydrological Sciences Journal*, *59*(3–4), 673–687. https://doi.org/10.1080/02626667.2013.818220

Puckridge, J. T., Sheldon, F., Walker, K. F., Boulton, A. J. (1998). Flow variability and the ecology of large rivers. *Sustainable Development*.

Ji, L., Geng, X., Sun, K., Zhao, Y., & Gong, P. (2015). Target Detection Method for Water Mapping Using Landsat 8 OLI/TIRS Imagery. *Water*, *7*(2), 794–817. https://doi.org/10.3390/w7020794

Ji, L., Zhang, L., & Wylie, B. (2009). Analysis of Dynamic Thresholds for the Normalized Difference Water Index. *Photogrammetric Engineering & Remote Sensing*, *75*(11), 1307–1317. https://doi.org/10.14358/PERS.75.11.1307

Jiang, H., Feng, M., Zhu, Y., Lu, N., Huang, J., & Xiao, T. (2014). An automated method for extracting rivers and lakes from Landsat imagery. *Remote Sensing*, *6*(6), 5067–5089. https://doi.org/10.3390/rs6065067

Jones, S. K., Fremier, A. K., DeClerck, F. A., Smedley, D., Pieck, A. O., & Mulligan, M. (2017). Big data and multiple methods for mapping small reservoirs: Comparing accuracies for applications in agricultural landscapes. *Remote Sensing*, *9*(12). https://doi.org/10.3390/rs9121307

Kapangaziwiri, E., Hughes, D. A., & Wagener, T. (2012). Incorporating uncertainty in hydrological predictions for gauged and ungauged basins in southern Africa. *Hydrological Sciences Journal*, *57*(5), 1000–1019. https://doi.org/10.1080/02626667.2012.690881

UNIVERSITY of the WESTERN CAPE

http://etd.uwc.ac.za/

Karimi, P., & Bastiaanssen, W. G. M. (2015). Spatial evapotranspiration, rainfall and land use data in water accounting - Part 1: Review of the accuracy of the remote sensing data. *Hydrology and Earth System Sciences*, *19*(1), 507–532. https://doi.org/10.5194/hess-19-507-2015

King, J. M., Brown, C. A., Paxton, B. R., & February, R. J. (2004). *Development of DRIFT, a scenario-based methodology for environmental flow assessments*.

Kustas, W. P., & Norman, J. M. (1996). Use of remote sensing for evapotranspiration monitoring over land surfaces. *Hydrological Sciences Journal*, *41*(4), 495–516. https://doi.org/10.1080/02626669609491522

Lacaux, J. P., Tourre, Y. M., Vignolles, C., Ndione, J. A., & Lafaye, M. (2007). Classification of ponds from high-spatial resolution remote sensing: Application to Rift Valley Fever epidemics in Senegal. *Remote Sensing of Environment*, *106*(1), 66–74. https://doi.org/10.1016/j.rse.2006.07.012

Li, W., Du, Z., Ling, F., Zhou, D., Wang, H., Gui, Y., Bingyu, S., Zhang, X. (2013). A comparison of land surface water mapping using the normalized difference water index from TM, ETM+ and ALI. *Remote Sensing*, *5*(11), 5530–5549. https://doi.org/10.3390/rs5115530

Liu, C., Liu, J., Hu, Y., Wang, H., & Zheng, C. (2016). Airborne Thermal Remote Sensing for Estimation of Groundwater Discharge to a River. *Groundwater*, *54*(3), 363–373. https://doi.org/10.1111/gwat.12362

Martha, T. R., Kerle, N., Jetten, V., van Westen, C. J., & Kumar, K. V. (2010). Characterising spectral, spatial and morphometric properties of landslides for semi-automatic detection using object-oriented methods. *Geomorphology*, *116*(1–2), 24–36. https://doi.org/10.1016/j.geomorph.2009.10.004

Martins, V. S., Barbosa, C. C. F., de Carvalho, L. A. S., Jorge, D. S. F., Lobo, F. de L., & de Moraes Novo, E. M. L. (2017). Assessment of atmospheric correction methods for Sentinel-2 MSI images applied to Amazon floodplain lakes. *Remote Sensing*, *9*(4). https://doi.org/10.3390/rs9040322

UNIVERSITY of the WESTERN CAPE

http://etd.uwc.ac.za/

Masocha, M., Dube, T., Makore, M., Shekede, M. D., & Funani, J. (2018). Surface water bodies mapping in Zimbabwe using Landsat 8 OLI multispectral imagery : A comparison of multiple water indices. *Physics and Chemistry of the Earth*, (March), 1–5. https://doi.org/10.1016/j.pce.2018.05.005

Mathews, R., & Richter, B. D. (2007). Application of the indicators of hydrologic alteration software in environmental flow setting. *Journal of the American Water Resources Association*, *43*(6), 1400–1413. https://doi.org/10.1111/j.1752-1688.2007.00099.x

Mcfeeters, S.K., (1996). The use of normalized difference water index (NDWI) in the delineation of open water features. International Journal of Remote Sensing, 17, pp. 1425–1432.

McFeeters, S. K. (2013). Using the normalized difference water index (ndwi) within a geographic information system to detect swimming pools for mosquito abatement: A practical approach. *Remote Sensing*, *5*(7), 3544–3561. https://doi.org/10.3390/rs5073544

Mishra, K., & Prasad, P. R. C. (2015). Automatic Extraction of Water Bodies from Landsat Imagery Using Perceptron Model. *Journal of Computational Environmental Sciences*, *2015*, 1–9. https://doi.org/10.1155/2015/903465

Montgomery, J. S., Hopkinson, C., Brisco, B., Patterson, S., & Rood, S. B. (2018). Wetland hydroperiod classification in the western prairies using multitemporal synthetic aperture radar. *Hydrological Processes*, *32*(10), 1476–1490. https://doi.org/10.1002/hyp.11506

Mueller, N., Lewis, A., Roberts, D., Ring, S., Melrose, R., Sixsmith, J., Lymburner, L., McIntyre, A., Tan, P., Curnow, S., Ip, A. (2016). Water observations from space: Mapping surface water from 25years of Landsat imagery across Australia. *Remote Sensing of Environment*, *174*, 341–352. https://doi.org/10.1016/j.rse.2015.11.003

Nguyen, H. C., Jung, J., Lee, J., Choi, S. U., Hong, S. Y., & Heo, J. (2015). Optimal atmospheric correction for above-ground forest biomass estimation with the ETM+ remote sensor. *Sensors (Switzerland)*, *15*(8), 18865–18886. https://doi.org/10.3390/s150818865

UNIVERSITY of the WESTERN CAPE

http://etd.uwc.ac.za/

Ogilvie, A., Belaud, G., Massuel, S., Mulligan, M., Le Goulven, P., & Calvez, R. (2018). Surface water monitoring in small water bodies: potential and limits of multi-sensor Landsat time series. *Hydrology and Earth System Sciences Discussions*, 1–35. https://doi.org/10.5194/hess-2018-19

Ollis D.J., Snaddon C.D., Job N.M., Mbona. N. (2013). *Classification System for Wetlands and other Aquatic Ecosystems in South Africa*. *Journal of Chemical Information and Modeling* (Vol. 53). https://doi.org/10.1017/CBO9781107415324.004

Omute, P., Corner, R., & Awange, J. L. (2012). The use of NDVI and its Derivatives for Monitoring Lake Victoria's Water Level and Drought Conditions. *Water Resources Management*. https://doi.org/10.1007/s11269-011-9974-z

Pasquini, L., Cowling, R. M., & Ziervogel, G. (2013). Facing the heat: Barriers to mainstreaming climate change adaptation in local government in the Western Cape Province, South Africa. *Habitat International*, *40*, 225–232. https://doi.org/10.1016/j.habitatint.2013.05.003

Pekel, J.-F., Cottam, A., Gorelick, N., & Belward, A. S. (2016). High-resolution mapping of global surface water and its long-term changes. *Nature*, *540*(7633), 1–19. https://doi.org/10.1038/nature20584

Poff, N. L., Allan, J. D., Bain, M. B., Karr, J. R., Prestegaard, K. L., Richter, B. D., R.E Sparks., Stromberg, J. C. (1997). The Natural Flow Regime: A paradigm for river conservation and restoration N. *BioScience*, *47*(11), 769–784. https://doi.org/10.2307/1313099

Pontius, R. G., & Millones, M. (2011). Death to Kappa: Birth of quantity disagreement and allocation disagreement for accuracy assessment. *International Journal of Remote Sensing*, *32*(15), 4407–4429. https://doi.org/10.1080/01431161.2011.552923

Provincial Spatial Development Framework. (2005). The Western Cape Province Today. *Development*, (November). Environmental & Spatial Planning Western Cape Department of Environmental Affairs and Development Planning. pp. 64

UNIVERSITY of the WESTERN CAPE

http://etd.uwc.ac.za/

Ren, J., Zheng, Z., Li, Y., Lv, G., Wang, Q., Lyu, H., Huang, Changchun., Liu, Ge., Du, Chenggong., Mu, Meng., Lei, Shaohua., Bi, S. (2018). Remote observation of water clarity patterns in Three Gorges Reservoir and Dongting Lake of China and their probable linkage to the Three Gorges Dam based on Landsat 8 imagery. *Science of the Total Environment*, , 1554–1566. https://doi.org/10.1016/j.scitotenv.2018.01.036

Rhazi, L., Grillas, P., Saber, E. R., Rhazi, M., Brendonck, L., & Waterkeyn, A. (2011). Vegetation of Mediterranean temporary pools: A fading jewel? *Hydrobiologia*, *689*(1), 23–36. https://doi.org/10.1007/s10750-011-0679-3

Riaño, D., Chuvieco, E., Salas, J., & Aguado, I. (2003). Assessment of different topographic corrections in Landsat-TM data for mapping vegetation types (2003). *IEEE Transactions on Geoscience and Remote Sensing*, *41*(5 PART 1), 1056–1061. https://doi.org/10.1109/TGRS.2003.811693

Richter, B. D., Baumgarther, J., Powell, J., Braun, D. P (1996). A Method for Assessing Hydrologic Alteration within Ecosystems. *Conservation Biology*. Vol. 10, Issue. 4, 1163-1174.

Richter, R., Kellenberger, T., & Kaufmann, H. (2009). Comparison of topographic correction methods. *Remote Sensing*, *1*(3), 184–196. https://doi.org/10.3390/rs1030184

UNIVERSITY of the
WESTERN CAPE

Rokni, K., Ahmad, A., Selamat, A., & Hazini, S. (2014). Water feature extraction and change detection using multitemporal landsat imagery. *Remote Sensing*, *6*(5), 4173–4189. https://doi.org/10.3390/rs6054173

Rokni, K., Ahmad, A., Solaimani, K., & Hazini, S. (2015). A new approach for surface water change detection: Integration of pixel level image fusion and image classification techniques. *International Journal of Applied Earth Observation and Geoinformation*, *34*(1), 226–234. https://doi.org/10.1016/j.jag.2014.08.014

L Rossouw, MF Avenant, MT Seaman, JM King, CH Barker, PJ du Preez, AJ Pelser, JC Roos, JJ van Staden, GJ van Tonder, and M Watson (2005). *Environmental Water Requirements in Non-Perennial Systems*. The Centre for Environmental Management. University of the Free State. pp 318.

http://etd.uwc.ac.za/

Rouse, J. W., Hass, R. H., Schell, J. A., & Deering, D. W. (1973). Monitoring vegetation systems in the great plains with ERTS. *Third Earth Resources Technology Satellite (ERTS) Symposium*, *1*, 309–317. https://doi.org/citeulike-article-id:12009708

Sader, S. A., Ahl, D., & Liou, W. S. (1995). Accuracy of landsat-TM and GIS rule-based methods for forest wetland classification in Maine. *Remote Sensing of Environment*, *53*(3), 133–144. https://doi.org/10.1016/0034-4257(95)00085-F

Sarp, G., & Ozcelik, M. (2017). Water body extraction and change detection using time series: A case study of Lake Burdur, Turkey. *Journal of Taibah University for Science*, *11*(3), 381–391. https://doi.org/10.1016/j.jtusci.2016.04.005

Sawunyama, T., Senzanje, A., & Mhizha, A. (2006). Estimation of small reservoir storage capacities in Limpopo River Basin using geographical information systems (GIS) and remotely sensed surface areas: Case of Mzingwane Catchment. *Physics and Chemistry of the Earth*, *31*(15–16), 935–943. https://doi.org/10.1016/j.pce.2006.08.008

Seaman, M., Watson, M., Avenant, M., Joubert, A., King, J., Barker, C., Esterhuyse, S., Graham, D., Kemp, M., Le Roux, P., Prucha, B., Redelinghuys, N., Rossouw, L., Rowntree, K., Sokolic, F., Van Rensburg, L., Van Der Waal, B., Van Tol, J Vos, T. (2016). DRIFT-ARID: Application of a method for environmental water requirements (EWRs) in a non-perennial river (Mokolo River) in South Africa. *Water SA*, *42*(3), 368–383. https://doi.org/10.4314/wsa.v42i3.02

UNIVERSITY of the
WESTERN CAPE

Sharma, R. C., Tateishi, R., Hara, K., & Nguyen, L. V. (2015). Developing Superfine Water Index (SWI) for global water cover mapping using MODIS data. *Remote Sensing*, *7*(10), 13807–13841. https://doi.org/10.3390/rs71013807

Sisay, A. (2016). Remote Sensing Based Water Surface Extraction and Change Detection in the Central Rift Valley Region of. *American Journal of Geographic Information System*, *5*(2), 33–39. https://doi.org/10.5923/j.ajgis.20160502.01

Smakhtin, V., Revenga, C., & Döll, P. (2004). A pilot global assessment of environmental water requirements and scarcity. *Water International*, *29*(3), 307–317. https://doi.org/10.1080/02508060408691785

http://etd.uwc.ac.za/

Smith, J. H., Wickham, J. D., Stehman, S. V, & Yang, L. (2002). Impacts of patch size and land-cover heterogeneity on thematic image classification accuracy. *Photogrammetric Engineering and Remote Sensing*, *68*(1), 65–70. Retrieved from http://www.scopus.com/inward/record.url?eid=2-s2.0-0036150948&partnerID=40

Smith, S. V., Renwick, W. H., Bartley, J. D., & Buddemeier, R. W. (2002). Distribution and significance of small, artificial water bodies across the United States landscape. *Science of the Total Environment*, *299*(1–3), 21–36. https://doi.org/10.1016/S0048-9697(02)00222-X

Solander, C., Reager, J., & Famiglietti, J. (2016). How well will the Surface Water and Ocean Topography (SWOT) mission observe global reservoirs?, 1–18. https://doi.org/10.1002/2016WR019804.

Song, C., Woodcock, C. E., Seto, K. C., Lenney, M. P., & Macomber, S. A. (2001). Classification and change detection using Landsat TM data: When and how to correct atmospheric effects? *Remote Sensing of Environment*, *75*(2), 230–244. https://doi.org/10.1016/S0034-4257(00)00169-3

Soti, V., Tran, A., Bailly, J. S., Puech, C., Seen, D. Lo, & Bégué, A. (2009). Assessing optical earth observation systems for mapping and monitoring temporary ponds in arid areas. *International Journal of Applied Earth Observation and Geoinformation*, *11*(5), 344–351. https://doi.org/10.1016/j.jag.2009.05.005

Toté, C., Patricio, D., Boogaard, H., van der Wijngaart, R., Tarnavsky, E., & Funk, C. (2015). Evaluation of satellite rainfall estimates for drought and flood monitoring in Mozambique. *Remote Sensing*, *7*(2), 1758–1776. https://doi.org/10.3390/rs70201758

USGS. (2016). Department of the interior geological survey. America, 8(1993), 1993–1993.

Wang, L., Qu, J. J., Zhang, S., Hao, X., & Dasgupta, S. (2007). Soil moisture estimation using MODIS and ground measurements in Eastern China. *International Journal of Remote Sensing*, *28*(6), 1413–1418. https://doi.org/10.1080/01431160601075525

Wang, S., Baig, M. H. A., Zhang, L., Jiang, H., Ji, Y., Zhao, H., & Tian, J. (2015). A simple enhanced water index (EWI) for percent surface water estimation using Landsat data. *IEEE Journal of Selected Topics in Applied Earth Observations and Remote Sensing*, *8*(1), 90–97. https://doi.org/10.1109/JSTARS.2014.2387196

http://etd.uwc.ac.za/

Wang, X., Xie, S., Zhang, X., Chen, C., Guo, H., Du, J., & Duan, Z. (2018). A robust Multi-Band Water Index (MBWI) for automated extraction of surface water from Landsat 8 OLI imagery. *International Journal of Applied Earth Observation and Geoinformation*, *68*(April 2017), 73–91. https://doi.org/10.1016/j.jag.2018.01.018

Wynne, B. R. H., Oderwald, R. G., Reams, A., & Scrivani, J. A. (2000). Optical remote sensing for forest area estimation. *Journal of Forestry*, *98*(5), 31–36.

Xie, Y., Sha, Z., & Yu, M. (2008). Remote sensing imagery in vegetation mapping: a review. *Journal of Plant Ecology*, *1*(1), 9–23. https://doi.org/10.1093/jpe/rtm005

Xu, H. (2006). Modification of normalised difference water index (NDWI) to enhance open water features in remotely sensed imagery. *International Journal of Remote Sensing*, *27*(14), 3025–3033. https://doi.org/10.1080/01431160600589179

Yamazaki, D., & Trigg, M. (2016). The dynamics of Earth's surface water. *Nature Int. J. Dig. Earth Limnol. Oceanogr. J. Geophys. Res. Lett. Int. J. Dig. Earth. Remote Sens. Environ. Nature Clim. Change*, *540*(185), 418–422. https://doi.org/10.1038/nature21100

Yamazaki, D., Trigg, M. A., & Ikeshima, D. (2015). Development of a global ~90m water body map using multi-temporal Landsat images. *Remote Sensing of Environment*, *171*, 337–351. https://doi.org/10.1016/j.rse.2015.10.014

Zacharias, I., & Zamparas, M. (2010). Mediterranean temporary ponds. A disappearing ecosystem. *Biodiversity and Conservation*, *19*(14), 3827–3834. https://doi.org/10.1007/s10531-010-9933-7

Zhou, Y., Chen, J., Guo, Q., Cao, R., & Zhu, X. (2014). Restoration of information obscured by mountainous shadows through landsat TM/ETM+ images without the use of DEM data: A new method. *IEEE Transactions on Geoscience and Remote Sensing*, *52*(1), 313–328. https://doi.org/10.1109/TGRS.2013.2239651

Zhou, Y., Dong, J., Xiao, X., Xiao, T., Yang, Z., Zhao, G., Zhenhua, Z., Qin, Y. (2017). Open surface water mapping algorithms: A comparison of water-related spectral indices and sensors. *Water (Switzerland)*, *9*(4). https://doi.org/10.3390/w9040256

UNIVERSITY of the
WESTERN CAPE

http://etd.uwc.ac.za/

Zhou, Y., Wenninger, J., Yang, Z., Yin, L., Huang, J., Hou, L., Wang, X., Zhang D., Uhlenbrook, S. (2013). Groundwater-surface water interactions, vegetation dependencies and implications for water resources management in the semi-arid Hailiutu River catchment, China - A synthesis. *Hydrology and Earth System Sciences*, *17*(7), 2435–2447. https://doi.org/10.5194/hess-17-2435-2013

http://etd.uwc.ac.za/

APPENDICES

Appendix 4.1 Variation of surface water colour for pools in the Touws River

TY of the
CAPE

http://etd.uwc.ac.za/

Appendix 5.1 Table of available weather stations used in this study

Weather Station	x-coordinate (longitude)	y-coordinate (latitude)
Spanjaardskloof	19°44'20,4"E	34°32'24"S
Moddervlei	19°47'50,815"E	34°36'18,158"S
Visserdrift	19°59'45,6"E	34°41'16,8"S
Swellendam	20°26'9,6"E	34°1'15,6"S
Swellendam: Napky	20°26'28,104"E	34°15'22,284"S
Laingsburg	20°51'43,2"E	33°11'24"S
Ladismith	21°15'54"E	33°30'0"S
Sutherland	20°39'43,2"E	32°23'56,4"S
Brakfontein: Die Bos Calvinia	19°31'51,096"E	32°20'34,152"S

Appendix 5.2 Example of shadow backdrop covering a pool in the Prins River

http://etd.uwc.ac.za/